PORTABLE FWD (PRIMA 100) FOR IN-SITU SUBGRADE EVALUATION

FINAL REPORT

by

K.P. George

Conducted by the

DEPARTMENT OF CIVIL ENGINEERING
UNIVERSITY OF MISSISSIPPI

In cooperation with

THE MISSISSIPPI DEPARTMENT OF TRANSPORTATION

And

U.S. DEPARTMENT OF TRANSPORTATION
FEDERAL HIGHWAY ADMINISTRATION

The University of Mississippi
University, Mississippi
June, 2006

Technical Report Documentation Page

1.Report No.	2. Government Accession No.	3. Recipient's Catalog No.
FHWA/MS-DOT-RD-06-179		

4. Title and Subtitle	5. Report Date
PORTABLE FWD (PRIMA 100) FOR IN-SITU SUBGRADE EVALUATION	June 2006
	6. Performing Organization Code

7. Author(s)	8. Performing Organization Report No.
K.P. George	MS-DOT-RD-06-179

9. Performing Organization Name and Address	10. Work Unit No. (TRAIS)
University of Mississippi Department of Civil Engineering University, MS 38677	11. Contract or Grant No. State Study 179

12. Sponsoring Agency Name and Address	13. Type Report and Period Covered
Mississippi Department of Transportation Research Division Jackson, MS 39215-1850	Final Report
	14. Sponsoring Agency Code

15. Supplementary Notes

16. Abstract

Subgrade soil characterization measured in terms of resilient modulus, M_R, has been a prerequisite for pavement design. For new pavement design, M_R is obtained by conducting repeated load triaxial tests on reconstituted/undisturbed cylindrical specimens, employing AASHTO T-307 test protocol. Because of the complexities encountered with the test, in-situ tests would be desirable, if reliable correlation can be established. Subgrade characterization for rehabilitation selection, however, in-situ tests are the norm than the exception. The focus of this study is to investigate the viability of Prima 100, a Portable Falling Weight Deflectometer (PFWD), for direct testing of subgrade with the objective of estimating resilient modulus, via a correlation between M_R and PFWD modulus (E_{PFWD}). Thirteen as-built subgrade sections reflecting typical subgrade soil materials in Mississippi, were selected and tested for elastic modulus employing a Falling Weight Deflectometer (FWD), followed by PFWD. In-situ unit weight and moisture were measured using a nuclear device. Soil samples collected from those sections were subjected to repeated load triaxial test (AASHTO T307) and to other routine laboratory tests for classification purposes.

The first step in analyzing the data was to authenticate the Prima elastic modulus, which was accomplished by establishing an acceptable relation between Prima modulus and FWD modulus (E_{FWD}). A statistically significant relation between M_R and E_{PFWD} and was derived, though three other explanatory variables emerged in the model equation. Since moisture and density of in-situ material rarely match those prescribed in the repeated load test sample, those two attributes were included in the model. A third variable, which was soil-related (namely, PI/P_{200}), emerged to account for the range of soil types, and intentionally retained in the model equation. A similar, but abbreviated version of the model was also derived, deleting the soil-related variable. An investigation of the significance of unit weight and moisture on the Prima modulus resulted in a correlation equation between E_{PFWD} and those two variables.

An exclusive program, PFWDSUBGRADE was developed to analyze Prima modulus and calculate resilient modulus. The program, in addition to calculating station-by-station resilient modulus, relying on what is known as "cumulative difference" technique, delineates 'homogeneous' subsections of the project, outputting mean and standard deviation of the resilient modulus for each homogeneous section. A graphical plot of resilient modulus of each station is another output of the program.

17. Key Words	18. Distribution Statement
Elastic Modulus, In-situ Test, Portable FWD, Resilient Modulus, Subgrade,	Unclassified

19. Security Classif. (of this report)	20. Security Classif. (of this page)	21. No. of Pages	22. Price
Unclassified	Unclassified	125	

Form DOT F 1700.7 (8-72)

Reproduction of completed page authorized

ACKNOWLEDGMENT

This report includes the results of a study titled "Portable FWD (Prima 100) for In-situ Subgrade Evaluation", conducted by the Department of Civil Engineering, The University of Mississippi, in cooperation with the Mississippi Department of Transportation (MDOT), and the U.S. Department of Transportation, Federal Highway Administration (FHWA). Funding of this project by MDOT and FHWA is gratefully acknowledged.

The author wishes to thank Bill Barstis with MDOT's Research Division for his efforts in coordinating the overall work plan of the project. M. Howard of MDOT coordinated the fieldwork, including FWD tests; Burns Cooley Dennis of Jackson conducted the repeated load triaxial tests.

Biplab Bhattacharya was the key personnel from the University conducting laboratory work and providing support in the field. The service of Sherra Jones in preparing this report is gratefully acknowledged.

ABSTRACT

Subgrade soil characterization measured in terms of resilient modulus, M_R, has been a prerequisite for pavement design. For new pavement design, M_R is obtained by conducting repeated load triaxial tests on reconstituted/undisturbed cylindrical specimens, employing AASHTO T-307 test protocol. Because of the complexities encountered with the test, in-situ tests would be desirable, if reliable correlation can be established. Subgrade characterization for rehabilitation selection, however, in-situ tests are the norm than the exception. The focus of this study is to investigate the viability of Prima 100, a Portable Falling Weight Deflectometer (PFWD), for direct testing of subgrade with the objective of estimating resilient modulus, via a correlation between M_R and PFWD modulus (E_{PFWD}). Thirteen as-built subgrade sections reflecting typical subgrade soil materials in Mississippi, were selected and tested for elastic modulus employing a Falling Weight Deflectometer (FWD), followed by PFWD. In-situ unit weight and moisture were measured using a nuclear device. Soil samples collected from those sections were subjected to repeated load triaxial test (AASHTO T-307) and to other routine laboratory tests for classification purposes.

The first step in analyzing the data was to authenticate the Prima elastic modulus, which was accomplished by establishing an acceptable relation between Prima modulus and FWD modulus (E_{FWD}). A statistically significant relation between M_R and E_{PFWD} was derived, though three other explanatory variables emerged in the model equation. Since moisture and density of in-situ material rarely match those prescribed in the repeated load test sample, those two attributes were included in the model. A third variable, which was soil-related (namely, PI/P_{200}), emerged to account for the range of soil types, and intentionally retained in the model equation. A similar, but abbreviated version of the model was also derived, deleting the soil-related

variable. An investigation of the significance of unit weight and moisture on the Prima modulus resulted in a correlation equation between E_{PFWD} and those two variables.

An exclusive program, PFWDSUBGRADE was developed to analyze Prima modulus and calculate resilient modulus. The program, in addition to calculating station-by-station resilient modulus, relying on what is known as "cumulative difference" technique, delineates 'homogeneous' subsections of the project, outputting mean and standard deviation of the resilient modulus for each homogeneous section. A graphical plot of resilient modulus of each station is another output of the program.

TABLE OF CONTENTS

LIST OF TABLES

LIST OF FIGURES

CHAPTER 1

INTRODUCTION

1.1 SUBGRADE CHARACTERIZATION IN MECHANISTIC EMPIRICAL PAVEMENT DESIGN GUIDE

Subgrade soil stiffness is an important parameter in pavement design. The resilient modulus (M_R) has become the standard parameter to characterize unbound pavement materials because a large amount of evidence has shown that the elastic (resilient) pavement deflection possesses a better correlation to field performance than the total pavement deflection (1). Resilient modulus is defined as the ratio of deviator stress, σ_d, to the recoverable strain, ε_r,

$$M_R = \sigma_d/\varepsilon_r \quad (1.1)$$

Now that MDOT has embarked on a program of implementing Mechanistic-Empirical Pavement Design Guide (M-EPDG), laboratory resilient modulus, M_R, of subgrade soil is a requisite input into the design software. The Department has already initiated a study to determine M_R of typical Mississippi soils, eventually developing a materials library of M_R values. With this materials library completed, a M_R value based on soil classification could be obtained for Level 2 pavement design. For Level 1 design, however, laboratory resilient modulus is a prerequisite, with AASHTO adopting the harmonized test protocol in NCHRP 1-28A (2). Meanwhile, the complexity of the laboratory test procedures has prompted highway agencies to explore other test methods, especially in situ field tests. Deflection measurements with the Falling Weight Deflectometer (FWD) and, in turn, modulus calculation through backcalculation have been routinely employed in evaluating pavement layers, and the underlying subgrade. Elastic stiffness modulus (abbreviated as stiffness modulus) of subgrade, however, could be determined employing forward calculation of the surface deflection induced by devices

similar to FWD. For routine use, it is imperative that the device be reliable, fast, and cost effective. The Mississippi Department of Transportation (MDOT) has funded this study to investigate the use of a Portable FWD (PFWD) for subgrade characterization.

The AASHTO Guide allows the use of both laboratory and in situ backcalculated moduli, but recognizes that the moduli determined by both procedures are not equal. The Guide, therefore, suggests that the stiffness modulus determined from deflection measurements on the pavement surface (E_{back}) needs to be adjusted by a factor of 0.33. However, other ratios have been documented. Ali and Khosla (3) compared the subgrade soil resilient modulus determined in the laboratory and backcalculated values from three pavement sections in North Carolina. The ratio of laboratory- measured modulus values to the corresponding backcalculated values varied from 0.18 to 2.44. Newcomb (4) reported results of similar tests in Washington State, suggesting a ratio in the range of 0.8 to 1.3. Von Quintus and Killingsworth (5) reported ratios in the range of 0.1 to 3.5 in a study based on data obtained from the Long Term Pavement Performance (LTPP) database. In the same reference, different average ratios were reported based on the type of layers atop the subgrade layer. Laboratory values were consistently higher (nearly double) than the backcalculated values, according to Chen et al. (6). Note that the previous studies relied on backcalculated moduli from deflection measurements on the top of the pavement structure. Many factors may have contributed to the disagreement between the laboratory measured and backcalculated moduli. One issue is the difficulty of obtaining representative samples from the field because of the inherent variability of the subgrade layer itself. A detailed discussion of the differences between laboratory measured M_R(lab) and backcalculated moduli can be found elsewhere (7).

While numerous studies have attempted FWD measurements on the pavement surface, only a few have targeted FWD tests conducted directly on the subgrade surface. In their study of the Minnesota Research Road Project (Mn/ROAD), Van Deusen et al. (8) reported that the laboratory resilient modulus tests conducted on the thin-wall samples yielded values that compared well with the backcalculated values from the deep layer of the subgrade. Resilient modulus vs. elastic stiffness modulus, E, relation was explored in a recent study titled "The Virginia Smart Road Project" (9). The one-to-one relationship sought, however, was less than satisfactory. A recent investigation, conducted for the Mississippi Department of Transportation (MDOT), showed that the backcalculated moduli (E_{back}) obtained from testing directly on the subgrade were in satisfactory agreement with the laboratory resilient modulus (10). On average, E_{back} was 3% larger than the resilient modulus. In a 2003 study (11), a concerted effort was made to correlate stiffness modulus from the light weight package of FWD to resilient modulus of undisturbed (Shelby tube) samples. The relation turned out to be of dual nature involving the first sensor and the offset sensors stiffness moduli. Note that stiffness modulus is directly related to resilient modulus in contrast to applying a correction factor to backcalculated modulus as customary when testing a pavement system.

1.2 CRITIQUE OF RESILIENT MODULUS TEST (AASHTO T-307)

Since AASHTO recommends using a laboratory resilient modulus test in a relatively small soil sample – one that is undisturbed or reconstituted – it is worthwhile to examine how realistic this test is. Despite several improvements made over the years, researchers have cited several uncertainties as well as limitations associated with this laboratory test procedure (12):

1. The laboratory resilient modulus sample is not completely representative of in situ

conditions because of sample disturbance and differences in aggregate orientation, moisture content, in-situ suction and level of compaction (or recompaction).

2 Laboratory specimens represent the properties of a small quantity of material, and not necessarily the average mass of the material that responds to a typical vehicle axle load.

3. Questionable accuracy in deflection measurement even employing internal LVDTs..

4. Lack of uniform equipment calibration and verification procedures lead to differences between labs.

5. The time, expense and potential impact associated with a statistically adequate sampling plan as well as testing add up to large expenditure.

Overall, these issues have kept the resilient modulus test from achieving general acceptance by the pavement and materials testing community, whereas a nondestructive test such as the FWD deflection test is credited with providing in-situ modulus, and is also capable of identifying inherent spatial variation. Some recent studies (13, 14, 15, 16) suggest that a Portable FWD (PFWD) could as well accomplish the same objective as that realized by a conventional FWD, at a fraction of the cost. Though the direct use of in-situ stiffness modulus is desirable for pavement design, its application should await until the M-EPDG model is calibrated with this input. This research, therefore, explored the viability of PFWD in estimating elastic stiffness modulus, a likely surrogate measure for resilient modulus in pavement design. Many different versions of PFWD have been introduced in recent years (13). A brief review of the

prominent PFWDs can be seen in chapter 2. Prima 100, manufactured by Carl Bros, Denmark, was selected as the most promising technology for this investigation.

1.3 OBJECTIVE AND SCOPE

The first objective of this study was to investigate the feasibility of employing Prima 100 to estimate in-situ stiffness modulus of constructed subgrade and/or embankments. In accomplishing this objective, a relation was sought between the in-situ stiffness modulus measured by Prima 100 and resilient modulus determined in accordance with the harmonized test procedure. Should a viable correlation exist between the two, PFWD tests could be advanced for subgrade characterization for Level 1 M-EPDG design. These objectives were accomplished by:

(i) Selecting 14 test sections covering a wide range of soils employed in subgrade construction in Mississippi.

(ii) Conducting in-situ tests with PFWD and conventional FWD at predetermined locations, characterizing those 14 subgrade soils.

(iii) Conducting resilient modulus tests as well as index tests (for soil classification) on bag samples collected from the 13 test sections (Note only 13 section-data were employed in the model development).

(iv) Performing correlation analysis between PFWD stiffness modulus (E_{PFWD}) and conventional FWD modulus (E_{FWD}) in order to authenticate the former test.

(v) Developing a prediction model, between PFWD stiffness modulus and laboratory resilient modulus, facilitating the transformation of PFWD modulus to resilient modulus.

(vi) Developing of a computer program to detect spatial variation of estimated resilient modulus along the road and thus facilitate subdividing the road way into

"uniform" sections, assigning representative "design resilient modulus" for each uniform section.

1.4 CHAPTER SUMMARY

This chapter discusses how resilient modulus evolved to become the primary subgrade characterizing parameters in M-EPDG. Despite the original recommendation of AASHTO to use laboratory resilient modulus, the current trend is to rely more on in-situ tests for assessing the subgrade design modulus.

This report comprises six chapters and three appendices. Chapter 2 presents a literature review of various in-situ devices for elastic stiffness modulus determination and correlations between the stiffness moduli from different impact testing devices. Results of in-situ tests (Prima 100, FWD and other supporting tests) on 13 test sections, five stations in each test section, are presented in Chapter 3. A comprehensive data analysis, culminating in a relation between elastic stiffness modulus and resilient modulus comprises chapter 4. A methodology for Prima 100 test is described in the first part of Chapter 5. Presented in the latter part is an outline of a computer program designated "PFWDSUBGRADE" for analyzing Prima 100 data, arriving at a design resilient modulus – mean and standard deviation of so-called uniform section. A summary and observations regarding the findings of the study constitute Chapter 6. Typical resilient modulus test results are presented in Appendix A, and optional prediction models in Appendix B. Detailed flow chart of the program, PFWDSUBGRADE, can be seen in Appendix C.

CHAPTER 2

LITERATURE REVIEW

2.1 OVERVIEW

This chapter presents a brief discussion of the significance of resilient modulus in pavement design, its laboratory determination including the factors affecting it. An overview of devices for in-situ modulus determination of pavement layers is also presented leading to selection of Prima 100 in this investigation. In addition, this chapter provides information on the existing correlations between the in-situ devices and resilient modulus.

2.2 RESILIENT MODULUS OF UNBOUND MATERIAL

The concept of a resilient modulus of a material was originally introduced by Seed et al. (17) in 1962. Seed et al. defined "resilient modulus" as the ratio of applied replicated deviatoric stress to the resilient or recoverable strain under a transient dynamic load. The resilient modulus has become the standard parameter to characterize unbound pavement materials because a large amount of evidence has shown that the elastic (resilient) pavement deflection possesses a better correlation to field performance than the total pavement deflection. In the last several decades, the resilient modulus has become a well recognized mode of material characterization for all pavement material layers (subgrade, subbase, and base).

2.2.1 Resilient Modulus Determination

The resilient modulus of soils can be determined from repeated load triaxial (RLT) tests in the laboratory or backcalculated from nondestructive (deflection) tests (NDT) in the field using methods such as falling weight deflectometer, Road Rater or Dynaflect. The 1986 AASHTO Guide, however, has stipulated and the 2002 Guide reaffirmed, that laboratory M_R be the parameter for characterizing the subgrade. Responding to the need, AASHTO T278-82

laboratory test was proposed to describe the behavior of pavement materials subjected to moving traffic. In 1991, AASHTO modified the T278-82 test procedure in terms of sample conditioning, load magnitude, and load application, with the revised test designation changed to TP292-92I, and subsequently to TP46-94. In conjunction with M-EPDG, a harmonized M_R test protocol was proposed in the NCHRP 1-28A study (18). For undisturbed test samples, Shelby tube sampling is relied upon. Reconstituted samples are molded in the laboratory to obtain desired density and moisture content representative of the field. The test method recommends kneading, impact or vibratory methods (depending on soil type) for sample preparation.

In accordance with the harmonized test protocol, a fine soil sample is subjected to a combination of four confining stresses and four deviator stresses, thus yielding 16 resilient modulus values for each sample. The stress factorial including the test sequence is listed in Table 2.1. Now, a constitutive model comprising M_R-stress relation is chosen, describing the resilient property of the material. The model employed in this study can be seen in equation 2.2. This model is then fitted to the data of each sample by regressing, and the resulting equation can be used for calculating M_R at any desired stress level.

Generally, the RLT test requires well-trained personnel, expensive laboratory equipment and is time-consuming, to say the least. The resilient modulus backcalculated from the field NDT deflection data can produce inconsistent backcalculated modulus results when different backcalculation programs are chosen. Many factors contribute to uncertain outcomes in backcalculated moduli, such as the use of elastic-layer theory, the static load assumption, variable and unknown depths of stiff layers at the bottom of subgrade in a pavement structure, to name a few.

Table 2.1 Test Sequence and Stress Levels in Harmonized Repeated Load Test (2)

Sequence	Confining Pressure		Contact Stress/Seating Stress		Cyclic (Deviator) Stress		Number of Load Applications
	kPa	psi	kPa	psi	kPa	psi	
0*	27.6	4.0	5.5	0.8	48.3	7.0	1000
1	55.2	8.0	11.0	1.6	27.6	4.0	100
2	41.4	6.0	8.3	1.2	27.6	4.0	100
3	27.6	4.0	5.5	0.8	27.6	4.0	100
4	13.8	2.0	2.8	0.4	27.6	4.0	100
5	55.2	8.0	11.0	1.6	48.3	7.0	100
6	41.4	6.0	8.3	1.2	48.3	7.0	100
7	27.6	4.0	5.5	0.8	48.3	7.0	100
8	13.8	2.0	2.8	0.4	48.3	7.0	100
9	55.2	8.0	11.0	1.6	69.0	10.0	100
10	41.4	6.0	8.3	1.2	69.0	10.0	100
11	27.6	4.0	5.5	0.8	69.0	10.0	100
12	13.8	2.0	2.8	0.4	69.0	10.0	100
13	55.2	8.0	11.0	1.6	96.6	14.0	100
14	41.4	6.0	8.3	1.2	96.6	14.0	100
15	27.6	4.0	5.5	0.8	96.6	14.0	100
16	13.8	2.0	2.8	0.4	96.6	14.0	100

(*Conditioning)

2.2.2 Resilient Modulus in M-EPDG

The general approach for selecting design inputs for materials and subgrade soils in 2002 Design Guide is a hierarchical system. In its simplest and most practical form, the hierarchical approach is based on the philosophy that the level of engineering effort in pavement design process should be consistent with the relative importance, size and cost of the design project

(18). In keeping with the hierarchical approach, material characterization is comprised of three input levels. Level 1 represents a design approach philosophy of the highest practically achievable reliability, Levels 2 and 3 have successfully lower reliability. A general tabulation of resilient modulus characterization methods is given in the Table 2.2.

Table 2.2 Input Levels for Mechanistic-Empirical Pavement Design

Material	Input Level 1	Input Level 2	Input Level 3
Granular Materials	Measured resilient modulus in laboratory	Estimated resilient modulus from correlations	Default resilient modulus
Cohesive Materials	Measured resilient modulus in laboratory	Estimated resilient modulus from correlations	Default resilient modulus

In selecting an appropriate M_R value for level 1 design, it is imperative that the stress state corresponding to typical rolling load be given consideration. M-EPDG suggests using a deviator stress, σ_d = 6 psi (41 kPa) and a confining stress, σ_c = 2 psi (14 kPa) in the stress dependent constitutive equation.

2.2.3 Estimation of M_R from Correlation Equations

Various empirical correlations have been proposed to determine the resilient modulus in the last three decades; most of them suit the level 2 requirements. Van Til et al. (19) related resilient modulus of subgrade soils to the soil support value employed in the earlier AASHTO design equation. He also made a correlation chart in which the values of M_R could be determined from R-value, CBR, and Texas triaxial classification value. Many other correlations between M_R, CBR, R-value and soil support values were also developed. A comparative study of the present M_R prediction equations had been completed for The Mississippi Department of Transportation (20), recommending LTPP equations for estimating it for level 2 design. The

writer has completed two other studies on relating Dynamic Cone Penetrometer Index (DCPI) to resilient modulus (21), and another establishing a relation between FWD elastic modulus and resilient modulus (11). Note that FWD tests were conducted directly on the subgrade and with modulus calculation employing forward technique.

2.2.3.1 Resilient Modulus Estimation Software: With numerous correlation models available for M_R prediction, a software program was recently developed by Han et al. (22), incorporating all of the 30 available models. The program was developed using an expert system approach. In this system (program), the information (soil properties) entered by the user is first examined for reasonableness and accuracy. Then, data searching processes are initiated, and over thirty estimation models can be invoked, depending on the availability of input data. All results are evaluated, based on certainty rules such as how well the data is meeting the limitations existing during the model's original development environment. The user is given four alternate methods on which to base the choice of resilient modulus that is most appropriate for the site: one based on certainty rules and others statistical average with different confidence intervals. Also included is a provision to estimate an average M_R, based on all of the 30 models. This option is employed to estimate M_{R95} of 18 soils, reported in Table 4.1.

2.3 FACTORS AFFECTING RESILIENT RESPONSE OF SOILS

Beginning with the 1986 AASHTO Guide (including the current M-EPDG), require that soil characterization to incorporate changes in material properties as a function of the state of stress (stress dependency), environmental conditions (moisture and temperature), aging and continual deterioration under traffic loading. A comprehensive discussion of the factors affecting resilient modulus is presented in M-EPDG report, Appendix DD1 (23). Those factors

are listed under the following three categories. The significance of those factors in the formulation of M_R-prediction models can be seen in section 4.5.1.

2.3.1 Factors Related to the State of Stress

The most often used stress parameters include bulk stress, octahedral sheer stress and pore pressure. For laboratory test conditions such as triaxial, volumetric (bulk) stress is determined from: $\theta = \sigma_1 + \sigma_2 + \sigma_3$

Octahedral Shear Stress is determined from: $\tau_{oct} = \frac{1}{3} \cdot \sqrt{(\sigma_1 - \sigma_2)^2 + (\sigma_1 - \sigma_3)^2 + (\sigma_2 + \sigma_3)^2}$.

Unbound materials used in pavement design are generally in a partly saturated state, especially if they fall above the groundwater table. The state of stress in unsaturated materials can be characterized by the following parameters (Fredlund et al. (24)):

$(\sigma_3 - u_a)$ = net confining pressure (also called net normal stress);

$(\sigma_1 - \sigma_3)$ = deviator stress, σ_d; and $(u_a - u_w)$ = matric suction, φ_m

where: σ_3 = total confining pressure;

σ_1 = total major principal stress;

u_a = pore air pressure; and

u_w = pore water pressure.

Matric suction greatly affects the state of stress and consequently the modulus (24, 25, 26, 27, 28). A resilient modulus model incorporating soil suction is proposed in a recent study (29). The equation is of the form:

$$M_R = k_1(\sigma_d + \chi\psi_m)^{k_2} \quad (2.1)$$

where: ψ_m = matrix section;

k_1, k_2 = regression constants; and

χ = a parameter thought to be a function of degree of saturation ($\chi = 0$ for dry soils, $\chi = 1$ for saturated soils)

Note that matrix suction complements the deviatoric stress increasing the rigidity of the soil skeleton, and in turn, the resilient modulus.

2.3.2 Factors Related to Soil Physical State

Moisture Content: All other conditions being equal, the higher the moisture content the lower the modulus; however, moisture has two separate effects: first, it can affect the state of stress through suction or pore water pressure because suction and water content are correlated through the "soil-water characteristic curve". Second, it can affect the structure of the soil, through destruction of the cementation between soil particles.

Dry Density: At low moisture contents, a lower density will give a lower M_R. The relationship is reversed for high moisture contents, as reported in reference 23. Any change in volume is reflected in a change in dry density; therefore, void ratio (*e*) can be used instead of dry density.

Degree of Saturation: A third parameter, uniquely defined by moisture content, dry density (or void ratio) and specific gravity of solids (*Gs*) is the degree of saturation (*S*). There is a unique relationship between the three physical state parameters depending on which parameter is used as a measure of volume changes (i.e. dry density or void ratio):

What it means is that knowing any two of the three parameters, *w*, *S* and γ_{dry}, the third may be found, provided G_s is known or can be estimated. The use of all three parameters as predictors in a model is therefore incorrect, due to redundancy. For cases where variations in moisture content are accompanied by volume changes, any two of the three parameters need to be used to correctly predict the change in modulus, together with known G_s.

Temperature: It becomes the most important factor in predicting the resilient modulus of frozen materials while for thawed materials it has little or no significant influence.

2.3.3 Factors Related to the Structure/Type of Material

Compaction Method: Roller compaction in addition to pre-stressing the material, results in microcracks which could affect resilient response of the material.

Particle Size (Grain Size Distribution): No doubt a well graded soil could result in improved rigidity of the soil skeleton, and in turn, larger resilient modulus.

Particle Shape: Frictional resistance, and in turn, stiffness of the soil, could be enhanced by irregular-shaped particles rather than spherical particles.

Cohesive Strength: Right quantity of fines (-#200 material) would enhance the bond between particles, and in turn, increase the resilient modulus.

2.4 MODELING RESILIENT MODULUS

Summarizing, the effect of various factors on resilient modulus, it is important to realize/recognize the three broad categories of factors in M_R prediction model. If the model for a given unbound material (UBM), at constant moisture and density is desired, bulk stress and octahedral shear stress could be the predictor variables. The M-EPDG model (Equation 2.2) is a prime example of this approach:

$$M_R = k_1 p_a \left(\frac{\theta}{p_a} \right)^{k_2} \left(\frac{\tau_{oct}}{p_a} + 1 \right)^{k_3} \tag{2.2}$$

where: p_a = atmospheric pressure

Should resilient modulus be desired for an unbound material subjected to varying environmental conditions (such as, moisture fluctuation), the explanatory variables in the constitutive model shall include a moisture-related factor. Equation 2.1, a deviator stress-matrix suction model, though simple, not only takes into account the state of stress but also suction-

generated internal stress resulting from moisture changes. Alternately, postulating that the state of stress and physical state factors are uncoupled, the moisture/density effect may be solved as an independent problem, and the latter used in tandem with equation 2.2. The M_R saturation level formulation proposed in M-EPDG is represented by Equation 2.3:

$$\log \frac{M_R}{M_{Ropt}} = k_s \cdot \left(S - S_{opt}\right) \tag{2.3}$$

where: M_R = resilient modulus at saturation level S (%);

$M_{R(opt)}$ = resilient modulus at maximum dry density and optimum moisture content;

S_{opt} = degree of saturation at maximum dry density and optimum moisture content, (%); and

k_s = gradient of log resilient modulus ratio (log (M_R/M_{Ropt})) with respect to variation in degree of saturation ($S - S_{opt}$) expressed in percent; k_s is a material constant and can be obtained by regression in the semi-log space.

The specific relation developed based on Equation 2.3, happens to be a sigmoidal equation, which can be seen in reference (23). Factors related to structure/type of material could be included in the model by introducing additional index properties of UBM (for example, material passing #200 sieve, PI etc.). General models, empirical though, encompassing all of the three categories of variables have been proposed in the past (30, 31, 32). The validity of those three and four other equations have been investigated by the author (20), and the LTPP equation (30) is found to be suitable for purposes of predicting resilient modulus of Mississippi subgrade soils. Specifically, in the LTPP equation, physical state factors include moisture content and density, state of stress factors are θ and τ, and finally, factors related to material type include

material passing 3/8" sieve, #4 sieve, percent silt and percent clay, and liquid limit and plasticity index.

2.5 NON-DESTRUCTIVE TEST DEVICES

Non-destructive testing of pavements, especially deflection testing, has been a vital part in evaluating the structural capacity of pavement. A detailed review of deflection measuring methods and analysis techniques to derive material property of the layered system can be seen elsewhere (33).

The Benkelman Beam, the LaCroix Deflectograph, and the Curviameter apply static or slow moving loads. Vibratory loads are applied by the Dynaflect, the Road Rater, the Corps of Engineers 16-kip (71-kN) Vibrator and the Federal Highway Administration's Cox Van. Geogauge is a portable device which again employs a vibratory load. Near field impulse loads are applied by the Dynatest, KUAB and Phoenix falling weight deflectometers. Small-scale impulse test devices include Loadman (34), German Dynamic Plate Bearing Test (GDP) (35), TRL Foundation Tester (TFT) (36) and Prima 100 (37). "Far field" impulse loads are again applied by the impact devices whose primary use is in Spectral Analysis of surface wave technique. Wave propagation is used by the Shell Vibrator, which loads the pavement harmonically and sets up standing surface waves, the peaks and nodes of which are found by using moveable sensors.

2.5.1 Non-destructive Impulse Test Devices for Stiffness Modulus

For a description of principal impulse test devices and others, including Geogauge and Dynamic Cone Penetration Test, the reader may consult references 15, 16 and 38. Impulse test devices described here include the Falling Weight Deflectometer (trailer mounted), and dynamic plate test devices such as GDP, TFT and Prima 100. All those devices mimic the moving vehicle

loading by measuring the response of a transient load pulse of 20 to 40 milliseconds and the load applied through a bearing plate of diameter between 300mm or 450mm at a contact stress of about 100 kPa to 200 kPa. Flexibility in the loading is facilitated in the FWD and Prima 100. The portable devices measure deflection via a central geophone (or accelerometer) except the Prima 100, which has an option to accommodate two more geophones. Table 2.3 presents pertinent features for easy comparison. Whereas a detailed description of all of the devices can be seen in reference 15, FWD and Prima 100 employed in this investigation will be summarized for ready reference:

2.5.1.1 Falling Weight Deflectometer (FWD): FWD has been a favored pavement evaluation device over the last 25 years. It is trailer-mounted and comprises a weight that is raised and dropped mechanically onto the 300 mm diameter steel bearing plate via a set of rubber buffers by in-vehicle computer control. The drop height, weight and plate size can be varied to

Table 2.3 Test Device Specification (Adapted from reference 14)

		Mass			Deflection Transducer		
Device	**Plate Diameter (mm)**	**Falling Weight (kg)**	**Bearing Plate (kg)**	**Total Load Pulse (ms)**	**Type**	**On Plate or On Ground**	**Stress Range[a] (kPa)**
GDP	300	10	17	18 ± 2	Accelerometer	Plate	100
TFT	300, 200	10	20	15-25	Velocity	Ground	<20
Prima	300, 200, 100	10, 20	16	15-20	Velocity	Ground	<200
FWD	300, 450	Adjustable	150[b]	30-40	Velocity	Ground	>100
SSG	114	10 kg (total weight		Pulse frequency 100 Hz to 196 Hz		Plate	<1

[a] With 300 mm diameter plate

[b] Estimate

[c] Applies a low amplitude vibration to the ground

obtain the required contact pressure, over a large range. The load pulse duration is 25 to 40 milliseconds dependent on the material under test. The applied stress and surface deflections, from up to seven radially spaced velocity transducers, are recorded automatically and can be backanalyzed to infer individual layer stiffnesses. However, for testing unbound materials it is customary to utilize only the central sensor and determine a 'composite foundation moduli. The central velocity transducer bears onto the ground through a hole in the bearing plate. In a recent study (11), both the central sensor and the third, fourth and fifth offset sensors were employed in characterizing subgrade soil. The FWD is a relatively heavy device, however, resulting in a relatively large preload to the material under test.

2.5.1.2 Prima 100: The Prima 100 is a device that has been relatively recently developed and marketed by Carl Bro Pavement Consultants (37). It weighs 26 kg in total and has a 10 kg falling mass that impacts the bearing plate via two, three or four rubber buffers to produce a load pulse of 15-25 milliseconds. It has a load range of 1-15 kN, i.e. up to 200 kPa with its 300 mm diameter bearing plate. It measures both force and deflection, utilizing a velocity transducer (maximum deflection of 2.2 mm). The velocity transducer measures the deflection of the ground through a hole in the plate. Up to two extra geophones can be deployed to provide a simple deflection bowl. The device requires a portable computer for data output and analysis, the proprietary software being provided with the device. It is a relatively new device, therefore, only few published data relating to its efficacy is available to date (13, 14, 15, 16).

2.6 RELATION BETWEEN RESILIENT MODULUS (M_R) AND IN-SITU STIFFNESS MODULUS (E)

This section reviews the relation between resilient modulus, M_R, and in-situ moduli from FWD or Portable FWD. Whereas, M_R is the input in M-EPD procedure, there is strong impetus

in using in-situ modulus because of its relevance in estimating the subgrade support, and in turn, contributing to a realistic design.

2.6.1 Relation Between M_R and FWD Modulus, E_{back} or E

The results of comparison overwhelmingly suggest that the laboratory resilient modulus is less than that determined from backcalculation, E_{back}. The AASHTO Guide (39) asserted that laboratory modulus is only a third of that determined from in-situ deflection of pavements. Other researchers, for example, Daleiden (40), Akram (41) and Nazarian (42) could not identify a unique relationship between moduli from laboratory and field tests. Having failed to establish a meaningful relationship between laboratory and backcalculated moduli, Von Quintus and Killingsworth (43) recommended correction factors (see Table 2.4) to be used with the AASHTO Design Guide. Based on the comparison study performed in regard to the WESTRACK road test, Seed et al. (12) asserted that their findings support the consensus that laboratory and NDT-based backcalculated moduli do not agree.

Whereas all of the above investigations relied on FWD measurements on pavement surface, only a few investigations had conducted the FWD test directly on the subgrade surface. In their study of the Minnesota Research Road Project (Mn/ROAD), difficulties were encountered in analyzing FWD measurements performed directly on a subgrade surface (44). Their results showed weak correlation between laboratory and backcalculated moduli. Yet another attempt to estimate resilient modulus via subgrade deflection testing and Boussinesq equation was made in the Virginia Test Road (45). Subgrade composite modulus, herein after referred to as elastic modulus, was calculated employing Equation 2.4.

$$E = \frac{S(1-\upsilon^2)\sigma_p a}{d_p} \tag{2.4}$$

Table 2.4 AASHTO Modulus Correction Values From Long-term Pavement Performance Sections (42). (Backcalculated value shall be multiplied by correction factor to get resilient modulus)

Layer Type and Location	C-Value, Correction Factor
Granular base/subbase under PCC	1.32
Granular base/subbase under AC	0.62
Granular base/subbase between stabilized layer and AC	1.43
Subgrade soils under stabilized subgrade	1.32
Subgrade under full-depth AC or PCC	0.52
Subgrade under granular base/subbase	0.35

Note: PCC, Portland cement concrete; AC, asphalt concrete

where: E = composite modulus/elastic modulus;

S = stress distribution factor, assumed 2.0;

σ_p = (peak) pressure of FWD impact load under loading plate;

a = radius of FWD loading plate

d_p = (peak) center FWD deflection; and

υ = Poisson's ratio

The one-to-one relation between elastic modulus and resilient modulus, turned out to be weak.

In a recent study completed for MDOT, twelve finished subgrades were tested for deflection employing FWD (21). As the subgrade exhibited three layers, indicated by the Dynamic Cone Penetrometer (DCP), modulus of those layers were backcalculated using MODULUS 5.0. Shelby tube samples from the twelve sections were tested in accordance with TP-46, and the resulting M_R showed satisfactory relation with the backcalculated value E_{back} (10). However, E_{back} of the same sections increased, 40 and 100 percent for fine- and coarse-

grained soil, respectively, upon completion of pavement construction and deflection measurements conducted on top of the pavement.

2.6.2 Relation Between M_R and E_{FWD} or E_{PFWD}: A Critique

In comparing laboratory M_R and in-situ modulus, for example, back-figured from deflection measurements, it is important to recognize spatial variability as well as variability in the vertical direction. No doubt, spatial variability would have strong influence on in-situ modulus, as the test encompasses a relatively large volume of material, and, therefore, a large variation. What follows is a discussion of important factors that could result in the two moduli–laboratory M_R and in-situ modulus–being different, nonetheless, portraying the basic stiffness characteristics of the material being tested.

Besides variability in the prepared subgrade, there are fundamental differences in the procedural aspects of the two test methods, yielding different moduli at a given location. Possible causes of difference in the moduli are briefly explained herein. First, different volumes of material are tested in the laboratory and in the field. Accordingly, the size effect phenomenon should result in the laboratory modulus being larger than the field modulus, provided the material tested is "homogeneous". Second, the confinement in AASHTO T-307 protocol is generated by compressed air, whereas in the field it is self-induced passive earth pressure. Air medium is compressible and, therefore, the laboratory sample is susceptible to relatively large lateral, and in turn, increased axial deformation. Clearly, the increased deformation in the laboratory sample results in smaller resilient modulus as compared to backcalculated field values. While these two factors are recognized as influencing the resilient modulus, their quantification is somewhat obscure at this time. It could be that the effects of those factors offset each other while averaging the results for some length of a subgrade.

While testing material compacted in the field (employing either static or vibratory rollers), residual stress becomes an issue. It has been documented that vertical compaction – especially under a roller compactor – causes lateral stress to increase with only partial recovery when the roller "walks out". The stress remaining, otherwise known as residual stress, has a profound effect on the deflection tests in-situ, whereas it has minimal effect on reconstituted samples recommended in T-307 protocol. Residual stresses are partially removed when the sample is extruded from the mold, an explanation for residual stress being not significant in T-307 samples. That the residual stress, relevant in material in-situ, could cause the resulting modulus to be larger than that obtained from reconstituted sample in which residual stress is practically nonexistent.

The stress-dependent nonlinearity of subgrade soil is yet another factor that influences a realistic comparison of the two sets of values. The laboratory sample being of finite size, the stress state is practically uniform for induced triaxial stress state. Besides, in the laboratory test only resilient deformation is measured and used in resilient modulus calculation. Whereas in FWD test the stress distribution is uniform neither in the vertical nor in the horizontal direction. More important, total deflections are monitored in contrast to the resilient deformation in the FWD test. The effect of nonlinearity, therefore, is likely to bring about a decrease in FWD modulus, in relation to AASHTO T-307 resilient modulus.

Another important factor is the dynamic effect of FWD loading. For example, the deflection of the bearing plate is out of phase (in time) with the maximum applied contact stress, and this phase difference becomes exaggerated for the largest bearing plate inertia and stiffest damper. Also, with the dynamic test (for example, FWD), stress in the material under testing extends to proportionally a larger depth, i.e. produces a more elongated pressure bulb. What it

amounts to is that the use of conventional static load theory for interpretation of dynamic deflection is inconsistent and will tend to underestimate the actual stiffness modulus (46).

With several factors influencing laboratory and in-situ moduli in a rather complicated manner, it is unlikely that they exhibit a one-to-one relation. More on this will be presented in Chapter 4, while discussing the test results.

2.6.3 Relation Between M_R and Portable FWD Modulus, E_{PFWD}

Hardly any published work has been identified relating M_R and E_{PFWD}, whereas several studies dealt with correlating E_{FWD} with a variety of portable drop weight devices (14, 15, 16, 38). Several coarse grained and fine grained soils were tested in test pits and in the field and samples collected from those sites were subjected to repeated load triaxial tests as well (16). Regression analysis of the data resulted in the following two equations, respectively, for coarse grained and fine grained soils:

$$M_R = 101.5 \frac{(E_{PFWD})0.25}{w} \tag{2.5}$$

$R^2 = 0.80$, Standard Error = 16.8

$$M_R = 101\frac{(E_{PFWD})^{0.21}}{w} + 2.53\gamma_d \tag{2.6}$$

$R^2 = 0.6$, Standard Error = 8.9

where: E_{PFWD} = measured PFWD modulus, MPa;

w = measured water content, percent; and

γ_d = measured dry density (unit weight), kN/m^3

A cursory examination of the models reveals that density variable plays a significant role in predicting M_R, whereas E_{PFWD} is the least significant explanatory variable. That M_R is marginally influenced by in-situ modulus, E_{PFWD}, is somewhat inconsistent, to say the least.

2.6.4 Relation Between E_{FWD} and E_{PFWD}

One of the earlier studies (14) presented data on comparative performance of several portable devices with respect to the FWD. This field data shows significant scatter and site-specific correlation. Three portable devices included in the study were German Dynamic Plate Bearing Test (GDP), TRL Foundation Tester (TFT) and Prima 100. Their results showed that E_{FWD} correlated best with Prima 100 moduli, as described in Equation 2.7.

$$E_{FWD} = 1.031\ E_{LFWD} \qquad (2.7)$$

$$R^2 = 0.60$$

Van Gurp et al. (46) determined that the Prima 100 elastic moduli are about 0.65 to 1.60 times the conventional FWD elastic moduli. This investigation took place on various base materials including stabilized soils, furnace slag, crushed rubble and sand.

Investigations that are more recent produced similar correlations. In a combined study performed by the USDA Forest Service, the U.S. Army ERDC Cold Regions Laboratory, New Hampshire DOT, and the University of Maine on low volume roads (including unsurfaced and thin asphalt pavements) produced a correlation coefficient (R^2) of approximately 0.7 for the Prima 100 LFWD to the standard FWD (47). Nazzal (38) obtained better results. He suggested the model to predict the FWD backcalculated elastic moduli, E_{FWD}, from the LFWD modulus, E_{PFWD}, as follows:

$$E_{FWD} = 0.97\ (E_{PFWD}) \quad \text{for } 12.5 \text{ MPa} < E_{PFWD} < 865 \text{ MPa} \qquad (2.8)$$

$$R^2 = 0.94$$

A number of factors influence the measured moduli from the PFWD (46). Various plate diameters, deflection sensor configurations, equipment weights, load pulse, and conversion equations from deflection to modulus lead to variation among researchers. Fleming (14) also

reported similar problems leading to variation in measured moduli stressing effects of variations in applied stress on the material behavior.

2.6.5 Relation Between In-situ Resilient Modulus and In-situ FWD Modulus

In-situ resilient modulus is (defined) derived by modifying the laboratory resilient modulus to stress state that exists in a real pavement. Groenendiji (48) proposed the following procedure for calculating the in-situ resilient modulus. Inputting the laboratory moduli in an appropriate nonlinear analysis program, deflection of a typical pavement structure was calculated. From these deflections a "calculated" or "predicted" surface moduli was determined which was then compared to the surface moduli determined in-situ by forward calculation (E_{PFWD}). The agreement between the calculated and in-situ stiffness moduli for a few portable devices was good. According to the researchers the good fit could be attributed to the calculation procedure capable of taking into account the stress dependency of the materials.

2.7 CHAPTER SUMMARY

With the resilient modulus of subgrade retained as the characterizing input in the M-EPDG, the pavement community is exploring in-situ methods of determining this parameter. In attempting to quantify seasonal variations of resilient modulus, a simple relation has been proposed in NCHRP Project 1-37A (23). That this relation totally depends upon moisture and density of the soil reinforces the need to rely on in-situ measurements rather than laboratory test results. Driven by mobility considerations and low cost, several portable devices have been introduced recently for in-situ tests. A review of various portable devices led to the conclusion that Prima 100 has the potential to be a viable device for in-situ characterization, judged by its being able to mimic the results of conventional FWD. For a comparison between devices the

conventional FWD has been adopted as a suitable benchmark for validation of current portable devices.

CHAPTER 3

EXPERIMENTAL WORK – FIELD AND LABORTORY

3.1 OVERVIEW

With the primary objective of determining in-situ modulus of finished subgrade employing the Prima 100, and relating this modulus to the laboratory resilient modulus, a field test program was planned. Thirteen test sections, 200 ft (61 m) in length – whose soil properties reflect typical soil types in Mississippi – were selected. Table 3.1 presents a summary of the location, test dates and various field tests performed at five stations on each test section. At each station, FWD test, with the light load package on 12-in. (300-mm) plate was first conducted followed by the Prima 100 test. Unit weight and moisture in the field were determined to assess the physical state of the in-situ material. From each station in a test section, except for the middle one, bag samples were collected for laboratory studies, including classification tests, and resilient modulus test.

3.2 FIELD TESTS

3.2.1 FWD Test on Prepared Subgrade and Modulus Calculation

Thirteen as-built test sections reflecting typical soil types throughout the State of Mississippi were selected and tested (see *Table 3.1*). The Mississippi Department of Transportation (MDOT) FWD was used for the deflection testing. As per experiment design, FWD modulus (E_{FWD}) was intended to establish a benchmark stiffness of the material tested, in order to authenticate the PRIMA 100 modulus.

In cases where the test station was unsuitable for testing due to loose surface material, wheel ruts, or other reasons, the surface was leveled to eliminate as far as possible erratic sensor deflections. Some sections were bladed and re-compacted before FWD testing to ensure surface

Table 3.1 Summary of Section Locations and Tests Performed

Section No.	County/Highway	Date Tested	Section Length (ft)	Tests Performed
2	Jeff. Davis / US 84	06/13/2005	200	FWD[a], Prima 100, Nuclear moisture & unit weight
3	Covington / US 84	06/13/2005	200	FWD[a], Prima 100, Nuclear moisture & unit weight
4	Covington / US 84	06/13/2005	200	FWD[a], Prima 100, Nuclear moisture & unit weight
5	Covington / US 84	06/13/2005	200	FWD[a], Prima 100, Nuclear moisture & unit weight
6	Desoto / MS 304	06/07/2005	200	FWD[a], Prima 100, Nuclear moisture & unit weight
7	Desoto / MS 304	06/07/2005	200	Prima 100, Nuclear moisture & unit weight
8	Desoto / MS 304	06/07/2005	200	Prima 100, Nuclear moisture & unit weight
9	Desoto / MS 304	06/22/2005	200	FWD[a], Prima 100, Nuclear moisture & unit weight
10	Desoto / MS 304	06/22/2005	200	FWD[a], Prima 100, Nuclear moisture & unit weight
11	Desoto / MS 304	06/22/2005	200	FWD[a], Prima 100, Nuclear moisture & unit weight
12	Desoto / MS 304	06/22/2005	200	FWD[a], Prima 100, Nuclear moisture & unit weight
13	Desoto / SR 713	08/22/2005	200	Prima 100, Nuclear moisture & unit weight
14	Tunica / SR 713	08/22/2005	200	Prima 100, Nuclear moisture & unit weight

[a] Falling Weight Deflectometer
1 ft = 30.5 cm

smoothness. Nonetheless, debris and improper sensor seating resulted in a few sporadic deflection basins, and in turn, elastic modulus.

By necessity, sensor deflections with negative slopes were excluded from the analysis. These erroneous deflections might be due to unevenness of the soil surface attributable to either a soft layer or debris on the surface. It could also be due in part to spatial variation resulting in soft pockets along the road leading to punching of the bearing plate and/or the sensor tip. Abnormal deflections primarily caused by plate vibration and/or soft surface layer were critically reviewed prior to data analysis.

3.2.1.1 Modulus from FWD Deflection Data: Researchers in previous studies employed a backcalculation routine for deriving subgrade modulus from deflection data (10, 44). The Minnesota Test Road Program adopted EVERCALC, and Mississippi researchers used MODULUS 5.1. The need for resorting to backcalculation in the Mississippi study stemmed from the fact that the subgrades exhibited layering, as determined by Dynamic Cone Penetrometer tests. The layering observed was more due to moisture gradient and lack of confinement at the surface than due to material variation. Invariably, the top 6 to 12 in. (152 to 305 mm) of the material remained at a lower moisture content than the underlying material, resulting in two nominal layers. Even with two layers, backcalculation methodology, often posed problems of non-uniqueness, demanding several trial-and-error calculations, which turned out to be time-consuming. A simple forward calculation based on Boussinesq solution for a uniformly distributed load on the surface of an isotropic elastic space deemed satisfactory for this study. Realizing that Prima 100 employs only one deflection sensor at the center of the loaded area, only the first sensor deflection is extracted from the FWD test. The equation used for calculating elastic stiffness modulus, E, is presented in Eq. 2.4.

Making use of the first sensor deflection of each drop, (composite) elastic stiffness modulus (herein after referred to as elastic stiffness modulus) was calculated, repeating the calculation for repeat drops at each station, extending this to other stations in each section. Mean values and coefficient of variations of the two load drops are presented in Table 3.2. Owing to mechanical problems, sections 7, 8, 13 and 14 and part of section 6 could not be tested with FWD, though Prima 100 tests were conducted on all of the 13 sections. Note that load in the FWD could not be precisely controlled, especially in sections 9, 10, 11 and 12.

3.2.2 Measuring In-Situ Modulus Employing PRIMA 100

3.2.2.1 Description and Operation of Prima 100: Prima 100 is a portable FWD (PFWD) device. Employing this device, the elastic stiffness modulus of the subgrade soil foundation is estimated from the measurement of the surface deflection due to impact loading applied to the subgrade. Figure 3.1 illustrates the Prima 100 device. The device has been commercialized with a software

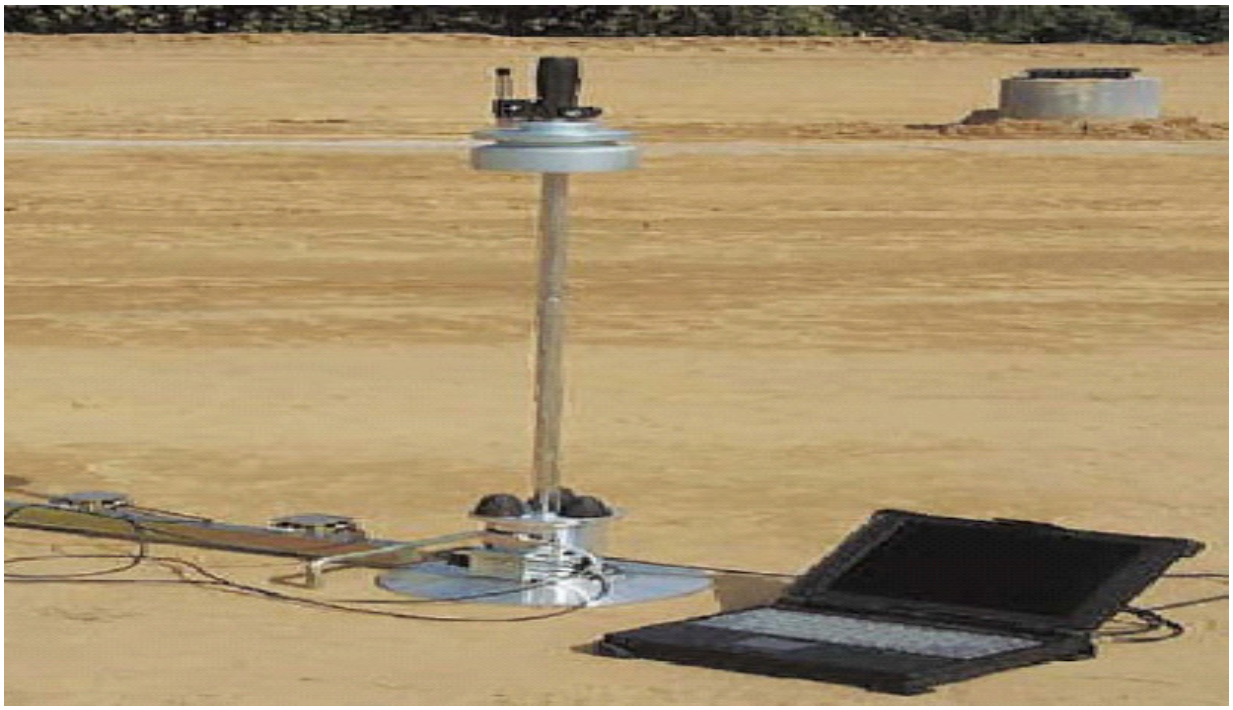

Figure 3.1 Prima 100, Portable Falling Weight Deflectometer (PFWD), with Laptop Computer

Table 3.2 Falling Weight Deflectometer and Portable Falling Weight Deflectometer Test Results

Section No.	Station No.	FWD			PFWD			FWD			PFWD		
		Average Load (lbs)	Elastic Modulus (psi)		Average Load (lbs)	Elastic Modulus (psi)		Average Load (lbs)	Elastic Modulus (psi)		Average Load (lbs)	Elastic Modulus (psi)	
			Mean	CV		Mean	CV		Mean	CV		Mean	CV
2	1	1605	17750	3.3	1723	12810	1.0	2201	17060	3.3	2427	12820	3.1
	2		17650	1.5		14420	1.8		16740	3.6		12910	2.8
	3		23910	2.0		11060	0.6		21740	1.9		10190	1.3
	4		13740	2.4		10890	1.0		12300	3.4		10310	0.7
	5		11750	0.7		14150	1.5		10410	1.8		10980	1.5
3	1	1484	7530	1.8	1717	9860	0.8	2010	6900	1.5	2335	8620	1.5
	2		6360	2.5		17920	0.9		5990	1.6		14810	2.3
	3		8500	1.8		10670	2.0		7470	1.1		600	2.8
	4		5170	2.4		5810	1.2		4740	2.2		5550	2.1
	5		3920	0.6		2240	3.5		3200	1.1		3350	14.4
4	1	1617	32520	1.5	1734	39980	2.3	2133	30970	1.8	2423	33170	0.9
	2		47630	1.8		14930	0.9		46720	0.7		17960	3.4
	3		35490	1.4		16990	1.1		33700	2.2		16780	2.3
	4		14250	3.0		17060	2.1		12880	3.0		18100	1.6
	5		12610	3.0		17810	0.9		11510	4.5		16190	2.7
5	1	1689	33260	1.2	1745	20920	2.7	2285	31910	0.2	2493	21960	0.0
	2		45270	0.5		22230	2.2		40620	0.5		21910	1.5
	3		40770	3.1		23994	2.3		41070	2.5		23920	1.9
	4		25120	3.0		16240	1.9		24320	1.0		15780	0.5
	5		31630	0.2		48250	0.9		31190	1.6		42530	0.4

(Continued next page)

1 psi = 6.89 kPa

1 lb = 4.448 kN

Table 3.2 (ctd) Falling Weight Deflectometer and Portable Falling Weight Deflectometer Test Results

Section No.	Station No.	FWD			PFWD			FWD			PFWD		
		Average Load (lbs)	Elastic Modulus (psi)		Average Load (lbs)	Elastic Modulus (psi)		Average Load (lbs)	Elastic Modulus (psi)		Average Load (lbs)	Elastic Modulus (psi)	
			Mean	CV		Mean	CV		Mean	CV		Mean	CV
6	1	2298	14760	1.1	1739	15170	2.3	2778	14680	2.2	2477	15710	0.4
	2		15160	0.4		14520	1.3		14290	1.3		14270	0.4
	3		NA[a]	NA		18200	1.1		NA	NA		16040	0.8
	4		NA	NA		15810	1.3		NA	NA		14910	0.3
	5		NA	NA		26060	1.4		NA	NA		23200	0.7
7	1	NA	NA	NA	1750	14840	1.0	NA	NA	NA	2442	13700	1.0
	2		NA	NA		17240	0.7		NA	NA		15300	0.7
	3		NA	NA		13040	0.0		NA	NA		12460	3.1
	4		NA	NA		11600	2.0		NA	NA		10930	1.9
	5		NA	NA		7770	0.8		NA	NA		7700	1.5
8	1	NA	NA	NA	1765	16110	1.6	NA	NA	NA	2475	16100	0.8
	2		NA	NA		16590	0.5		NA	NA		15920	1.5
	3		NA	NA		12010	1.4		NA	NA		12380	0.9
	4		NA	NA		17920	0.7		NA	NA		18340	1.1
	5		NA	NA		17750	0.6		NA	NA		17110	1.6
9	1	2001	13310	0.9	1713	12590	1.4	3086	13100	0.2	2455	12510	0.8
	2		17660	1.1		16110	0.7		17870	0.8		16000	0.7
	3		10710	1.1		11700	1.1		10660	1.4		11840	0.0
	4		8740	2.1		11520	1.2		8270	1.1		10250	1.1
	5		5710	2.7		7820	2.5		5500	2.5		7230	0.9

(Continued next page)

[a] Not Available

1 psi = 6.89 kPa

1 lb = 4.448 kN

Table 3.2 (ctd) Falling Weight Deflectometer and Portable Falling Weight Deflectometer Test Results

Section No.	Station No.	FWD			PFWD			FWD			PFWD		
		Average Load (lbs)	Elastic Modulus (psi)		Average Load (lbs)	Elastic Modulus (psi)		Average Load (lbs)	Elastic Modulus (psi)		Average Load (lbs)	Elastic Modulus (psi)	
			Mean	CV		Mean	CV		Mean	CV		Mean	CV
10	1	2125	18830	1.4	1719	20500	0.7	3358	18140	0.5	2496	20430	1.5
	2		24090	1.1		20770	1.3		25140	0.2		22170	0.6
	3		24220	1.0		23800	1.1		24260	0.6		24640	0.8
	4		45710	0.4		30740	1.0		43070	0.9		31540	1.0
	5		32270	1.1		28850	1.3		32170	0.7		29660	1.1
11	1	2078	20200	3.9	1710	23450	1.4	3237	20930	0.7	2478	24100	2.0
	2		25790	1.1		23140	1.0		24250	0.9		23890	0.8
	3		15380	0.8		24180	0.3		15840	0.6		25160	0.8
	4		28100	1.4		26100	1.7		27780	0.1		26600	1.5
	5		16310	1.0		24970	1.1		16970	0.4		25840	1.1
12	1	1901	11920	0.3	1736	12270	1.0	3013	10960	0.4	2460	11700	1.4
	2		13410	5.3		16680	0.7		12160	11.9		15840	1.4
	3		17010	0.4		12880	1.6		15900	0.2		13010	0.5
	4		12380	0.4		13560	0.0		10930	0.2		12890	1.5
	5		15440	1.1		13330	1.1		13960	0.6		12700	2.6
13	1	NA	NA[a]	NA	1735	22490	0.6	NA	NA	NA	2447	24260	1.0
	2		NA	NA		30240	1.0		NA	NA		30210	1.0
	3		NA	NA		23970	1.7		NA	NA		24170	2.9
	4		NA	NA		21720	0.6		NA	NA		22090	1.3
	5		NA	NA		24870	1.1		NA	NA		26010	1.8
14	1	NA	NA	NA	1731	21470	5.3	NA	NA	NA	2460	22260	2.9
	2		NA	NA		21980	0.7		NA	NA		24170	1.8

[a] Not Available
1 psi = 6.89 kPa
1 lb = 4.448 kN

program for data acquisition and interpretation from a laptop computer. Alternately, data may be transmitted to a hand-held computer (PDA) in conjunction with a Bluetooth device. The software, developed for a Microsoft Windows© environment, enables a user to choose the test setup, and visualize and save the test results. Displayed results include time histories and peak values of load and displacement, as well as calculated value of elastic stiffness modulus. Maximum applied stress and load pulse duration also are displayed. A sample data collection screen of Prima 100 software can be seen in Figure 3.2. Prima 100 User's Manual (49) may be consulted for details of operation, data collection, and sample data reduction.

Two options are available for data collection:

1. Prima 100 with RS232 cable connection in conjunction with a laptop computer.
2. Prima 100 with a Bluetooth, wireless HF connection and a hand-held computer (PDA).

Different data collection software is made available for each mode of operation. A majority of the project data collection was carried out employing the cable connection and laptop; however, toward the last phase of the project the wireless system became available, and was successfully used. Data analysis software, described in Chapter 5, for arriving at 'uniform' sections for design purposes, developed as a part of the project, has been fully integrated with the data collection software. The data collection software is described in reference 49.

In the current test program, a 12-inch (300-mm) diameter rigid plate (with center opening of 40 mm) is employed, though in calculations the presence of the center hole is disregarded. While employing a 10-kg sliding hammer, the height of fall is adjusted to result in ≃7.7 kN and≃10.9 kN forces, successively. The corresponding contact stresses underneath the bearing plate were about 16 psi (109 kPa) and 23 psi (158 kPa), respectively. The duration of the

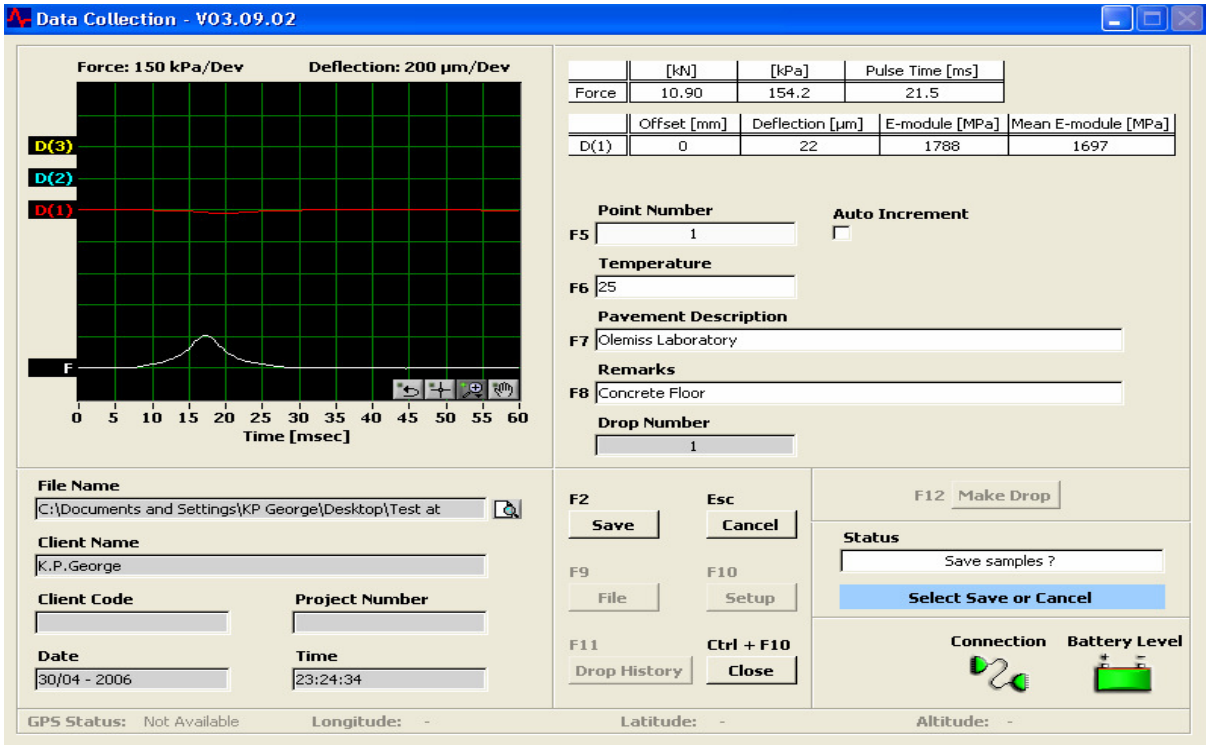

Figure 3.2 Data Collection Screen (49)

recorded force and deflection signals was set to 60 ms. As can be seen in Figure 3.3, the load pulse shape resembles a half-sine wave form. With only two relatively soft rubber buffers installed on top of the housing, the load pulse duration has been extended to 20-24 ms, in contrast to typically, 18 ms with regular four-buffer combination.

The peak values of load and deflection are employed in the software for calculating the elastic stiffness modulus, E. Elastic half-space solution, Equation 2.4.a, analogous to Equation 2.4 is embedded in the program where stress distribution factor, S, and Poisson's ratio, υ, are user defined.

$$E = \frac{S(1-\upsilon^2)\sigma_p a}{d_p} \qquad (2.4.a)$$

where: σ_p = peak force;

d_p = peak deflection; and

a = radius of the load plate

Poisson's ratio, a material property, though important in equation 2.4.a, it is seldom measured. Based on the literature (Huang, 50), and relying on the often recommended numbers, 0.35 and 0.4, respectively, were assigned to coarse- and fine-grained soils.

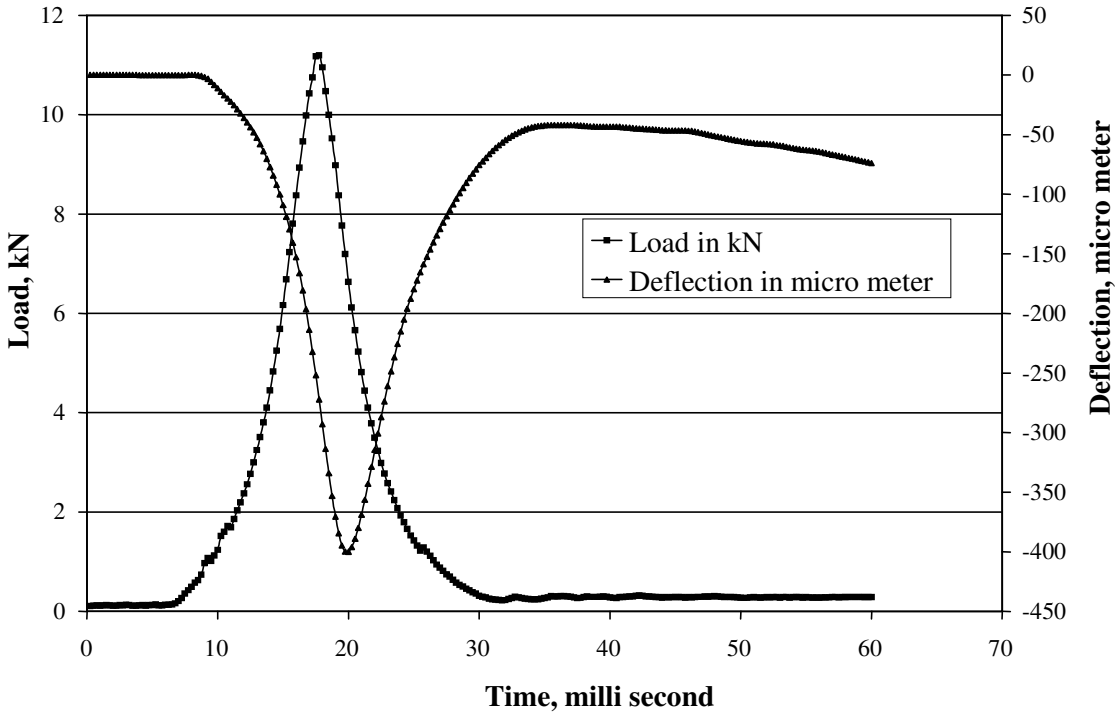

Figure 3.3 Load Pulse and Corresponding Deflection Bowls from Prima 100 Software, 1 lb = 4.448 kN, 1 in. = 2.54 cm

The two user inputs include stress distribution factor S and Poisson's ratio υ. The magnitude of S depends on the stress distribution under the loading plate which in turn depends on the relative rigidity of the plate to that of the medium being tested, in this case, subgrade soil. Under a perfectly rigid plate, the deflection is uniform over the plate area, and stress peaks around the perimeter of the plate. When testing with a perfectly flexible plate, however, deflections decrease from the center towards the edge of the plate, with uniform contact stress. Figure 3.4 compares the deflection bowls of those two plates, revealing the shape of the stress

distribution becoming irrelevant when deflection is measured at a radial distance of 80% of plate radius. According to Boussineq solution in S = π/2 for rigid plate and S = 2 for flexible plate for a uniform stress distribution. In practice the plate can be neither completely rigid nor

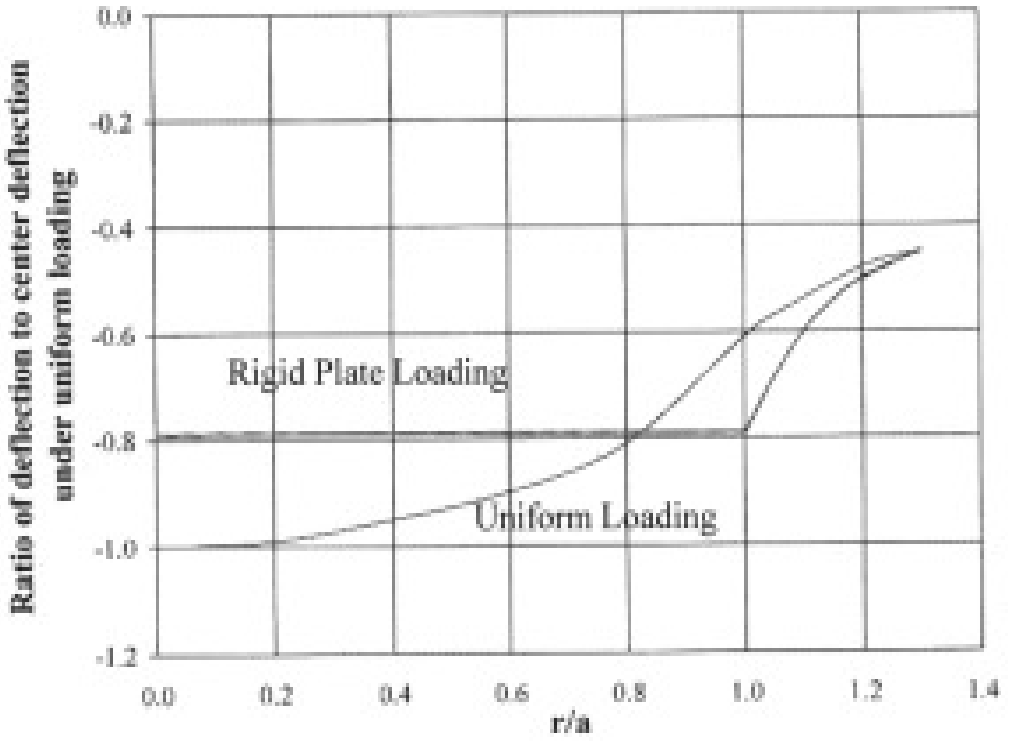

Figure 3.4 Effect of Plate Rigidity on Deflection, r = Radial Distance and a = Plate Radius (Adapted from Reference 48)

perfectly flexible, with rigidity something in between. Therefore, an average of the two extremes ($\pi/_2$+2)/$_2$ =1.79), rounded off to 1.8 would be a good approximation.

In addition, a material-related issue inherent in impulse tests is the apparent phase lag of peak deflection in relation to the peak force (see Figure 3.3). The data interpretation method that is used for stiffness modulus employs peak values of force and displacement records (herein referred to as peak method) in lieu of their static counterparts. There is some suggestion to use peak load and corresponding deflection, however, this approach invariably results in a larger modulus than using the peak method. Neither of these methodologies provides the 'actual'

modulus, because the inertia effects and dynamic load effects are not adequately addressed. One method to improve this modulus calculation is to employ the entire load deflection time history instead of the peak load and peak deflection. A brief description of this approach is discussed in the next section.

3.2.2.2 Spectral Analysis of Time History of Load and Deflection: One method of tapping the additional information of the history data file is to perform Fast Fourier Transform (FFT) on the force-time impulse and on deflection-time response. If the transform of the deflection signal is divided, frequency by frequency, by the transform of the load impulse, the result is a transfer function, which is a complex number and a function of frequency. The compliance, that is, deflection per unit force, can be extracted from this transfer function for any given frequency.

A recent study (Hoffman et al., 51) extracted modulus from an analysis of the complete time history of deflection and load, employing a footing-on-a-half-space model. They concluded that the peak method tends to overestimate the stiffness associated with very soft soils and to underestimate the stiffness in soft to stiff soils. Those results have not been substantiated so far with field testing in conjunction with spectral analysis. In view of the complexity of the procedure and lack of substantive results to promote spectral analysis, a decision has been made to employ the peak method in equation 2.4.a, which is the recommended method in the Prima 100 software.

How to mitigate the problems arising from using dynamic response in a static equation (such as Eq. 2.4.a), thereby improving the peak method? The peak method was shown to be strongly and non-linearly dependent on the duration of the force pulse duration, stiffness of the material tested, and the stiffness of buffer, among others (51). Recognizing those factors, we have selected very soft buffers, and also limited the number to two instead of the typical four-

buffer configuration. Resulting force pulse duration lies in the range of 20 to 24 milliseconds. Yet another factor that could improve the results of peak method is the use of a large loading plate. Note that a 300-mm bearing plate was employed throughout the study.

3.2.2.3 Prima 100 Modulus Data: The field test program called for Prima 100 tests at the same five locations immediately following the FWD tests. Followed by two seating drops, four to six drops of each load (7.7 kN and 10.9 kN) were applied, and the elastic stiffness modulus of each station was checked for outliers, employing Chaunaut's criterion (52). Reported in Table 3.2 (columns 6 and 11) are the mean and coefficient of variation (CV) of the modulus at each station for the two loads, namely, 7.7 kN and 10.9 kN. Range of CV observed is relatively small, 0% to 3.5%. Figure 3.5 depicts the variation of the CV of each station with its corresponding average E_{PFWD} stiffness moduli. The general trend is that the CV value decreases with the increase in stiffness moduli.

3.2.2.4 Factors Affecting PRIMA 100 Tests: The factors affecting the modulus measurements could be listed under two categories: 1) Fundamental aspects of the equipment, and 2) Operational problems/drawbacks. The factors that can be grouped under the first category include (a) the use of static elastic equation (Boussinesq) for analyzing dynamic test results, (b) effect of the mass of the assembly, (c) effect of drop weight (d) rubber buffer stiffness, and (e) phase lag between the load and deflection time-histories.

The use of Eq. 2.4.a and its implications in regard to stress distribution factor and Poisson's ratio were discussed in section 3.2.2.1. Stress distribution factor is dependent on the relative rigidity of the plate and no rational procedure exists to assign an appropriate value. Its selection is in the most part subjective, to say the least.

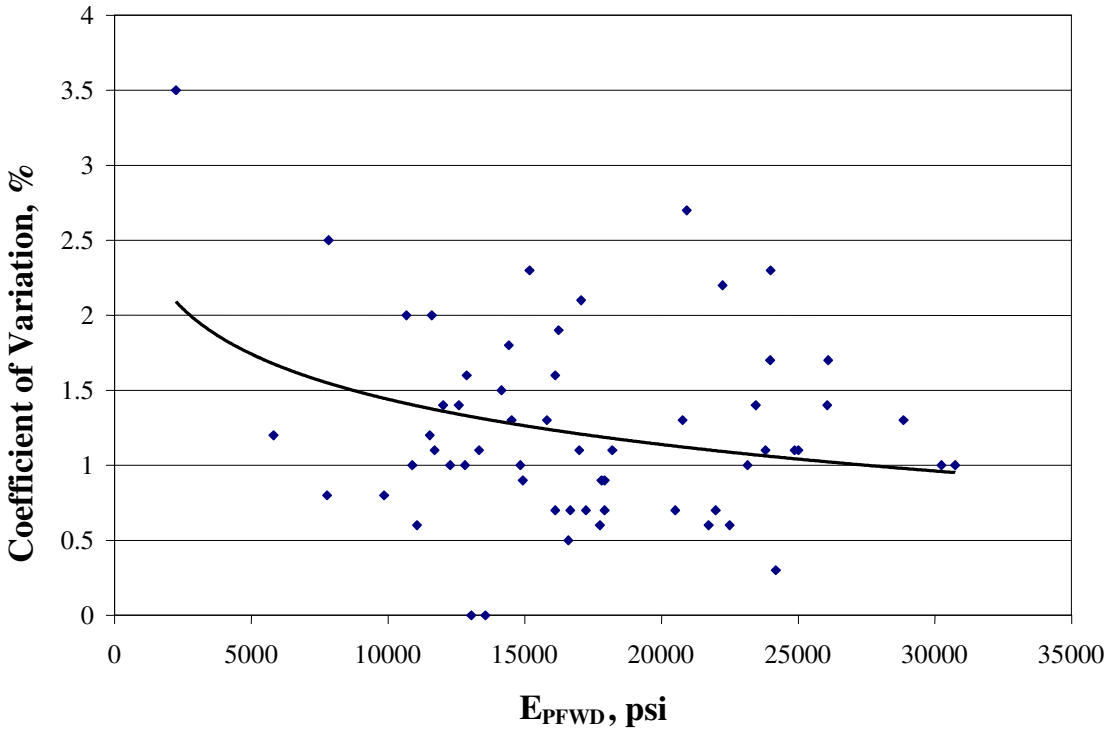

Figure 3.5 Repeatability of Prima 100 Modulus (E_{PFWD}) Test, 1 psi = 6.89 kPa

The effect of increasing the mass of the assembly (bearing plate, the housing and guide rod) has been found to reduce the inferred peak deflection owing primarily to increased resistance to motion. The increase in the bearing plate mass resulted in a decrease in recorded soil pressure, decrease in peak deflection with no substantial change in the load pulse duration (14).

Adjusting the rubber buffer stiffness has the effect of increasing the inertia; the stiffer the damper the more significant the phase difference between the peak load and the peak deflection. A reduction in buffer stiffness not only reduces the phase difference but it increases the duration of the load pulse as well. Two soft buffers were used in this study, resulting in a load pulse duration of 20-24 milliseconds.

The operational problems/drawbacks include the following: (a) problem arising from the guide rod being not plumb, (b) slipping or lateral displacement of the bearing plate upon

dropping the load, and (c) punching of the ground especially in soft ground. If the guide rod is out of plumb, the falling mass is likely to rub against the rod, resulting in an eccentric force. An amateur operator is encouraged to run through a repeatability study before undertaking a full-scale field test.

With no rubber pad provided at the contact face of the bearing plate, it tends to slip laterally, especially on stiff subgrade surface often resulting in spurious results. This problem is exacerbated should the road surface is sloping. The use of Prima on surface with slopes exceeding 10% is discouraged by the equipment supplier. Choosing another spot close by may be a solution to circumvent this problem. Out of the total 62 stations that were tested in this project, location shifting was necessary in less than 10% of the stations.

3.2.3 In-Place Density and Moisture

Since the modulus, or any strength parameter for that matter, is dependent on density and moisture of the material, they were determined in-place. Note that those attributes generally exhibit significant spatial variation. At each station, where the FWD test was performed, density (moist density, and in turn, dry density) and moisture content were determined by nuclear gauge. An 8-inch (20-mm) probe was employed estimating density and moisture, and they are tabulated in Table 3.3, comparing them with the optimum moisture and corresponding density of bag samples. The moisture content reported in column 4 is the average of nuclear moisture and the moisture of bag sample determined by gravimetric method. It should be worth mentioning that the nuclear moisture was consistently lower than that of the bag sample, the difference being an average of 2%.

Table 3.3 Soil Properties of Bag Samples and Comparison of Nuclear Dry Unit Weight and Moisture to Maximum Dry Unit Weight and Optimum Moisture

Section No.	Sample No.	Nuclear Test(field)		Tests on Bag Samples					Classification AASHTO / USCS	
				AASHTO T-99		Index Properties				
		Dry Unit Weight (pcf)	Mois-ture (%)	Max. Dry Unit Weight (pcf)	Optimum Moisture (%)	P_{200} (%)	LL (%)	PI (%)	Bag Sample Data	As per MDOT Soil Profile Data
2	2-(1,2)	106.8	12.6	116.3	13.9	47	34	20	A-6(5)/SC	A-7(16)/CL
	2-(4)	107.5	13.7	117.6	13.1	63	32	19	A-6(6)/CL	A-7(16)/CL
	2-(5)	106.3	14.4	117.6	13.6	46	30	16	A-6(4)/CL	A-7(16)/CL
3	3-(1,2)	109.4	10.2	120.9	11.3	48	19	8	A-4(1)/SC	A-6(12)/CL
	3-(3)	107.4	10.8	116.9	12.9	67	24	14	A-6(6)/CL	A-6(12)/CL
	3-(4)	110.1	10.4	123.3	10.8	44	18	6	A-4(0)SMd	A-6(12)/CL
	3-(5)	104.9	17.6	120.7	11.7	49	20	9	A-4(1)/SC	A-6(12)/CL
4	4-(1)	117.4	10.9	121.8	11.7	48	22	11	A-6(2)/SC	A-2-4(0)/SMd
	4-(2)	111.3	10.4	123.3	10.4	35	20	8	A-2-4(0)/SC	A-2-4(0)/SMd
	4-(4,5)	114.0	8.8	123.0	10.7	25	21	7	A-2-4(0)SM	A-2-4(0)/SMd
5	5-(1,2)	109.1	11.4	116.5	13.0	78	26	11	A-6(6)/CL	A-4(0)/CL
	5-(4)	111.2	9.3	121.0	10.6	66	17	2	A-4(0)/CL	A-4(0)/CL
	5-(5)	111.3	11.5	118.0	12.6	76	28	14	A-6(8)/CL	A-6-5/CL
6	6-(1)	104.9	14.6	112.5	16.1	83	31	15	A-6(11)/CL	A-4(3)/ML
	6-(2,4)	104.3	14.5	110.2	17.1	95	31	12	A-6(11)/CL	A-4(3)/ML
	6-(5)	103.9	15.4	108.3	16.0	98	34	14	A-6(14)/CL	A-4(3)/ML
7	7-(1)	104.2	13.3	110.7	15.4	98	31	11	A-6(11)/CL	A-4(1)/ML
	7-(2)	104.0	14.2	110.4	16.3	98	32	12	A-6(12)CL	A-4(1)/ML
	7-(4,5)	101.4	17.2	106.2	17.7	99	31	9	A-4(9)/CL	A-4(1)/ML
8	8-(1,2)	104.6	12.9	110.8	15.7	94	28	9	A-4(7)/CL	A-4(3)/ML
	8-(4,5)	104.6	14.4	111.7	15.2	94	30	12	A-6(10)/CL	A-4(3)/ML
9	9-(2)	100.3	16.6	107.5	15.8	88	29	9	A-4(8)/CL	A-4(1)/ML
	9-(4)	102.6	14.7	110.9	15.5	98	27	8	A-4(7)/CL	A-4(1)/ML

1 pcf = 0.157 kN/m^3

(Continued next page)

Table 3.3 (ctd) Soil Properties of Bag Samples and Comparison of Nuclear Dry Unit Weight and Moisture to Maximum Dry Unit Weight and Optimum Moisture

Section No.	Sample No.	Nuclear Test(field)		Tests on Bag Samples					Classification AASHTO / USCS	
				AASHTO T-99		Index Properties				
		Dry Unit Weight (pcf)	Mois-ture (%)	Max. Dry Unit Weight (pcf)	Optimum Moisture (%)	P_{200} (%)	LL (%)	PI (%)	Bag Sample Data	As per MDOT Soil Profile Data
10	10-(1)	107.4	8.7	117.9	12.6	67	25	13	A-6(6)/CL	A-2-4(0)/SMd
	10-(2,4)	112.1	7.0	120.1	12.1	49	20	10	A-4(1)/SC	A-2-4(0)/SMd
	10-(5)	115.0	7.2	121.4	11.7	53	23	12	A-6(3)/CL	A-2-4(0)/SMd
11	11-(1,2)	111.1	10.1	117.7	12.7	74	21	7	A-4(2)/ML-CL	A-4(5)/ML-CL
	11-(4,5)	108.3	8.7	117.2	13.0	76	26	12	A-6(7)/CL	A-4(5)/ML-CL
12	12-(1,2)	102.9	14.3	111.1	14.3	82	30	15	A-6(10)/CL	A-6(9)/CL
	12-(4,5)	100.1	14.2	110.3	15.8	92	32	15	A-6(13)/CL	A-6(9)/CL
13	13-(1)	114.9	6.9	118.0	13.3	30	22	0	A-2-4(0)/SMd	A-4(0)/SC
	13-(2)	114.7	8.3	116.9	13.0	55	20	9	A-4(2)/CL	A-4(0)/SC
	13-(5)	115.3	8.1	121.1	11.6	37	20	9	A-4(0)/SC	A-4(0)/SC
14	14-(4)	109.6	8.0	117.8	12.5	12	20	0	A-2-4(0)/SP-SM	A-4(0)/SMd
	14-(5)	111.7	8.5	118.9	12.0	28	20	4	A-2-4(0)/SMd	A-4(0)/SMd

1 pcf = 0.157 kN/m^3

3.2.4 Soil Sampling and Tests

Bag samples from each location (up to 18 inch depth) of each test section were collected using a power drill. After being air-dried, based on color, texture, field density, field moisture and E_{PFWD} trend, the samples of nearly identical properties were combined. The grouping process resulted in 35 soil samples (see Table 3.3) starting with 52 samples collected from the field. A battery of tests was conducted on those 35 samples, including:

1. Particle size analysis and Atterberg Limits for soil classification
2. Moisture density tests (Proctor, AASHTO T99-90)
3. Repeated load triaxial tests in accordance with test Protocol NCHRP 1-28A (AASHTO T-307).

3.2.4.1 Routine Laboratory Tests on Bag Samples: In order to classify the 35 soil samples, they were subjected to particle size analysis (AASHTO T88-90), Atterberg limits (AASHTO T89-90 and T90-87), and Standard Proctor test (AASHTO T99-90). Those tests and soil classifications were carried out in the MDOT Soils Laboratory. Table 3.3 lists the results of those tests for all of the 35 samples along with the soil classification (column 10). For comparison, the classification reported in the MDOT Project Profile Studies are entered in column 11 of the same table. A scrutiny of those results suggests significant spatial (natural) variation existing over a short distance as little as 50 ft (15m).

3.2.4.2 Resilient Modulus Tests on Reconstituted Samples: Resilient modulus test (Test Protocol AASHTO T-307), on reconstituted samples of 4 in. (102mm) diameter and 8 in. (204mm) tall specimens, were conducted in the Burns Cooley Dennis, Inc. Laboratory. A question arose early as to what density and moisture the reconstituted samples to be prepared? With due consideration to the MDOT specifications and in consultation with M-EPDG implementation

team, a decision was made to mold the test samples at 95% compaction (95% maximum density) and optimum moisture.

The testing machine, supplied by Interlaken Technology, is computer controlled with deformation in the samples recorded using three Linear Variable Differential Transducers (LVDTs) mounted inside the triaxial chamber. Deformation and applied load readings were digitally recorded, from which the deviator stresses and resilient strains were calculated. The average M_R values for the last five loading cycles of a 100-cycle sequence yielded the resilient modulus. Typical laboratory M_R test results of two fine-grained soils and two coarse-grained soils are presented in Appendix A. As expected, all of the soils, laboratory M_R decreases with increase in deviator stress, σ_d, as well as bulk stress, θ. In theory, for a given confining stress, M_R vs. σ_d and M_R vs. θ plots should demonstrate identical negative slope, as can be verified in the plots.

3.*2.4.3 Representative Resilient Modulus Form AASHTO T-307 Tests:* The T-307 test was performed over a range of cyclic stresses and confining pressures (16 stress combinations) to measure the nonlinear (stress-sensitive) elastic behavior of soils. Numerous relationships have been employed for describing the nonlinear behavior of subgrade soils; a summary of those models can be seen in reference 20. As recommended in the NCHRP M-EPDG (18), Equation 2.2 included in section 2.4 is adopted in this study. Equation 2.2 serves to model stress dependency of resilient modulus. The k_1 to k_3 coefficients are determined from the 16 modulus values resulted from each AASHTO T-307 test. Multiple regression analysis of the 16 sets of M_R and corresponding stress states for each sample resulted in k_1 to k_3. As expected, k_1 is positive. Constant k_2 also turned out to be positive, signifying stress hardening with increasing bulk stress. Stress softening is even more dominant, as indicated by a larger negative k_3

exponent. The regression constants k_1, k_2, and k_3 of all of the 42 samples (tested for resilient modulus) are listed in Table 3.4.

The question now arises as to what stress state should be used to calculate the representative resilient modulus for relating it to in-situ elastic stiffness moduli. Two load scenarios were considered: first, a stress state resulting from a typical 18-in. (457-mm) pavement overlying subgrade, in conjunction with a 9000-lb. (9-kN) wheel load at 100 psi (690 kPa) tire pressure and second, a 1730-lb. (7.7-kN) load on a 12-in (300-mm) plate on top of the subgrade. The stress states calculated at two depths for the 9000-lb load, employing KENLAYER, are tabulated in Table 3.5, so also the stress induced by PFWD load, 1730 lbs (7.7 kN). M_R of reconstituted samples at a stress state corresponding to the Prima 100 load (σ_1 = 10.2 psi (70 kPa), $\sigma_2 = \sigma_3$ =1.6 psi (10 kPa) were calculated and listed in column 8 of Table 3.4. Also calculated were a set of moduli corresponding to stress state (σ_1 = 8 psi; (55 kPa), $\sigma_2 = \sigma_3$ = 2 psi (14 kPa)), which are listed in column 9 of Table 3.4. As this stress state is the choice of AASHTO M-EPDG, it seems logical to employ them for estimating the representative resilient modulus, which in turn will be related to Prima 100 modulus.

3.3 CHAPTER SUMMARY

The data required to fulfill the objective of this study includes: 1) the Prima 100 elastic stiffness modulus, and 2) the resilient modulus on the same soil. The elastic modulus data was collected from in-situ tests on thirteen as-built subgrades. Side by side tests were conducted with conventional FWD and Prima 100 calculating a pair of moduli for each test station. In-situ density and moisture were determined employing a nuclear gauge, and bag samples were collected for resilient modulus tests and standard classification tests. AASHTO T-307 protocol was employed for repeated triaxial tests, and the test results were synthesized to derive a stress-

Table 3.4 Resilient Modulus Calculated at Different Stress States Employing Regression Constants k_1, k_2 and k_3 (see equation 2.2)

Section No.	Station No. (Sample No.)	Regression Constants from AASHTO T-307 Test					Resilient Modulus Calculated with σ_1[a]=10.2 psi, σ_2[a]=σ_3[a]=1.6 psi, (psi)	Resilient Modulus Calculated with σ_1=8 psi, σ_2=σ_3=2 psi, (psi)
		k_1	k_2	k_3	R^2	S_e/S_y		
2	2-(1,2)	2017.4	0.628	-2.683	0.971	0.169	14140	16100
		2054.3	0.544	-2.523	0.968	0.178	15100	17140
		2049.5	0.589	-2.641	0.973	0.163	14560	16600
	2-(5)	2094.6	0.540	-2.554	0.975	0.159	15280	17400
		2164.7	0.531	-2.105	0.992	0.091	17680	19510
		2039.1	0.521	-2.520	0.954	0.214	15030	17100
3	3-(3)	2272.9	0.448	-2.945	0.989	0.104	15170	17910
		2308.4	0.395	-3.045	0.982	0.133	15110	18050
		2518.8	0.364	-3.009	0.982	0.133	16680	19940
	3-(4)	2256.8	0.587	-3.010	0.974	0.161	14630	17120
		2022.3	0.664	-3.186	0.967	0.183	12460	14650
		2178.0	0.599	-3.132	0.973	0.166	13680	16130
4	4-(4,5)	1720.8	0.848	-2.071	0.982	0.133	13760	14700
		1921.4	0.790	-2.000	0.976	0.156	15720	16800
		1868.3	0.839	-2.090	0.979	0.145	14880	15930
5	5-(1,2)	2602.5	0.490	-2.236	0.980	0.142	20650	23090
		2630.4	0.453	-2.111	0.976	0.155	21610	24030
		2776.8	0.413	-2.042	0.978	0.148	23290	25880
	5-(4)	1979.6	0.914	-2.495	0.974	0.162	14150	15475
6	6-(2,4)	1386.1	0.777	-2.728	0.961	0.198	9470	10670
7	7-(1)	1426.4	0.647	-2.265	0.969	0.177	11070	12220
		1625.1	0.614	-2.236	0.968	0.179	12740	14080

(Continued next page)

[a] These stresses derived from a stress analysis with 1730 lbs load (see Table 3.5)

1 psi = 6.89 kPa

Table 3.4 (ctd) Resilient Modulus Calculated at Different Stress States Employing Regression Constants k_1, k_2 and k_3 (see equation 2.2)

Section No.	Station No. (Sample No.)	Regression Constants from AASHTO T-307 Test					Resilient Modulus Calculated with σ_1[a]=10.2 psi, σ_2[a]=σ_3[a]=1.6 psi, (psi)	Resilient Modulus Calculated with σ_1=8 psi, σ_2=σ_3=2 psi, (psi)
		k_1	k_2	k_3	R^2	S_e/S_y		
8	8-(1,2)	1460.2	0.601	-1.860	0.994	13570	12590	13570
		1324.8	0.693	-1.922	0.986	11960	11150	11960
9	9-(2)	1537.2	0.566	-1.883	0.961	14320	13220	14320
10	10-(1)	2476.4	0.541	-2.753	0.984	19850	17190	19850
11	11-(1,2)	1980.4	0.603	-1.891	0.981	18290	16940	18290
		2007.5	0.558	-1.873	0.973	18760	17320	18760
		2009.5	0.566	-1.868	0.981	18770	17350	18770
12	12-(4,5)	1632.7	0.580	-2.520	0.971	13540	11970	13540
		1784.7	0.546	-2.547	0.968	14820	13040	14820
13	13-(1)	2404.9	0.864	-2.706	0.962	18280	16390	18280
		2036.4	0.888	-2.553	0.964	15830	14380	15830
		2181.6	0.903	-2.572	0.962	16860	15310	16860
	13-(5)	2460.7	0.606	-2.348	0.970	20930	18780	20930
		2478.2	0.602	-2.259	0.984	21430	19350	21430
		2144.7	0.646	-2.050	0.987	19100	17560	19100
14	14-(4)	1788.2	0.795	-1.815	0.976	16140	15310	16140
		1738.0	0.787	-1.780	0.970	15810	15020	15810
		1745.7	0.808	-1.818	0.971	15710	14920	15710
	14-(5)	2009.3	0.684	-1.947	0.975	18090	16820	18090
		1869.9	0.713	-1.863	0.982	17000	15940	17000

[a] These stresses derived from a stress analysis with 1730 lbs load (see Table 3.5)

1 psi = 6.89 kPa

Table 3.5 Calculated Stress State in Subgrade under Different Loads Including Overburden

Load Description	Stress		
	Location	σ_1 (psi)	$\sigma_2=\sigma_3$ (psi)
9000-lb wheel load over 18- in. pavement	6 in. below subgrade surface	4.3	1
	18 in. below subgrade surface	4	1.3
1730-lb load on 12- in. PFWD plate	6 in. below subgrade surface	10.2	1.6

1 lb = 4.448 kN
1 in. = 2.54 cm
1 psi = 6.89 kPa

dependent equation for M_R, calculated from which were: 1) M_R corresponding to the Prima 100 stress state, and 2) M_R corresponding to σ_1 = 8 psi and $\sigma_2 = \sigma_3$ = 2 psi. A detailed discussion of the results and correlation analysis will be the topic of the next chapter.

CHAPTER 4

ANALYSIS AND DISCUSSION OF RESULTS

4.1 INTRODUCTION

With in-situ stiffness elastic modulus from Prima 100, and resilient modulus determined employing AASHTO T-307 Protocol, a relation will be sought between the two. The credibility of Prima 100 modulus is authenticated by establishing an acceptable relation between Prima modulus (E_{PFWD}) and FWD modulus (E_{FWD}). Selection of independent variables and the methodology employed to arrive at a model form and the development of the model itself comprise a major part of this chapter. Typically, only a year or more after the grading contract is completed, Prima 100 test would be conducted at the time when the subgrade may have undergone seasonal changes in moisture and attendant density. To what extent those changes affect Prima modulus will also be discussed.

4.2 PRIMA 100 TEST RESULTS

4.2.1 Unreliable E_{PFWD} Measurements Owing to Uneven Surface

The field test program was comprised of 14 test sections. Test section #1 was supposed to be an A-2-4 (0) soil; it consisted of relatively large amount of gravel retained on #4 sieve, however. And, having undergone a prolonged drought in May 2005, the surface remained extremely hard and uneven. Primarily because of the seating problem, the Prima modulus measurements were excessively large, failing to fit the overall trend of the remaining 13 sections. Accordingly, a decision was made to delete section #1 from the database of this study.

4.2.2 Outliers of Prima Modulus, E_{PFWD}

Section #14 was selected to increase the presence of coarse-grained soil in the project database and also to substitute for section #1 which was initially classified as an A-2-4 soil. The

timing of the test was such that the final grading was not completed throughout the length as we arrived for the field tests. For some unknown reason, the Prima modulus of the first three stations was unreasonably large compared to the measurements on nominally similar soils on the same road. Test results of the last two stations, by virtue of its reasonably good comparison to the overall test results were, however, included in the analysis. As alluded to before, the conventional FWD results on section #14 were not available for verification of the Prima modulus, therefore, the measurements at the first three stations of section #14 were deleted, leaving 62 data points for further analysis.

4.3 PRIMA MODULUS RELATED TO FWD MODULUS

The comparison between E_{PFWD} and E_{FWD} is appropriate because both devices operate basically on the same principle, with provision to adjust the contact stress as desired. And, since E_{FWD} is generally considered acceptable for in-situ material characterization, it could be advanced as a benchmark value for comparison with that from the relatively new Prima 100 device.

A total of 42 FWD moduli and 62 Prima moduli data were available from the field test. The moduli determined at the 1730-lb (7.7 kN) load range were selected for both devices. For correlation purpose, only those stations where FWD moduli existed were considered, i.e., 42 stations. After critically reviewing the data, having not met the general trend of the pair wise plot, 6 out of 42 were not considered in the analysis, resulting in 36 pairs. The pair wise plot of E_{FWD} vs. E_{PFWD} of the remaining data is shown in Figure 4.1. A zero intercept regression analysis with MS EXCEL resulted in the following one-to-one relation:

$$E_{PFWD} = 1.09\, E_{PFWD}, \quad 2240 \text{ psi} < E_{PFWD} < 30740 \text{ psi} \tag{4.1}$$

$$R^2 = 0.64; \text{ Standard Error (RMSE)} = 5731$$

The calculated value of F = 60.99 larger than the tabulated F (90, 1, 34) = 2.86, indicates a significant relation between E_{FWD} and E_{PFWD}, despite a marginal R^2 value.

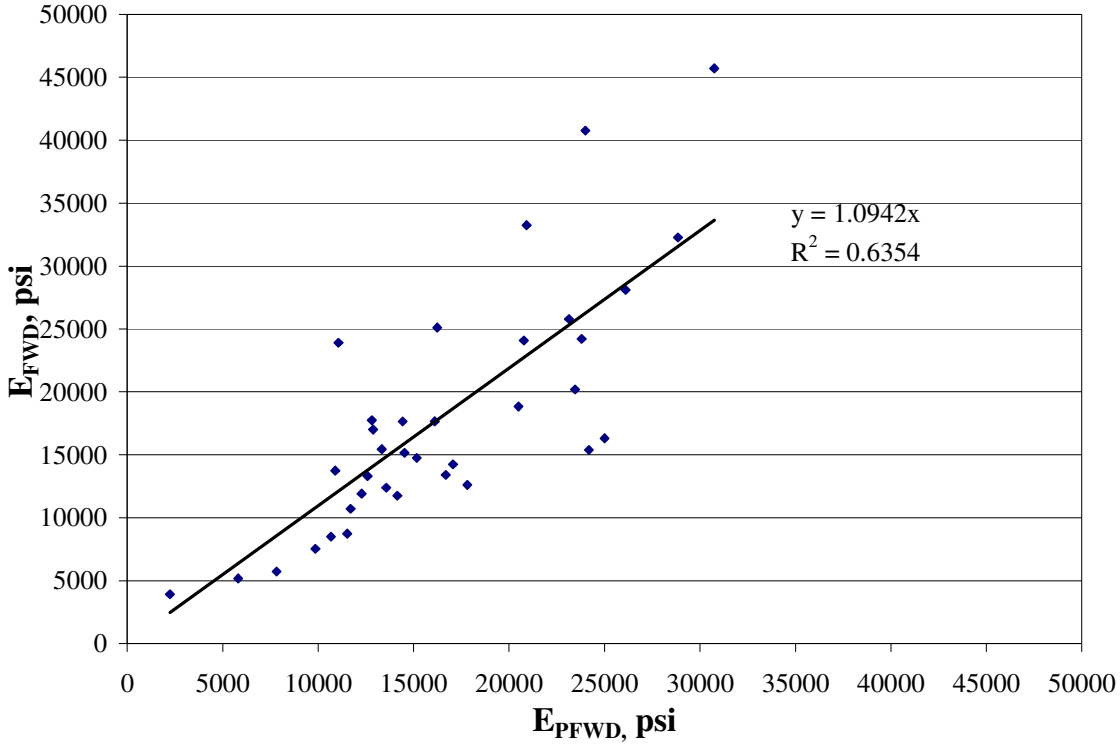

Figure 4.1 FWD Modulus (E_{FWD}) Compared to Prima 100 Modulus (E_{PFWD}), 1 psi = 6.89 kpa

This relation suggests that E_{FWD} on average is 1.09 times the Prima 100 modulus, a relatively higher ratio compared to Fleming (13) and Nazzal (38). They reported 1.03 and 0.97 ratios, respectively. Even a higher ratio of 1.23 was reported by Philips (15). What follows is a discussion as to why the E_{FWD} could be larger than E_{PFWD}. First the mass or the self-weight of the drop assembly of the FWD is at least one order of magnitude larger than that of the Prima 100 inducing a larger static preload stress (50 kPa vs. 4 kPa) on a 12-in. (300 mm) diameter bearing plate. This difference between the two devices may be expected to affect their respective measurements, especially when measuring on highly stress-dependent materials. When subjected to a larger preload, the stress-hardening material is known to result in larger modulus,

as observed with the conventional FWD. The bearing plate of FWD, which is a part of the drop assembly, is also heavier than that of Prima 100. As reported by Fleming et al. (14), the increased mass of the bearing plate from 15 kg to 25 kg did increase the peak acceleration of the bearing plate (i.e. increased resistance to motion) and produced a 25% reduction in the inferred peak deflection with only a moderate (≃10%) increase in soil pressure. Larger moduli, therefore, can be expected when using the FWD with the same drop load, but with a heavier bearing plate.

4.4 PROJECT DATABASE

Starting with 13 test sections (section #1 deleted), and 52 soil samples collected from the field, the number was reduced to 35 by combining similar samples based on visual examination (for example, color and texture) and the trend of Prima 100 modulus. All of those samples were subjected to particle size analysis, Atterberg limits and Proctor (AASHTO T99) tests for optimum moisture and maximum density (see Table 3.3). A second tier selection was made from the 35 samples, to encompass as many different classes of soils as recognized by MDOT (53), using CBR as the criterion. The MDOT manual recognizes 52 soil categories, assigning a CBR value for each soil, in the range of 1 to 25. The final selection cuts down the number of samples to 18, 14 fine-grained and 4 coarse-grained soils. Both laboratory and field test results, especially employed for model development, can be seen in Table 4.1. Only those 18 soils were tested for RLT test in accordance with AASHTO T-307 protocol, and those results are listed in column 9 of Table 4.1. A quick survey of the Prima modulus and corresponding resilient modulus of those 18 soils suggests that Prima modulus is, on average 13%, larger than the resilient modulus counterpart, excluding soil 3(3) and 3(4). This difference is more pronounced in coarse-grained soils. A brief discussion of why in-situ elastic modulus could differ from laboratory M_R is discussed in section 2.6.2.

Table 4.1 List of Soils and Their Properties Employed in Regression Analysis

Soil No.	Field Moisture (%)	Field Dry Unit Weight (pcf)	Optimum Moisture (%)	Dry Unit Weight at 95% Compac-tion (pcf)	PI (%)	P_{200} (%)	E_{PFWD} (psi)	M_{R95} (psi)	Estimated[c] Average M_{R95} (psi)	Density Ratio, $D_{(f/95)}$	Moisture Ratio, $M_{(f/o)}$	PI/P_{200}	E_{PFWD}/M_{R95}
2(1,2)	12.6	106.8	13.9	110.5	20	47	13620	16610	17200	0.97	0.91	0.43	0.82
2(5)	14.4	106.3	13.6	111.7	16	46	14150	18000	18080	0.95	1.06	0.35	0.79
3(3)	10.8	107.4	12.9	111.1	14	67	10670[a]	18630	12910	0.97	0.84	0.21	0.57
3(4)	10.4	110.1	10.8	117.1	6	44	5810[a]	15970	24410	0.94	0.96	0.14	0.36
4(4,5)[b]	8.8	114.0	10.7	116.9	7	25	17430	15800	21500	0.98	0.82	0.28	1.10
5(1,2)	11.4	109.1	13.0	110.7	11	78	21570	19840	12810	0.99	0.88	0.14	1.09
5(4)	9.3	111.2	10.6	115.0	2	66	16240	15480	15530	0.97	0.88	0.03	1.05
6(2,4)	14.5	104.3	17.1	104.7	12	95	15170	12610	12610	1.00	0.85	0.13	1.20
7(1)	13.3	104.2	15.4	105.2	11	98	14840	12220	13160	0.99	0.86	0.11	1.21
8(1,2)	12.9	104.6	15.7	105.3	9	94	16350	12760	12720	0.99	0.82	0.10	1.28
9(2)	16.6	100.3	15.8	102.1	9	88	16110	14320	13250	0.98	1.05	0.10	1.13
10(1)	8.7	107.4	12.6	112.0	13	67	20500	19840	13130	0.96	0.69	0.19	1.03
11(1,2)	10.1	111.1	12.7	111.8	7	74	23290	18600	14010	0.99	0.80	0.09	1.25
12(4,5)	14.2	100.1	15.8	104.8	15	92	13450	14180	12960	0.96	0.90	0.16	0.95
13(1)[b]	6.9	114.9	13.3	112.1	1	30	22490	16990	23260	1.02	0.52	0.03	1.33
13(5)	8.1	115.3	11.6	115.1	9	37	24870	20490	20000	1.00	0.70	0.24	1.21
14(4)[b]	8.0	109.6	12.5	111.9	1	12	21470	15890	23260	0.98	0.64	0.08	1.35
14(5)[b]	8.5	111.7	12.0	113.0	4	28	21980	17540	20000	0.99	0.71	0.14	1.25

[a] Not Considered for regression analysis
[b] Coarse-grained Soil
[c] Resilient Modulus estimated by employing MrAll1 Program, averaged over several models
1 psi = 6.89 kPa
1 pcf = 0.157 kN/m^3

Soils 3(3) and 3(4) were not considered in the final regression analysis because of unreasonably low values of E_{PFWD}, namely, 10670 psi (74 MPa) and 5810 psi (40 MPa), respectively (see Column 8 in Table 4.1), resulting in 16 soils data available for regression analysis. Those low values in part could be attributed to the synergism from low compaction ratio (92% and 89%, respectively) and relatively high moisture content.

4.4.1 Resilient Modulus Test Results

Resilient modulus tests were conducted by Burns Cooley Dennis soils laboratory, a subcontract with MDOT and The University of Mississippi. Three replicate samples were tested from most of the soils, with few exceptions where only one or two were tested, owing primarily to funding restrictions. One of those soils, 6 (2, 4), tested at 10,668 psi (84 MPa) at 95% compaction ratio. Comparing that M_R-value to those of other similar soils, 7 (1) and 12 (4, 5), with nearly identical physical properties, it is felt that an upward revision of the test value of 6(2, 4) is justified. The resilient modulus of the soils 7(1) and 12(4, 5) were, respectively, 12,220 psi (96 MPa) and 14,180 psi (112 MPa). Now, M_{R95} of 6 (2, 4), 7(1) and 12 (4, 5) were estimated using MrAll1 program, (Hans et al. 22) extracting the average value of 30 established models, resulting in resilient moduli of 12,610 psi (87 MPa), 13,160 psi (91 MPa) and 12,960 (89 MPa), respectively (see column 10 of Table 4.1). Accordingly, the laboratory resilient modulus of 6 (2, 4) is revised to 12,610 psi.

Soil 5 (1, 2) was tested with a resilient modulus value of 24,330 psi (192 MPa). This M_R-value is judged high compared to that of 10 (1) with nearly identical properties, which tested at 19,840 psi (137 MPa). Suspecting some experimental error in the high test value, the author recommended a repeat test on the soil, but not followed up by the BCD laboratories. The estimated M_R-values for those two soils according to Mrll1 program was 12,810 psi (88 MPa)

and 13,130 psi (90 MPa). A revision of soil 5 (1, 2) M_R to 19,840 psi (137 MPa) appears reasonable.

4.5 PREDICTION OF M_R AT 95% COMPACTION (M_{R95}) FROM PRIMA MODULUS (E_{PFWD})

The resilient modulus predicted from the perceived relation would be a surrogate measure for the laboratory resilient modulus (in accordance with AASHTO T-307), mandated in the M-EPDG. If a reasonably satisfactory model can be established, Prima 100 stands a good chance for use in QC/QA of subgrade construction as well.

4.5.1 Development of Statistical Model to Predict M_{R95}

In view of the different test procedures employed in the repeated load triaxial test and in-situ test, the likelihood of a one-to-one relationship between M_{R95} and E_{PFWD} is rather remote. Besides, the prediction model shall encompass a wide range of soils, requiring that soil physical/index properties be included in predicting M_{R95}. Therefore, properties such as field unit weight, field moisture, optimum moisture, maximum unit weight, plasticity index (PI), passing sieve size no. 200 (P_{200}), saturation level, and saturation level at 95% compaction were preliminarily considered in the correlation analysis. Table 4.1 presents the physical properties of 18 soils including M_{R95}, and, E_{PFWD}.

The first step in the analysis entailed selecting the appropriate independent variables to be included in the prediction model. Three categories of factors affecting resilient modulus include soil physical state, state of stress, and structure/type of material. The stress effect was taken into account by choosing the stress combination, σ_d = 6 psi (41 kPa) and σ_3 = 2 psi (14 kPa) in calculating the resilient modulus (18). Note that these stresses more or less match those under the bearing plate of Prima 100. The question of soil structure is somewhat an issue, especially

from the point of view of compaction method. This is apparently one of the drawbacks in using M_R in the MEPDG model. Since only one model is anticipated for a variety of soil types, however, variable(s) reflecting soil type shall be included in the model. The primary factors to be included in the model, therefore, would be those related to soil physical state, for example, unit weight, moisture content and saturation level. Since variations in moisture are generally accompanied by volume changes, any two of the three variables need to be included in the model. Based on this premise, a set of eight variables were chosen computing the pair wise correlation coefficient (CC) between those variables (see Table 4.2). Correlation coefficient provides a convenient index of strength of the linear relation between two variables. The maximum value of CC varies from -1 to +1, with the sign determining a positive or negative relation. Normally a CC of greater than 0.60 is considered a good correlation (45).

Employing the Statistical Package for Social Science (SPSS) a resulting correlation matrix, was developed involving all of the nine independent variables, and is presented in Table 4.3. As expected, M_{R95} and E_{PFWD} are well-correlated, so also M_{R95} and field unit weight, field moisture and P_{200} in that order. Some of the independent variables are also highly correlated, for example, the CC between moisture and unit weight is -0.89. This implies out of those two independent variables only one would be sufficient for development of the prediction model. With the objective of minimizing the correlation between the independent variables, dimensionless transformed variables were sought for regression analysis. Another desired feature of non dimensionless variables is that the model can be employed with any unit system. With the transformation, dependent variable became E_{PFWD}/M_{R95} instead of M_{R95}, and independent variables, for example, density ratio, $D_{(f/o)}$, (ratio of field unit weight to unit weight at 95% compaction), moisture ratio, $M_{(f/o)}$ (ratio of field moisture to optimum moisture) and ratio of saturation level, $S_{(f/o)}$ (ratio of saturation at field conditions to saturation at optimum conditions).

Table 4.2 Dependent and Independent Variables Considered and Their Ranges in Developing Prediction Model

Type of Variable	Symbol Used for the Variable	Description of Variable	Range
Dependent	M_{R95}	Measured Laboratory Resilient Modulus at 95% Compaction , psi	12220-20490
Independent or Explanatory	E_{PFWD}	Measured PFWD Elastic Modulus, psi	13450-24870
	w	Field Moisture, %	6.9 - 16.6
	γ_d	Field Dry Unit Weight, pcf	100.1- 115.3
	w_{opt}	Optimum Moisture Content, %	10.6 - 17.1
	$\gamma_{d\,max}$	Maximum Dry Unit Weight, pcf	107.5 – 123.0
	PI	Plasticity Index, %	1 – 20
	P_{200}	Passing Sieve Size 200	12 - 98
	S	Degree of Saturation with Field Moisture and Field Dry Unit Weight, %	41.6-68.7
	S_{95}	Degree of Saturation with Optimum Moisture and Dry Unit Weight at 95% Compaction , %	64.1-78.2

1 psi = 6.89 kPa
1 pcf = 0.157 kN/m^3

Table 4.3 Correlation Matrix of Basic Variables Considered in Developing Prediction Model

Variables	M_{R95}	E_{PFWD}	γ_d	w	S	S_{95}	PI	P_{200}
M_{R95}	1	0.688	0.595	-0.544	-0.402	-0.212	-0.008	-0.487
E_{PFWD}	0.688	1	0.729	-0.760	-0.684	-0.291	-0.575	-0.472
γ_d	0.595	0.729	1	-0.890	-0.673	-0.270	-0.561	-0.737
w	-0.544	-0.760	-0.890	1	0.932	0.355	0.636	0.718
S	-0.402	-0.684	-0.673	0.932	1	0.371	0.641	0.611
S_{95}	-0.212	-0.291	-0.270	0.355	0.371	1	0.514	0.183
PI	-0.008	-0.575	-0.561	0.636	0.641	0.514	1	0.411
P_{200}	-0.487	-0.472	-0.737	0.718	0.611	0.183	0.411	1

The soil type-related variable was coined with PI and P_{200}, their ratio, PI/P_{200}, though a direct comparison is not feasible, the indications are the CCs between the dependent variable and the independent variables after transformation (see Table 4.4) have improved compared to that before transformation (see Table 4.3). In addition, the correlation coefficient between each pair of transformed independent variables is lower than those in Table 4.3, suggesting no strong multicollinearity between those independent variables. The implications of multicollinearity will be discussed in detail in a later section. With these transformed variables selected, pair-wise correlations were developed and plotted in Figures 4.2 through 4.4. As expected, E_{PFWD}/M_{R95} shows good correlation with density ratio and with moisture ratio, respectively, direct relation and inverse relation. In so far as soil type is concerned, large PI/P_{200} ratio-soils (typically, fine-grained),

Table 4.4 Correlation Matrix of Transformed-Dependent and -Independent Variables Considered in Developing Prediction Model

Variables	E_{PFWD}/M_{R95}	$D_{(f/95)}$	$M_{(f/o)}$	PI/P_{200}	$S_{(f/95)}$	$S_{95} - S$	$w_{opt} - w$
E_{PFWD}/M_{R95}	1	0.799	-0.668	-0.729	-0.462	0.463	0.681
$D_{(f/95)}$	0.799	1	-0.575	-0.495	-0.308	0.342	0.609
$M_{(f/o)}$	-0.668	-0.575	1	0.358	0.953	-0.959	-0.986
PI/P_{200}	-0.729	-0.495	0.358	1	0.222	-0.213	-0.393
$S_{(f/95)}$	-0.462	-0.308	0.953	0.222	1	-0.996	-0.922
$S_{95} - S$	0.463	0.342	-0.959	-0.213	-0.996	1	0.939
$w_{opt} - w$	0.681	0.609	-0.986	-0.393	-0.922	0.939	1

exhibit relatively small in-situ modulus owing primarily to its susceptibility to seasonal volume change, a partial explanation for the negative relation. Further support of the negative relation can be offered on the premise that coarse-grained soil, with low PI/P_{200} ratio, often results in relatively large in-situ modulus in comparison to the resilient modulus. The superior confinement offered by the surrounding soil is the reason for this larger in-situ modulus.

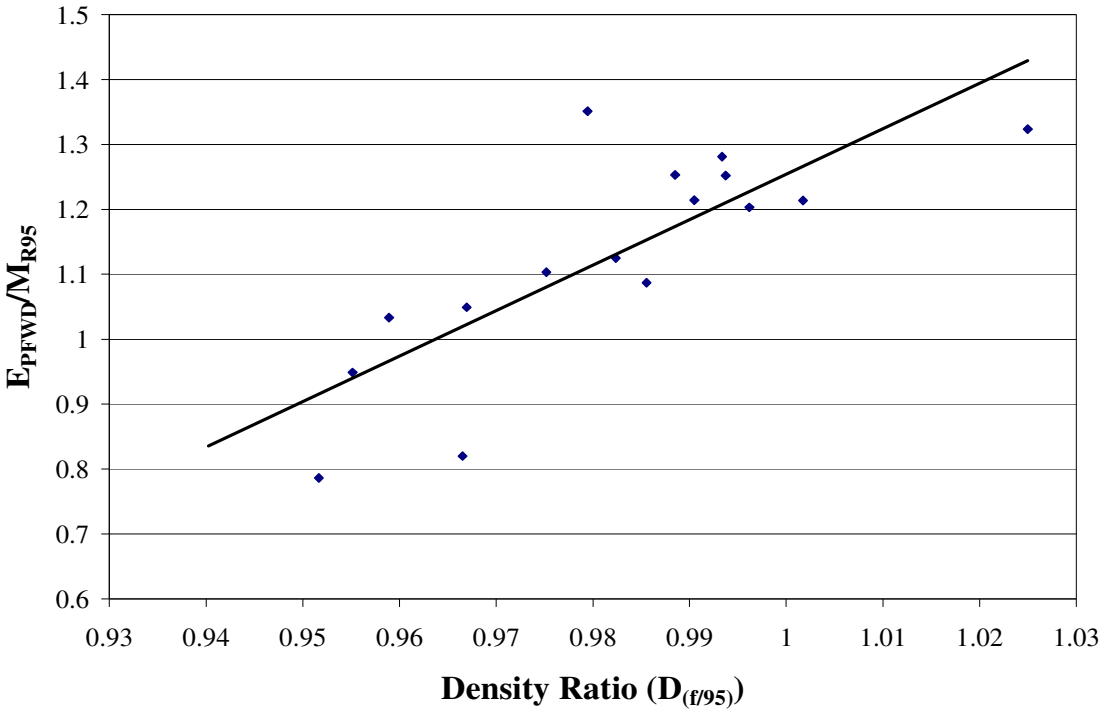

Figure 4.2 Scatter Plot of Modulus Ratio (E_{PFWD}/ M_{R95}) versus Density Ratio ($D_{(f/95)}$)

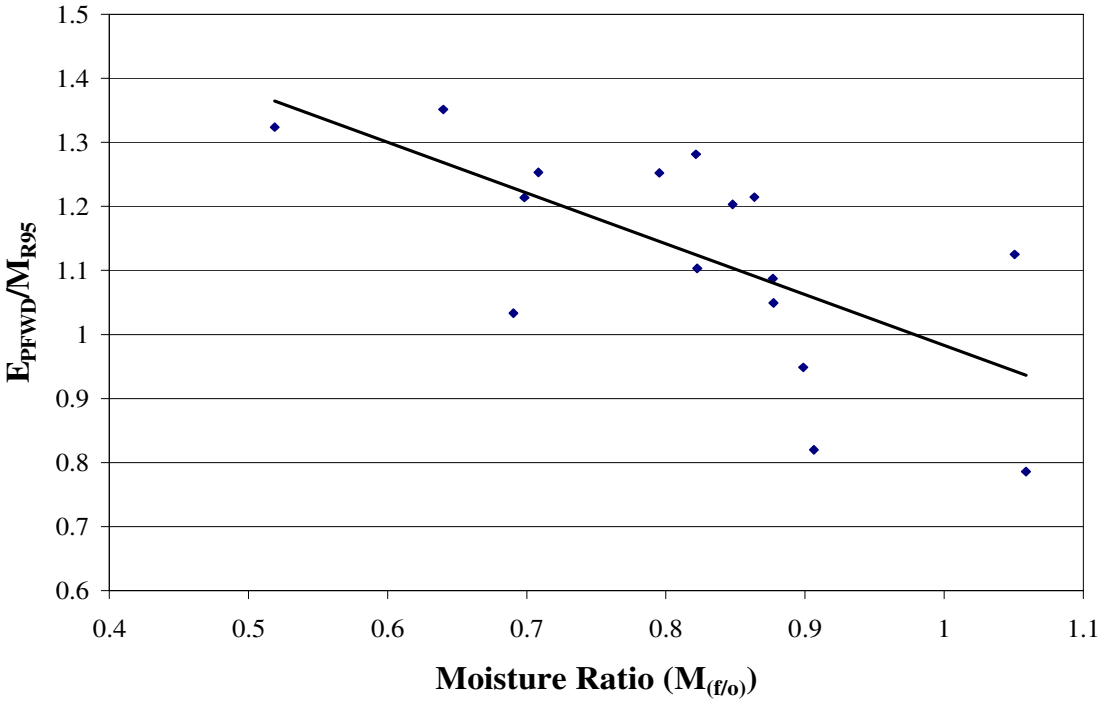

Figure 4.3 Scatter Plot of Modulus Ratio (E_{PFWD}/ M_{R95}) versus Moisture Ratio ($M_{(f/o)}$)

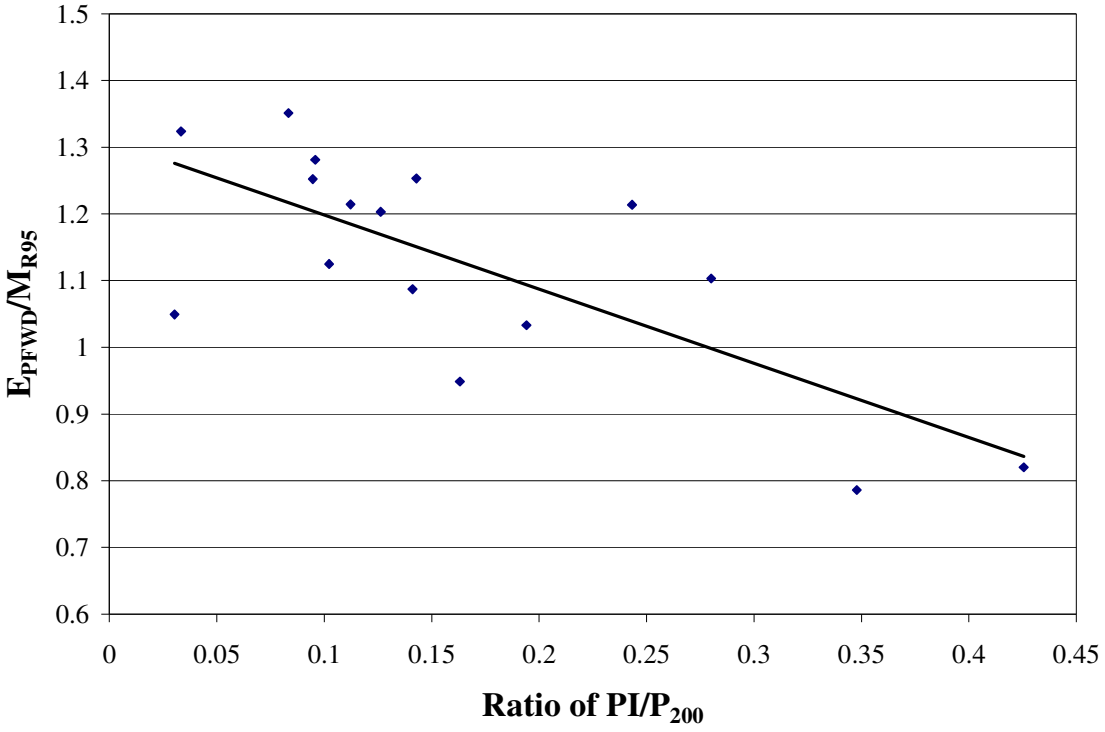

Figure 4.4 Scatter Plot of Modulus Ratio (E_{PFWD}/ M_{R95}) versus PI/P_{200}

Multivariable linear option in SPSS was employed to conduct regression analysis with 'enter method' option. The special features of curve estimation option and stepwise option were also tapped in, as required.

In order to select a model, some basic principles are followed: first, minimum Root Mean Square Error (RMSE) otherwise referred to as Standard Error (SE); the smallest Standard Error would result in the narrowest confidence intervals and largest test statistics. The model with the smallest SE involving the least number of independent variables would be the most appropriate. A model with the absolute smallest SE may not provide the best intuitive model, however. That is, a model providing a slightly larger RMSE but with explanatory variables that are more relevant to the problem may be more desirable. Second, the model should be as simple as possible; that is, it should have as few explanatory variables as possible. Third, the larger the coefficient of determination (R^2), the better the model will be. Fourth, the cause-and-effect

relationship between the dependent variable and each of the explanatory variables should be relevant. Fifth, the model should satisfy the physical requirements of boundary conditions. For example, the dependent variable should never become zero or infinite.

After numerous trials with several combinations of independent variables, a linear model (accommodating multiple variables), referred to as comprehensive model in this report, was selected over other likely models, based on its simplicity (with few independent variables), relevant cause-and-effect relation, and reasonably good statistics. The resulting model is listed in Eq. 4.2.

$$\frac{E_{PFWD}}{M_{R95}} = -2.30 + 3.860 D_{\left(f/95\right)} - 0.316 M_{\left(f/o\right)} - 0.635 \, PI/P_{200} \qquad (4.2)$$

$R^2 = 0.83$; Standard Error = 0.077

where: E_{PFWD}/M_{R95} = ratio of measured PFWD elastic modulus to laboratory determined resilient modulus at 95% compaction;

$D_{(f/95)}$ = ratio of field unit weight to unit weight at 95% compaction;

$M_{(f/o)}$ = ratio of field moisture to optimum moisture; and

PI/P_{200} = ratio of plasticity index (%) to passing sieve size #200 (%).

A summary statistic of this model is listed in Table 4.5. *F*-test for multiple linear regression relation was conducted to validate the significance of the relationship between dependent and independent variables included in the model. The calculated value of F=19.92 being larger than the tabulated F (90, 3, 12) = 2.61 indicates a significant relation between modulus ratio and selected independent variables. Significance of individual regression coefficients was tested employing the t-test. The calculated t of each of three coefficients meets 90% confidence level, except the constant regression coefficient, where the calculated t = -1.606 is less than the tabulated t (90, 15) = 1.753, indicating some uncertainty as to this coefficient

Table 4.5 Summary Statistics of Prediction Models

Model	Regre-ssion Coeffi-cints	Values	t-Statistics	t-Critical	F-Statistics	F-Critical	RMSE	R^2
Compre-hensive	a_1	-2.30	-1.610	1.753	19.921	2.61	0.07692	0.83
	a_2	3.860	2.824					
	a_3	-0.316	-1.831					
	a_4	-0.635	-3.047					
Abbre-viated	a_1	-3.907	-2.299	1.753	15.419	2.76	0.09842	0.70
	a_2	5.435	3.358					
	a_3	-0.370	-1.687					

being non-zero. To enhance the result, however, another transformation was made by transposing -2.30, and adding to E_{PFWD}/M_{R95}. Another regression analysis with this new dependent variable (E_{PFWD}/M_{R95} + 2.30) showed that the regression constant in the enhanced model is zero, with a significance level of 100%. It is worthwhile noting that the coefficients in equation 4.2 remained unchanged with the new dependent variable. This exercise confirms the premise of a non-zero constant regression coefficient.

As a further validation of the model, the predicted modulus ratio (E_{PFWD}/M_{R95}) is plotted versus the measured ratio, as shown in Figure 4.5. The fact that the majority of the points are aligned along the line of equality confirms the reliability of the model. On further examination of the model, it is encouraging to note that the model fully recognizes the cause and effect relationship between dependent and independent variables.

Having employed seemingly related variables as explanatory variables, it is imperative that problems associated with multicollinearity be checked. Multicollinearity arises when two or more independent variables are highly correlated. For example, an analysis of the correlation matrix reveals that any two variables with a correlation coefficient of 0.6 and above could result in multicollinearity problem. Multicollinearity, when present, is always associated with unstable

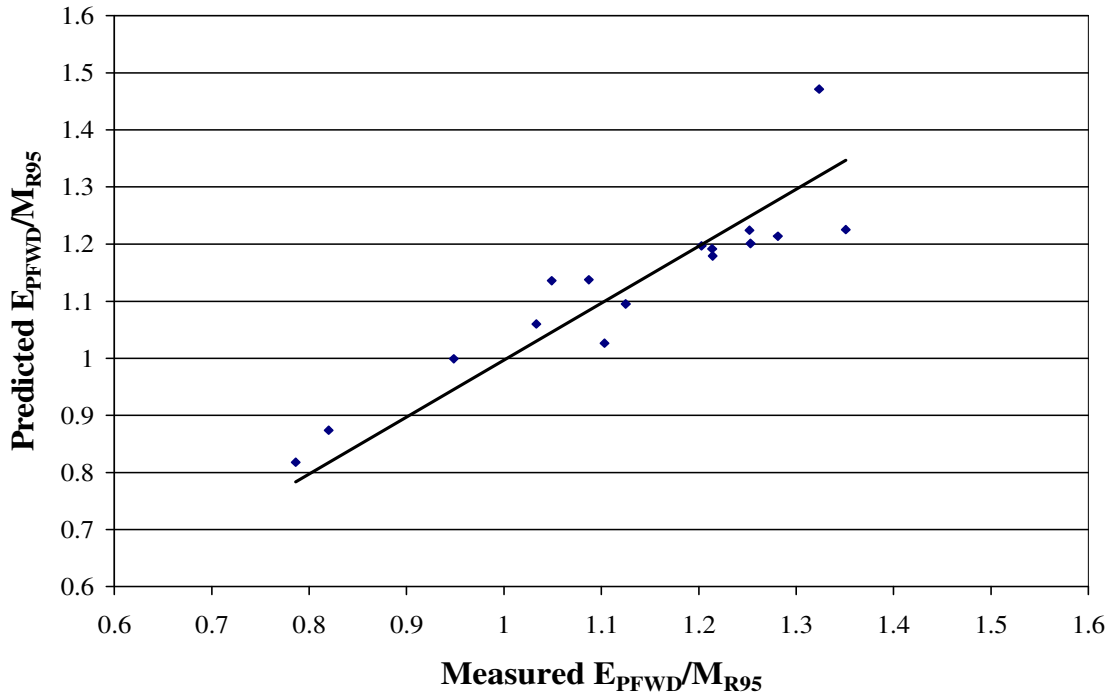

Figure 4.5 Modulus Ratio (measured) versus Modulus Ratio (predicted) [Comprehensive Model]

estimated regression coefficients. To check for possible multicollinearity for the specified model, residuals are plotted against the predicted E_{PFWD}/M_{R95} values. From Figure 4.6, it is evident that there is no distinct pattern among the residuals, ruling out the multicollinearity, concluding that the model is well-specified.

Yet another concern is the lack of homoscedasticity, or presence of heteroscedasticity in the data employed to derive the regression model. One of the standard assumptions of least square theory is that the constancy of error variance, which is often referred to as the assumption of homoscedasticity. When the error variance is not constant over all of the observations, the error is said to be heteroscedastic, violating the standard assumption of least square theory. To detect the heteroscedastic error in a regression model, the residuals are plotted against independent variables on the x-axis (see Figures 4.7, 4.8 and 4.9). That the residuals in all three

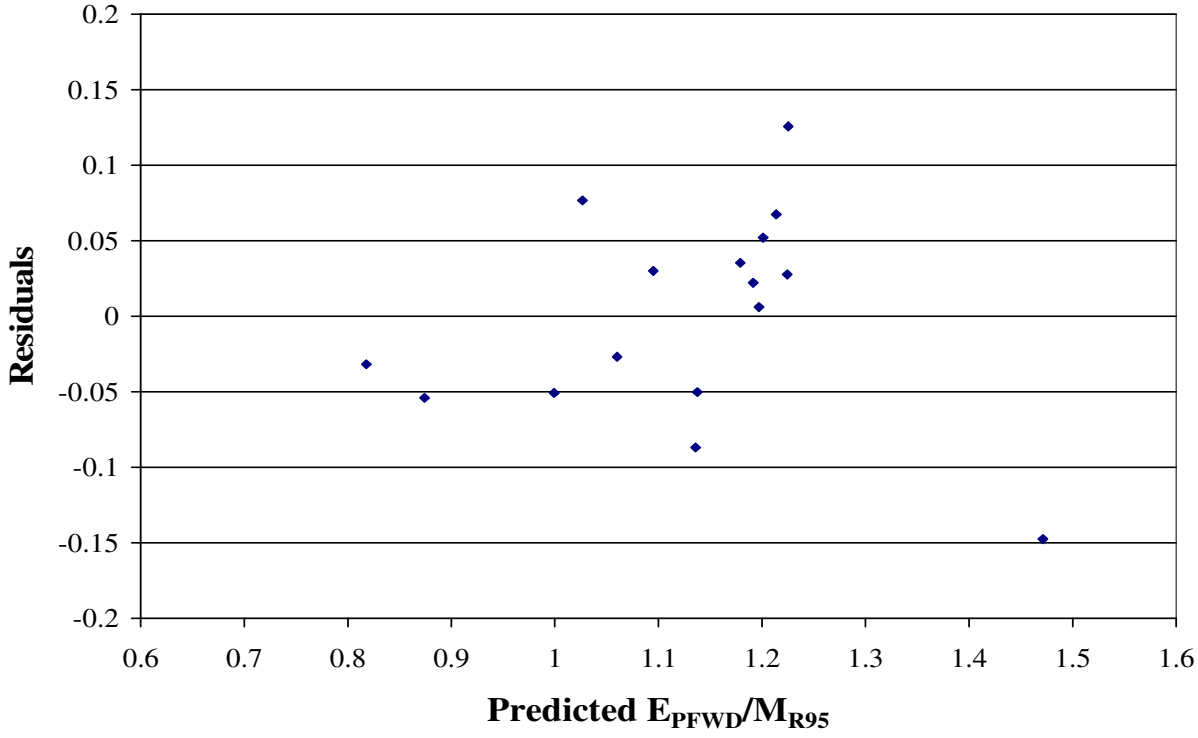

Figure 4.6 Residuals Plotted Against Predicted Modulus Ratio, E_{PFWD}/M_{R95}

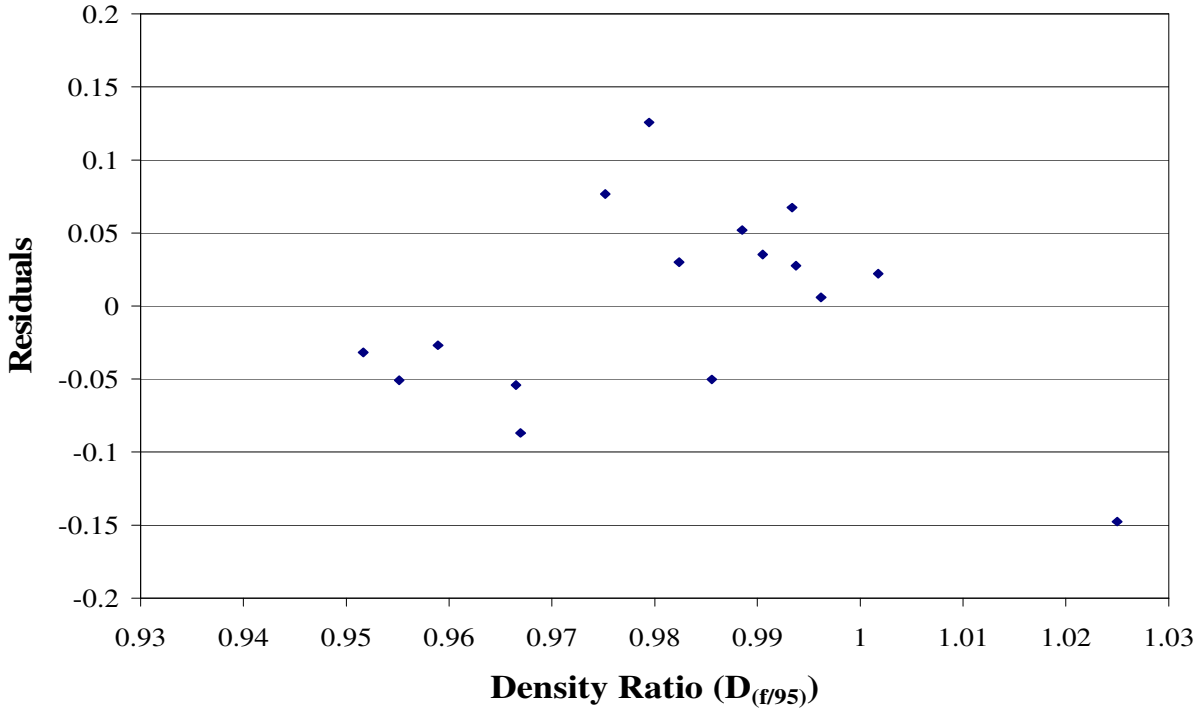

Figure 4.7 Residuals Plotted Against Independent Variable $D_{(f/95)}$

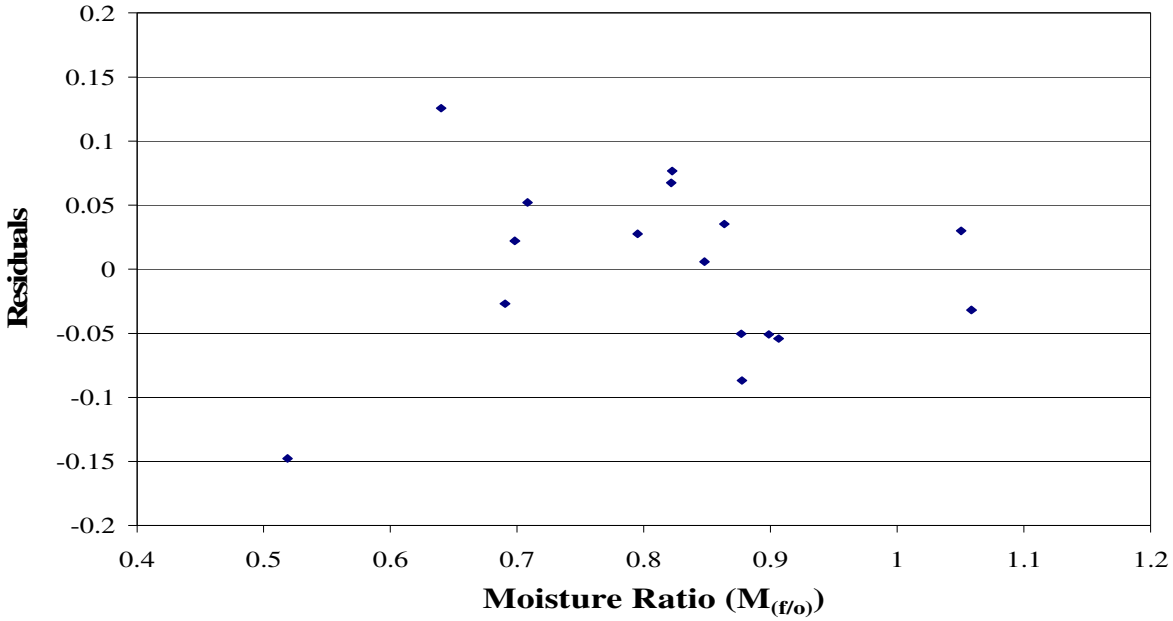

Figure 4.8 Residuals Plotted Against Independent Variable $M_{(f/o)}$

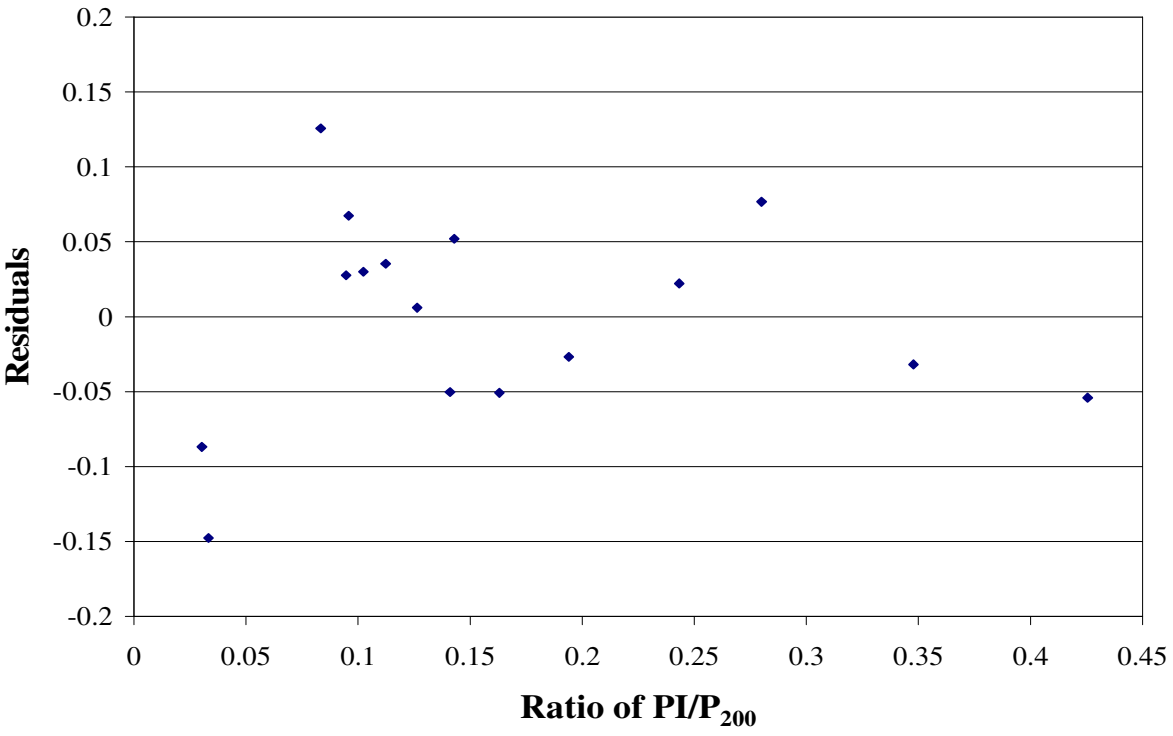

Figure 4.9 Residuals Plotted Against Independent Variable (PI/P_{200})

of the plots fall in a band parallel to the x-axis, indicating no evidence of heteroscedasticity, and in turn, no obvious violation of the least square theory assumption.

4.5.2 Sensitivity of the Model

The sensitivity analysis examines the effect of each independent (explanatory) variable on the predicted modulus ratio. The methodology of sensitive study entails changing the mean value of each independent variable by +/- one standard deviation and calculating the corresponding change in the predicted modulus ratio. The mean value of each independent variable is nothing but its probable value, for example, one for density ratio. With assumed values of coefficient of variation for density ratio, moisture ratio and PI/P_{200}, respectively, 5%, 15% (absolute change of 1.8%) and 20%, the dependent variable changes are calculated to be 17.3%, 4.3% and 2.4%. Clearly, density is a significant variable in estimating the resilient modulus of subgrade soils. Jin et al. (54), reported the effect of moisture and density on resilient modulus of coarse-grained soils, compiled from two field test sites, concluding that moisture having a minor influence on resilient modulus (≃4.9% modulus decrease for a 15% moisture increase). This result compares favorably with what was observed in the current field study, though Jin et al. M_R-prediction equation was derived from a laboratory investigation, where samples were casted and tested at different levels of moisture density and temperature. The effect of density has been shown to be even smaller than that arising from moisture variation (54). In soil samples subjected to wetting/drying in the laboratory, however, moisture was shown to have a significant effect on resilient modulus. A detailed analysis of laboratory test results reported a 1% (absolute value) increase in moisture, resulting in, on average, a 13% reduction in modulus in fine-grained soils, and 10% reduction in coarse-grained soils (23). The database included results on 49 different soils from seven researchers.

Two more model equations were developed, essentially employing the same three explanatory variables. The response variable moisture ratio in equation 4.2 was substituted by simply moisture in the first alternate model. In the second model, M_R value calculated from stress states σ_1 = 10.2 psi and $\sigma_2 = \sigma_3$ = 1.6 psi were used instead of those calculated with σ_1 = 8 psi and $\sigma_2 = \sigma_3$ = 2 psi (moduli in columns 8 and 9, respectively, of Table 3.4). Those two models and their statistics are presented in Appendix B.

4.6 ABBREVIATED PREDICTION MODEL

As much as the model (Eq. 4.2) has shown potential in predicting resilient modulus from in-situ measurement of stiffness elastic modulus employing Prima 100, there were some reservations amongst MDOT engineers as to the availability of the soil index properties, namely PI and P_{200}. The researchers were encouraged to develop another model (referred to as abbreviated model) with the same data set by deleting PI/P_{200} term. Proceeding in an identical manner employing SPSS program, both power and linear model forms were attempted with only two independent variables. Again, the multiple linear models fitted the data better than a power model. The resulting equation, presented in equation 4.3, has acceptable statistics.

$$\frac{E_{PFWD}}{M_{R95}} = -3.907 + 5.435D_{\left(f/95\right)} - 0.370M_{\left(f/o\right)} \tag{4.3}$$

R^2 = 0.70; Standard Error = 0.098

The variables are explained in equation 4.2. A summary statistic of this model can be seen in Table 4.5. The calculated value of F = 15.42 being larger than the tabulated F (90, 2, 13) = 2.76, indicates a significant relation between modulus ratio and selected independent variables. Significance of individual coefficients was tested employing t-test. The calculated t of each of the two coefficients meets 90% confidence level, but one does not. The regression coefficient of moisture ratio term had calculated t = 1.687, less than the tabulated t (90, 15) = 1.753. In view of

very close t-values, almost passing the t-test, the moisture ratio is retained in equation 4.3. The validity of the model was further established by plotting the measured E_{PFWD}/M_{R95} versus predicted E_{PFWD}/M_{R95} (see Figure 4.10), with majority of the points lying on the line of equality. To check any possibility of multicollinearity in the abbreviated model, residuals were plotted against the predicted E_{PFWD}/M_{R95} values. Realizing no distinct pattern among the residuals, as can be verified in Figure 4.11, multicollinearity is not an issue in this model either.

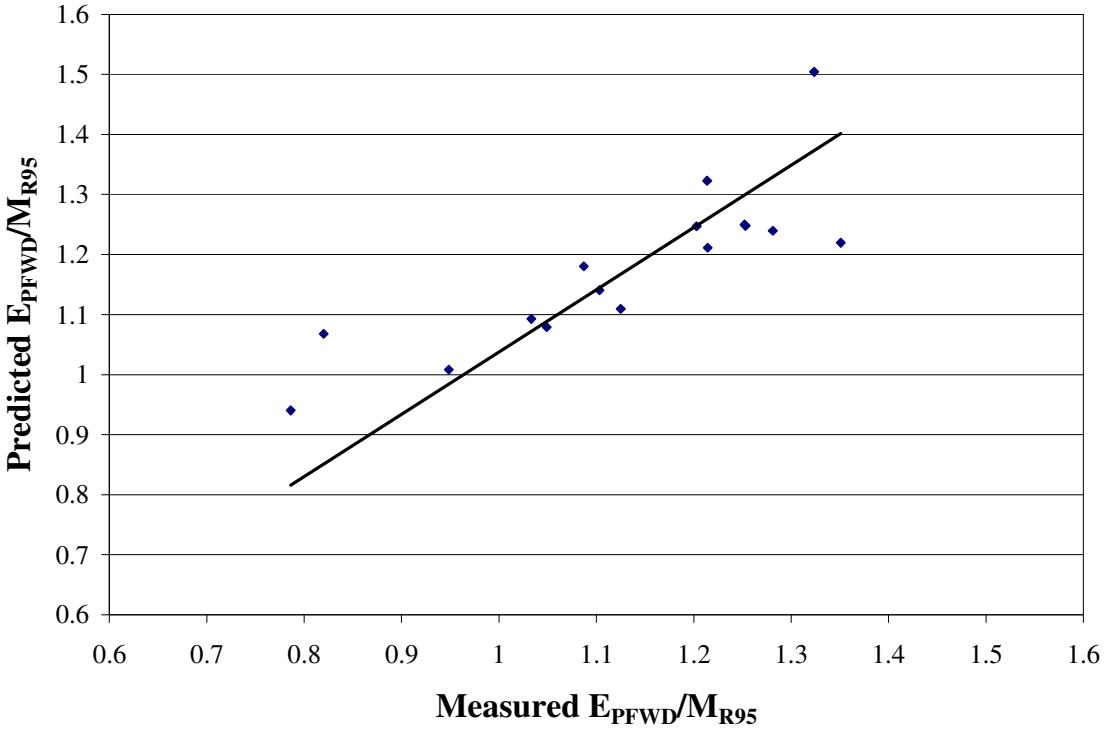

Figure 4.10 Modulus Ratio (Measured) versus Modulus Ratio (Predicted) [Abbreviated Model]

Applying the adopted coefficient of variation of 5% and 15%, respectively, in the density ratio and moisture ratio, the predicted modulus ratio changed by 23.4% and 4.8% respectively. Note that the sensitivity of density ratio increased from 17.3% to 23.4% compared to the comprehensive model, with the role of moisture ratio practically unchanged.

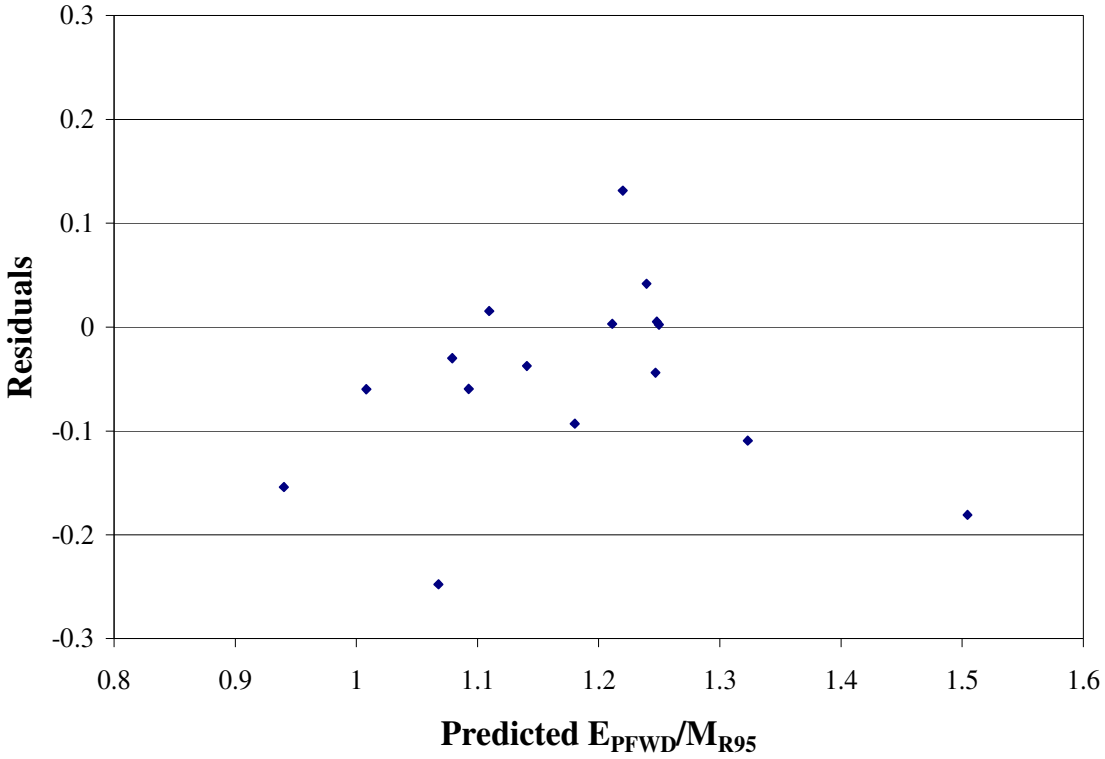

Figure 4.11 Residuals Plotted Against Predicted Modulus Ratio [Abbreviated Model]

4.7 IN-SITU TESTS INFLUENCED BY SEASONAL VARIATION

4.7.1 Timing of Prima Test

Typical sequence of new highway construction entails completion of grading contract followed by typically two years or more of no activity before the pavement contract is awarded. For example, the test sections available for in-situ tests were constructed some two years ago, others more than two, some up to 5 years. Because of the time lapse, sections 2, 3 10 and 11 have undergone severe weathering, some with grass and weeds growing. In the remaining sections, final grading work was in progress resulting in relatively even surface for testing. Since final grading calls for several inches of deep cutting, that will be an opportune time for planning in-situ Prima tests.

4.7.2 Prima Modulus Influenced by In-situ Moisture and Unit Weight

As can be seen in Table 3.3, dry unit weight and moisture content of each test location were determined employing a nuclear device. Comparing the field unit weight, with the maximum unit weight, it is noted that a majority of the field unit weights, 83% (column 3 of Table 3.3), turned out to be less than 95% compaction, which was MDOT QC/QA specification. One explanation for this gross mismatch of field density and specified density could be that the subgrade soil, presumably compacted to (say 95% compaction) meeting the Department specifications, had undergone some expansion upon wetting and drying. Density deficiency observed during in-situ tests in fine- and coarse-grained soils was not significantly different, however. Field moisture was invariably 1.5 to 4.5% below the optimum moisture. Note that the field tests were scheduled at a minimum of two days or more after a rain event, ensuring uniform moisture through the depth of subgrade formation. It should be remarked here that once the subgrade is overlain by an 'impervious' surface, the field moisture tends to attain the 'equilibrium moisture', which generally is one or two percent more than the optimum moisture.

As in a typical field test operation, the moisture and consequently dry unit weight cannot be controlled at the specified values as they are directly influenced by the seasonal climatic changes, especially precipitation, evapo-transpiration, ground cover and so forth. Moisture and unit weight profoundly influence the elastic modulus and, therefore, an understanding of their relative significance would help the engineer in scheduling field tests. Should a relation be developed to predict elastic modulus as affected by moisture and unit weight, the sensitivity of each independent variable could be quantified, thus providing valuable information on accuracy required for their estimation. For example, if one variable turns out to be significantly more sensitive than the other, special attention could be directed in estimating that particular variable

over the other. Solely for the purpose of establishing how in-situ modulus is influenced by the two significant variables (inherent in field operation), a relation is sought between E_{PFWD} and in-situ moisture and in-situ unit weight.

A database is developed with 31 data points each representing a test location. Soils 3(4), 3(5), 4(1) and 5(5) were deleted in view of the unreasonably low/high E_{PFWD} values. Scatter plots of dependent variable, E_{PFWD}, versus each of the two primary independent variables were plotted which can be seen in Figure 4.12 and 4.13. As expected, E_{PFWD} increases with dry unit weight and decreases with moisture content. Table 4.6 lists the dependent and all of the independent variables and their ranges considered in the modeling. The next step was to perform pair wise correlation between all the potential dependent and independent variables, with the correlation matrix presented in Table 4.7. Though, unit weight, moisture and degree of saturation showed a satisfactory correlation with E_{PFWD}, those independent variables were highly correlated among them, which implies, only one independent variable from those three is sufficient to develop the model. The Prima modulus in the field, nonetheless, is dependent on moisture and unit weight. The degree of saturation which is a function of unit weight and moisture showed a satisfactory correlation with E_{PFWD}, however, the model resulted in a low R^2 value. With this in mind, a set of transformed variables were coined and their correlation matrix calculated, as listed in Table 4.8. Among the set of transformed independent variables, density ratio and field moisture resulted in a better overall correlation with E_{PFWD}, despite moisture ratio showing a larger CC than the moisture.

With independent variables tentatively chosen, scatter plots of the dependent variable versus each potential explanatory variable were plotted. It is anticipated that the value of E_{PFWD} increases with the increase of field density and decreases with the increase of field moisture,

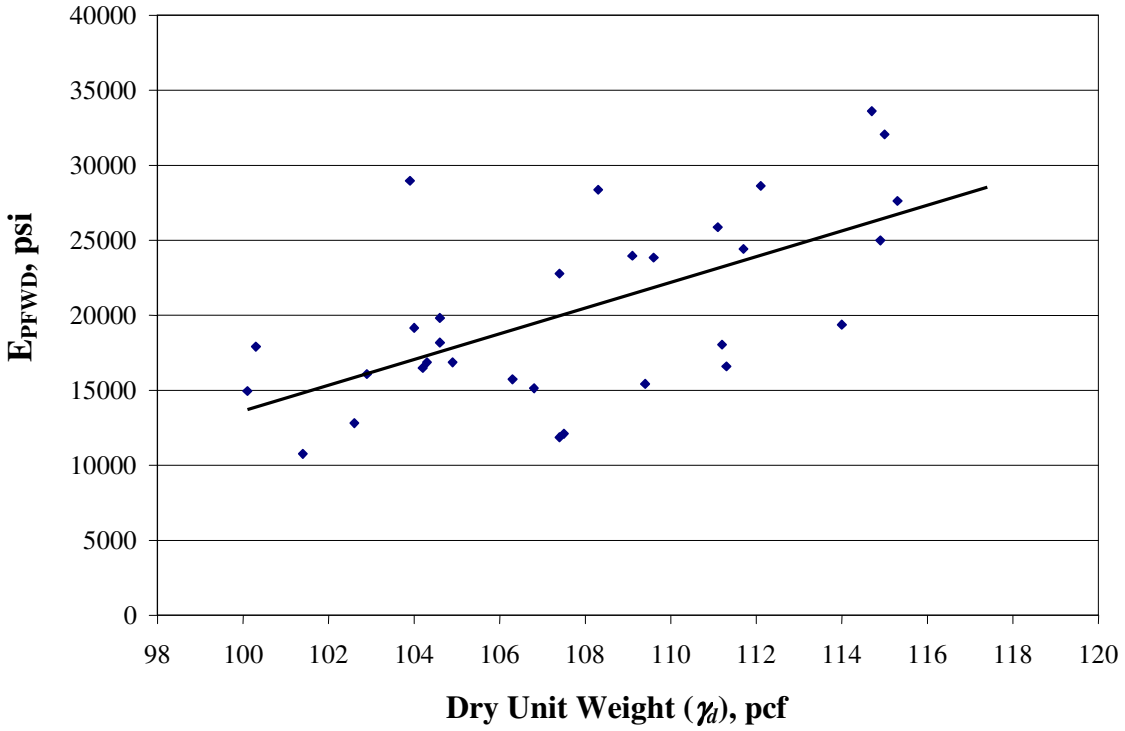

Figure 4.12 Scatter Plot of Prima 100 Modulus (E_{PFWD}) versus Dry Unit Weight (γ_d)
1 psi = 6.89 kPa, 1 pcf = 0.157 kN/m^3

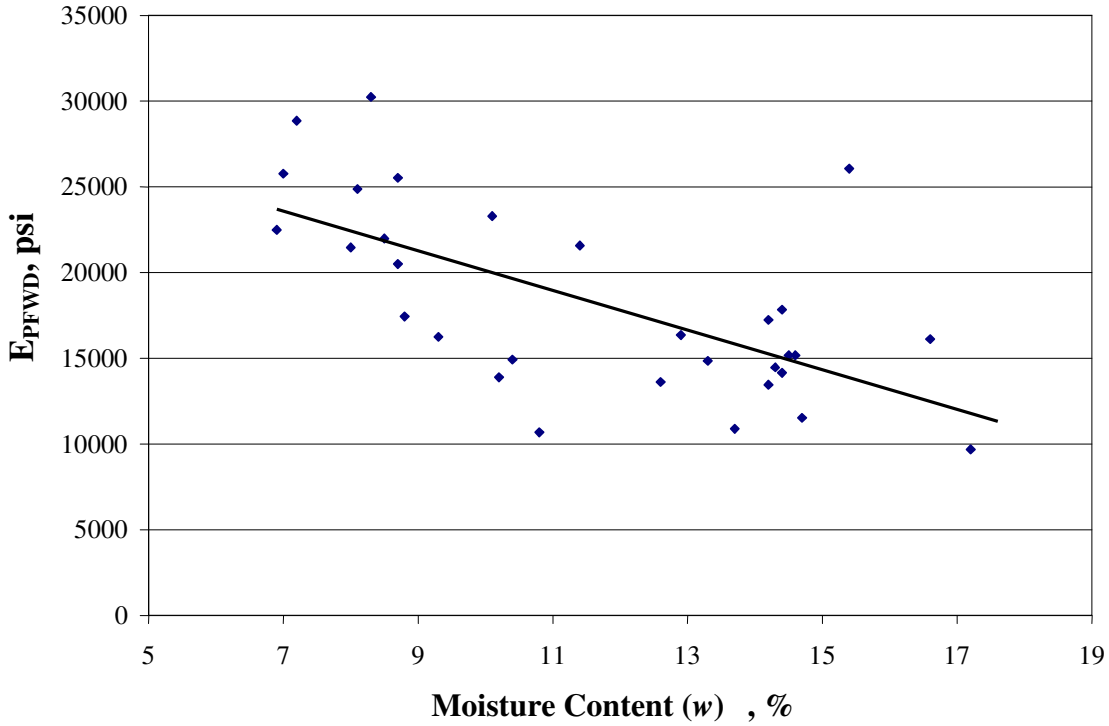

Figure 4.13 Scatter Plot of Prima 100 Modulus (E_{PFWD}) versus Moisture Content (w)
1 psi = 6.89 kPa

Table 4.6 Dependent and Independent Variables Considered and Their Ranges in Developing Correction Equation

Type of Variable	Symbol Used for the Variable	Description of Variable	Range
Dependent	E_{PFWD}	Measured PFWD Elastic Modulus, psi	9680-30240
Independent or Explanatory	w	Field Moisture, %	6.9 - 17.2
	γ_d	Field Dry Unit Weight, pcf	100.1- 115.3
	w_{opt}	Optimum Moisture Content, %	10.4 - 17.7
	$\gamma_{d\ max}$	Maximum Dry Unit Weight, pcf	106.2 – 123.3
	PI	Plasticity Index, %	1 – 20
	P_{200}	Passing Sieve Size 200	12 - 99
	S	Degree of Saturation with Field Moisture and Field Dry Unit Weight, %	41.6-72.3
	S_{opt}	Degree of Saturation with Optimum Moisture and Maximum Dry Unit Weight, %	76.6-90.8

1 psi = 6.89 kPa
1 pcf = 0.157 kN/m^3

Table 4.7 Correlation Matrix of Basic Variables Considered in Developing Correction Equation

Variables	E_{PFWD}	γ_d	w	S	PI	P_{200}
E_{PFWD}	1	0.626	-0.643	-0.610	-0.289	-0.305
γ_d	0.626	1	-0.902	-0.739	-0.446	-0.781
w	-0.643	-0.902	1	0.954	0.492	0.749
S	-0.610	-0.739	0.954	1	0.502	0.641
PI	-0.289	-0.446	0.492	0.502	1	0.410
P_{200}	-0.305	-0.781	0.749	0.641	0.410	1

Table 4.8 Correlation Matrix of Transformed-Dependent and -Independent Variables of Correction Equation

Variables	E_{PFWD}	$D_{(f/o)}$	$M_{(f/o)}$	PI/P_{200}	S	S/S_{opt}	γ_d	w
E_{PFWD}	1	0.558	-0.728	-0.115	-0.610	-0.592	0.626	-0.643
$D_{(f/o)}$	0.558	1	-0.460	-0.422	-0.076	-0.100	0.243	-0.114
$M_{(f/o)}$	-0.728	-0.460	1	0.201	0.885	0.922	-0.680	0.841
PI/P_{200}	-0.115	-0.422	0.201	1	0.090	0.011	0.152	-0.030
S	-0.610	-0.076	0.885	0.090	1	0.968	-0.739	0.954
S/S_{opt}	-0.592	-0.100	0.922	0.011	0.968	1	-0.742	0.936
γ_d	0.626	0.243	-0.680	0.152	-0.739	-0.742	1	-0.902
w	-0.643	-0.114	0.841	-0.030	0.954	0.936	-0.902	1

whereas, maximum density will remain unchanged for a given soil. Therefore, the density ratio has a positive and moisture, a negative relation with E_{FPWD}. Figures 4.14 and 4.13 present the trend lines generated by density ratio and moisture. After determining the trend between dependent and independent variables the next step was to perform the multiple linear regression on the selected variables. A statistical analysis employing SPSS was performed with the two selected variables. Linear regression model showed a poor R^2 value, therefore, a nonlinear regression was sought. After numerous trials with several combinations of regression constants (seed values), the following power model (referred to as a correction equation) Eq. 4.4, was selected based on relevant cause-and-effect relation, and reasonably good statistics. Note that the soil parameter PI/P_{200} could not be retained in the equation because of its unacceptable significance level.

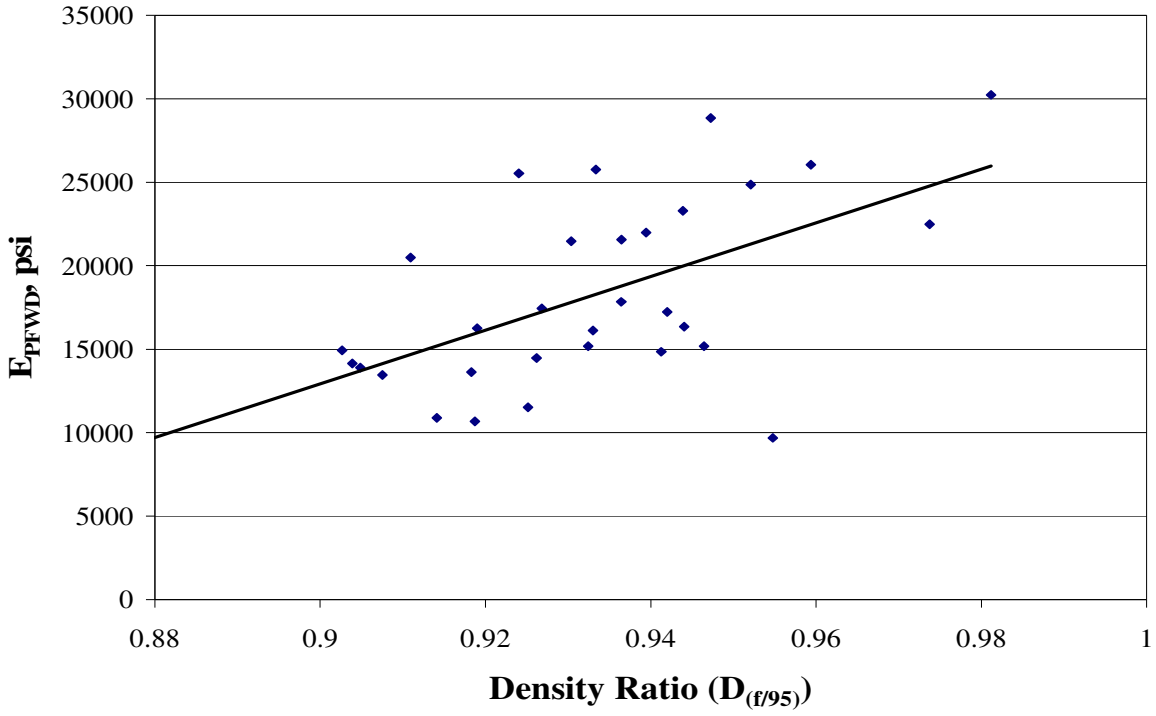

Figure 4.14 Scatter Plot of Prima 100 Modulus (E_{PFWD}) versus Density Ratio ($D_{(f/95)}$)
1 psi = 6.89 kPa

$$E_{PFWD} = 109{,}988\left(D_{\left(f/o\right)}\right)^{5.544}\left(w_{(f)}\right)^{-0.594} \qquad (4.4)$$

$R^2 = 0.63$; Standard Error = 3925

where: E_{PFWD} = measured PFWD elastic modulus (psi);

$D_{(f/o)}$ = ratio of field unit weight to unit weight at optimum moisture; and

$w_{(f)}$ = field moisture (%)

A summary statistics of this model is shown in Table 4.9. The calculated F = 46.67 of this model well exceeds the tabulated F (90, 2, 28) = 2.50, confirming the strong relationship between dependent and independent variables.

Table 4.9 Summary Statistics of Correction Equation

Model	Regression Coefficients	Values	t-Statistics	t-Critical	F-Statistics	F-Critical	RMSE	R^2
Correction-equation	a_1	109987.6	20.118	1.697	46.67	2.50	3925	0.63
	a_2	5.544	19.401					
	a_3	-0.594	-26.248					

In so far as the robustness of the individual regression coefficients is concerned, calculated t values of all of the three coefficients meet 90% confidence levels. The significance of the model was further established by plotting the measured versus predicted E_{PFWD} in Figure 4.15, where they show reasonable agreement. A sensitivity study shows that a 5% change of density

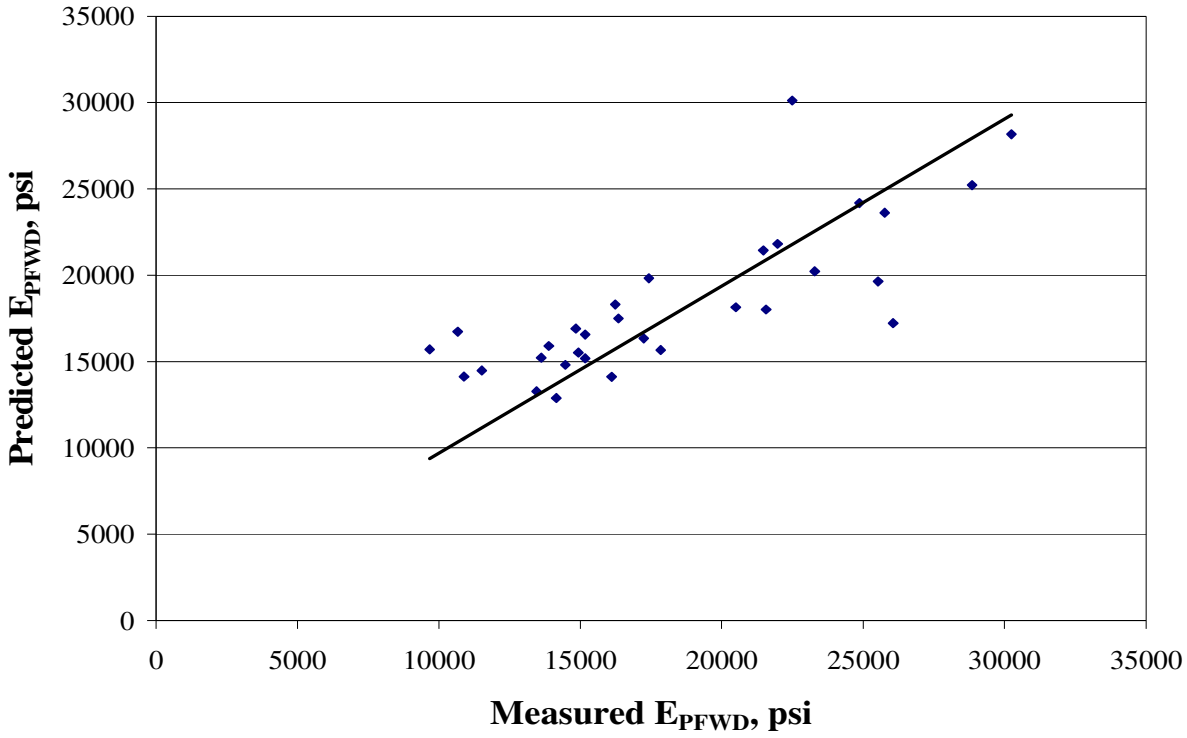

Figure 4.15 Prima 100 Modulus Measured versus Prima 100 Modulus Predicted, 1 psi = 6.89 kPa

ratio brings about 31.1% changes in E_{PFWD}. On the other hand, a 15% (absolute change of 1.8%) change of moisture results in only 10.4% change of E_{PFWD}. Clearly, the compaction has more effect on E_{PFWD} than moisture, suggesting that extreme care should be taken in the field density measurement.

Equations 4.2, 4.3 and 4.4 show that moisture influence on stiffness modulus is relatively minor compared to the effect of compaction. Previous studies summarized in reference 23, where the soil samples were subjected to wetting/drying in the laboratory, moisture was shown to have a significant effect on resilient modulus. In other words, the effect of moisture on field samples is relatively small compared to that on laboratory samples. One possible explanation for this anomalous result is that the laboratory samples undergo unrestrained volume change as they are free to expand/contract with moisture absorption/desorption. It would be worthwhile to pursue the seemingly contradictory effect of moisture on the laboratory tests versus in-situ tests.

4.8 DATA ANALYSIS SOFTWARE

The task at hand in determining a design resilient modulus for new pavement design starts with Prima 100 tests followed by an analysis of the modulus data. Each subgrade section tested may show substantial spatial variation in response (deflection), and in turn, elastic modulus, so that the section in question may, in effect, comprise one or more uniform sections or 'homogeneous units'. A software program to perform two tasks namely, resilient modulus calculation from elastic modulus, and subsectioning to homogeneous units, if warranted, is developed as a part of this study, the details of which can be seen in Chapter 5. This program, employing equation 4.2, calculates station-by-station resilient modulus. With the resilient modulus, we employ cumulative difference approach technique (39) for testing and delineating homogeneous units for the subgrade in question. By way of output, the program prints out the

length of each uniform section, the mean and standard deviation of design resilient modulus for each uniform section, and a resilient modulus of each station plotted with distance along the road.

4.9 CHAPTER SUMMARY

Investigating the applicability of Prima 100 for characterizing subgrade soil by correlating it to resilient modulus, the following empirical relations were developed:

i) E_{FWD} versus E_{PFWD} authenticating the PFWD elastic modulus.

ii) A comprehensive multi-variate linear model with three transformed independent variables, namely, density ratio, moisture ratio, and PI/P_{200} to predict M_{R95} from E_{PFWD}.

iii) An abbreviated linear model with only two transformed independent variables (deleting PI/P_{200}), only to be used if soil index properties are unavailable.

iv) A correction equation with density ratio and moisture assessing the importance of field moisture and field unit weight on E_{PFWD}.

A software program titled PFWDSUBGRADE, developed as a part of this study, performs all of the calculations, and identifies subsections, if any, on the roadway in question. A detailed discussion of this program will be presented in Chapter 5.

CHAPTER 5

PLANNING PRIMA 100 TEST AND CALCULATION OF DESIGN RESILIENT MODULUS

5.1 OVERVIEW

A methodology for choosing a design resilient modulus, relying on Prima 100 test, and corresponding elastic modulus, were the topic of discussion in Chapter 4. Planning Prima test for collecting field data is an important component that supports this methodology. A brief description of field test procedure and advance field preparation required will be covered in the first part of this chapter. Each subgrade project under consideration may be a fraction of a mile or a few miles in length. Regardless inherent spatial variation along the road shall be recognized. If the variation of modulus is statistically significant, the project should be divided into subsections or homogeneous units, as described in the second part of this chapter. Included in the third part of this chapter is a brief description of the exclusive computer program, PFWDSUBGRADE, for arriving at homogeneous unit(s), if warranted.

5.2 PLANNING PRIMA 100 TEST IN THE FIELD

The field test needs to be planned with extreme care ensuring that the data collected from Prima 100 will be minimally affected by spatial variations in the field. The planning of the field test includes the following:

1. Equipment preparation
2. When and where to test?
3. Additional data required for resilient modulus calculation

5.2.1 Equipment Selection

The Prima 100 shall be configured with a light load, ±1730 lbs (7.7 kN), which can be

accomplished by employing the 10 kg falling mass with a drop height adjusted to ±32 in. (813mm). One central sensor will be adequate for routine tests. The overall calibration of the device should be checked by testing a pre-selected site, for example, the laboratory floor ensuring consistent modulus values on repeat tests. This calibration test is recommended on alternate days of a continuous testing program or on the first day after the device has been in storage for a prolonged period.

While Prima 100 is manually operated, the data collection can be accomplished by either a laptop computer or a pocket PC (PDA) in conjunction with a Bluetooth. Bluetooth networking transmits data via low-power radio waves. The low-power limits the range of a Bluetooth device to about 35 feet. From the point of view of portability and ease of handling, the PDA is recommended for field tests.

5.2.1.1 Test Procedure: At each station two seating loads followed by four or more load drops of 1730 ± pounds shall be applied. The load and deflection history displayed on the monitor needs to be reviewed, checked for any anomalies and recorded, and the data collection should be repeated for all of the load repetitions. In a few instances, the measured modulus at a station was relatively large (50 to 100% more) compared to that at an adjacent station in a nominally identical test section. Lateral shifting of the bearing plate upon the load impact could be a reason for this anomaly. A typical screen display after a load drop is displayed in Figure 3.3. Tests shall be repeated at constant intervals (or uniform spacing) from the beginning to the end of the project. Note that the last station (or the project end) needs be tested, regardless if the last section is equal to or smaller than the predetermined interval. Though the test interval (spacing) is left to the discretion of the project engineer, based on the precision required and practicality, a test interval of 100 ft. (30 m) is recommended.

5.2.2 When and Where to Test?

Subgrade soil, though compacted to specified density and moisture, could become soft when it absorbs excessive moisture resulting from precipitation for an extended period of time. Likewise, it could become hard when dry, as can be expected during a prolonged dry spell. Especially, some coarse-grain soils could lose strength when subject to extreme drought. For these reasons, it is important to schedule FWD testing when the prevailing moisture is close to optimum moisture. From practical considerations, the moisture during tests shall be within the upper limit of optimum moisture +2 percent, and the lower limit of 75 percent of optimum. Soon after a blading operation, either preceding the acceptance of the 'grading contract' or preparing for subbase/base construction, will be an opportune time for Prima 100 test.

Test locations along the road shall be so chosen as to avoid loose surface material and wheel ruts due to construction traffic. Uneven subgrade surface could result in load plate not being seated properly, giving rise to asymmetrical stress distribution affecting sensor deflections. The test location shall be horizontal as far as practical, though the limiting slope, according to Carl Bro (37) is 10%. Loose surface material also affects the sensor deflection. Experience suggests that loose particulate material shifts while the load is being dropped. Figure 5.1 is an illustration of a sensor imprint where coarse loose particles congregate around the sensor tip, caused primarily by vibration due to impacting load. If subgrade to be tested is uneven and/or rutted, it shall be bladed and lightly recompacted before Prima 100 testing to ensure a reasonably smooth surface for proper seating of the plate, and the sensors. Finally, test locations shall be aligned such that they are within 10 ft. of the centerline of the paved surface in 14 ft. wide lanes or 8 ft. in 12 ft. wide lanes.

5.2.3 Additional Data Required

The desired state of subgrade soil during in-situ test shall be moisture at the optimum level and unit weight at the MDOT specification level, for example, 95% compaction. This is seldom feasible because it would be impractical to perform Prima 100 test immediately after the compaction and finishing operation of the grading contract, or any time sooner. Even during this window of opportunity, moisture and density may not be at the desired level – the

Figure 5.1 Photograph of Imprint Showing Loose Coarse Particles Congregating Around the First Sensor Tip

specified values as permitted during construction – as a practical measure. In order to overcome this problem, the prediction equation includes the field unit weight and moisture as independent variables, which should be measured in conjunction with Prima 100 test. The Nuclear device shall be employed for this purpose.

Also for solving the prediction model equation, Eq. 4.2, unit weight at 95% compaction and optimum moisture of the soil being tested are required. The project files include this data, developed routinely for QC/QA of the grading contract. An alternate method would be to employ the following empirical equations proposed in a study in conjunction with the development of M-EPDG (55). The optimum moisture for standard compaction can be estimated by equation 5.1:

$$\begin{aligned} w_o &= 1.3 wPI^{0.73} + 11 \quad && wPI > 0 \\ w_o &= 8.6425 D_{60}^{-0.1038} \quad && wPI = 0 \end{aligned} \tag{5.1}$$

where: w_o = optimum moisture content at maximum dry density obtained by standard compaction (AASHTO T99);

wPI = plasticity index (PI) times the percent passing the #200 sieve (in decimal); and

D_{60} = particle size for which 60% of the material is finer in mm.

The degree of saturation at optimum moisture content and maximum dry density, S_o, shall be obtained from equation 5.2:

$$S_o = 6.752 wPI^{0.147} + 78 \tag{5.2}$$

Equation 5.3 represents the correlation developed for G_s (specific gravity of solids):

$$G_s = 0.041 wPI^{0.29} + 2.65 \tag{5.3}$$

With known w_o, S_o and G_s, and employing equation 5.4, dry unit weight at optimum condition, γ_{do}, shall be determined.

$$\gamma_{do} = \frac{G_s \gamma_w}{1 + \frac{w_o}{S_o}} \tag{5.4}$$

where: γ_w = unit weight of water

Unit weight at 95% compaction, required in equation 4.2, can thus be estimated, based on soil index properties, or by AASHTO T99 tests conducted in conjunction with the grading contract.

In order to authenticate these equations, optimum moisture content and dry unit weight at optimum condition are calculated for the 35 soils tested in this project and listed in columns 4 and 5 in Table 5.1. Comparing these values with the laboratory counterparts, listed in columns 2 and 3 in the same table, it is noted that 88% of T-99 optimum moisture measurements are below the empirically derived moisture, whereas, an opposite trend is observed with maximum dry unit weight, 85% of the T99 unit weights top their empirical counterpart. That is, the empirical equations over predict the optimum moisture and under predict the maximum unit weight.

5.3 SELECTION OF DESIGN UNIT

When considering a reasonably large pavement project, Prima modulus along the prepared subgrade could experience significant variability, signaling statistically different units within a given project. Frequently, the engineer must rely on the analysis of a measured pavement response variable (e.g., modulus) for unit delineation. The designer could develop a plot of measured response variable as a function of the distance along the project. This can be done manually or through computerized data analysis-graphic software. To illustrate the approach, the problem of sectioning a highway based on friction number (FN (40)) is included herein. Figure 5.2 is a plot of friction number results, FN (40), versus station number along an actual highway system. The proposed methodology is adopted from 1993 AASHTO Guide (39).

Once a spatial plot of subgrade modulus has been generated, it may be used to delineate units through several methods. The simplest of these is a visual examination to subjectively determine where relatively unique units occur. In addition, several analytical methods are

Table 5.1 Comparison of AASHTO T-99 Optimum Moisture and Maximum Dry Unit Weight with Those Calculated from Empirical Equations

Soil No.	AASHTO T-99		Empirical Equations	
	Optimum Moisture (%)	Maximum Dry Unit Weight (pcf)	Optimum Moisture (%)	Maximum Dry Unit Weight (pcf)
2-(1,2)	13.9	116.3	17.7	109.7
2-(4)	13.1	117.6	19.0	107.2
2-(5)	13.6	117.6	16.6	111.9
3-(1,2)	11.3	120.9	14.5	116.3
3-(3)	12.9	116.9	17.7	109.7
3-(4)	10.8	123.3	13.6	118.0
3-(5)	11.7	120.7	14.8	115.5
4-(1)	11.7	121.8	15.4	114.4
4-(2)	10.4	123.3	13.8	117.8
4-(4,5)	10.7	123	13.0	119.4
5-(1,2)	13	116.5	17.2	110.6
5-(4)	10.6	121	12.6	120.2
5-(5)	12.6	118	18.3	108.5
6-(1)	16.1	112.5	19.2	106.8
6-(2,4)	17.1	110.2	18.7	107.8
6-(5)	16	108.3	19.8	105.7
7-(1)	15.4	110.7	18.4	108.4
7-(2)	16.3	110.4	18.9	107.4
7-(4,5)	17.7	106.2	17.4	110.2
8-(1,2)	15.7	110.8	17.2	110.7
8-(4,5)	15.2	111.7	18.6	107.9
9-(2)	15.8	107.5	16.9	111.3
9-(4)	15.5	110.9	16.8	111.4
10-(1)	12.6	117.9	17.3	110.4
10-(2,4)	12.1	120.1	15.1	114.8
10-(5)	11.7	121.4	16.0	113.0
11-(1,2)	12.7	117.7	15.3	114.5
11-(4,5)	13	117.2	17.5	110.0
12-(1,2)	14.3	111.1	19.1	106.9
12-(4,5)	15.8	110.3	19.8	105.6
13-(1)	13.3	118	11.5	122.1
13-(2)	13	116.9	15.2	114.8
13-(5)	11.6	121.1	14.1	117.0
14-(4)	12.5	117.8	11.3	122.3
14-(5)	12	118.9	12.4	120.5

1 pcf = 0.157 kN/m^3

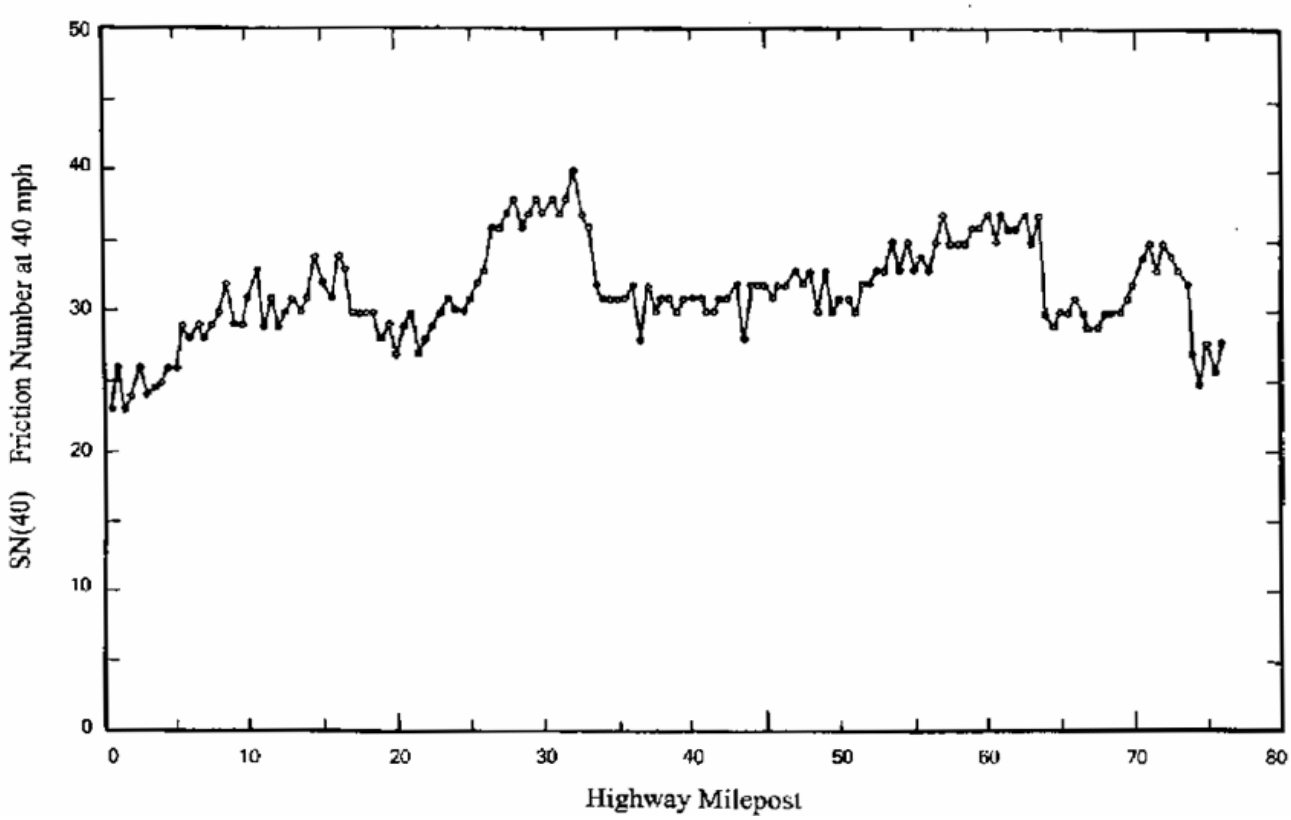

Figure 5.2 FN (40) Results versus Distance Along Project (Adapted From Reference 39)

available to help delineate units, with the recommended procedure being the "cumulative difference". When this report was reviewed, it was suggested that the sensitivity of M_R on pavement thickness/life could be another criterion to delineate subsections. This would require the development of an entirely different algorithm warranting extensive additional resources. The cumulative difference procedure, readily adaptable to computerized evaluation, relies on the simple mathematical fact that when the variable Z_c is plotted as a function of distance along the project, unit boundaries occur at the location where the slopes (Z_c vs. distance) change sign. Zc, designated cumulative difference variable, is defined as the difference between the area under the response curve at any distance and the total area developed from the overall project average response at the same distance. Figure 5.3 is a plot of the cumulative difference variable for the data shown in Figure 5.2. For this example, 11 preliminary analysis units are defined. The

engineer must then evaluate the resulting length of each unit to determine whether two or

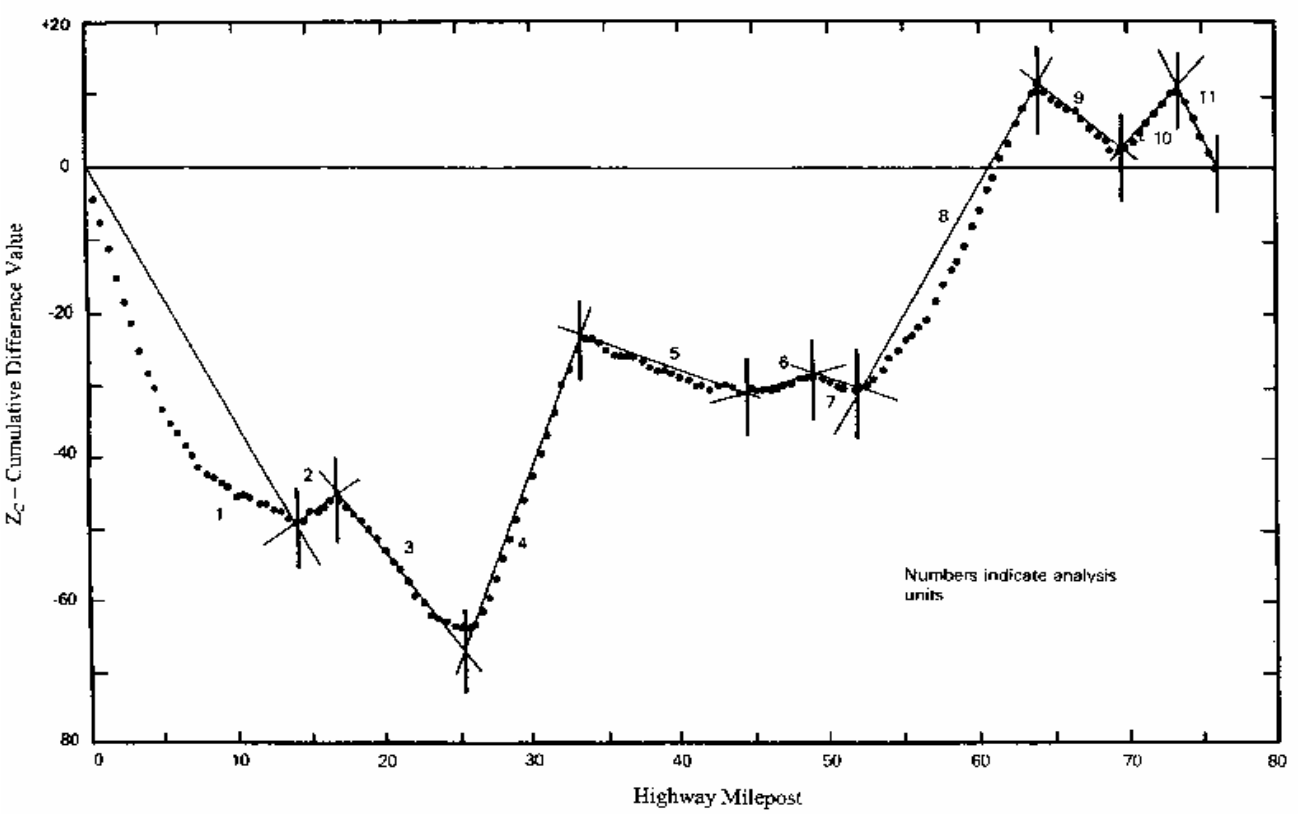

Figure 5.3 Delineating Analysis Units by Cumulative Difference Approach (Adapted From Reference 39)

more units should be combined for practical construction considerations and economic reasons. The combination of units should be done considering the sensitivity of the mean modulus values of each unit upon performance of future designs.

5.4 COMPUTER PROGRAM, PFWDSUBGRADE, TO CALCULATE DESIGN MODULUS

As alluded to before, the program, PFWDSUBGRADE, performs two major tasks in arriving at a design modulus. First, accepting elastic modulus data from Prima 100 software, it calculates/derives resilient modulus of soil at each station employing Eq. 4.2. Second, employing these station-by-station resilient moduli in an analytical procedure known as

cumulative difference, the program delineates homogeneous units, outputting the length of each unit (in the event of identifying multiple units) and the corresponding resilient moduli – both mean and standard deviation – which shall form the design resilient moduli. The logic of these operations is presented in the flow chart in Figure 5.4. Detailed operation of the program is charted in *Appendix C*. Note that the output of the program includes a plot of the resilient modulus at each station as a function of distance along the project. This plot should serve as a guide in combining adjacent units to form "design units". Practical construction considerations and economic reasons are likely to govern these decisions. For example, should there be short sections of relatively soft material, they are to be upgraded with additives (cement, lime, lime-fly ash, etc.) to facilitate merger with contiguous homogeneous units.

5.5 CHAPTER SUMMARY

Planning the Prima 100 test in the field, including configuring the device and site preparation for subgrade modulus measurement, is described. Test specifics, for example, seating load and repetitions required, are also a part of this discussion. With the calculated modulus response in each project, a methodology for unit delineation is presented. Finally, a flow chart outlining the operations necessary to accept Prima 100 modulus data and to output homogeneous units (with boundaries identified) and corresponding design resilient modulus constitute the last section of this chapter.

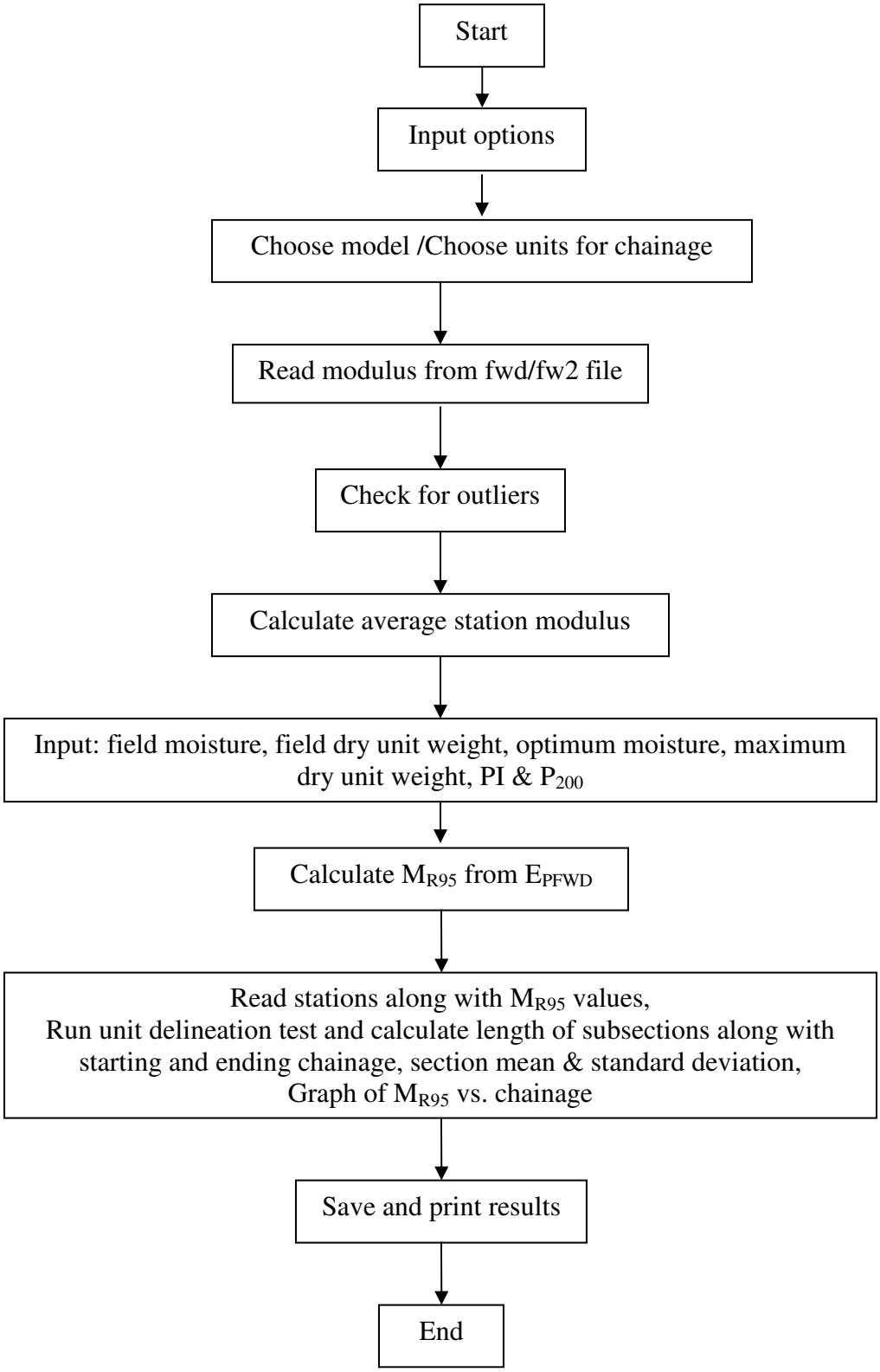

Figure 5.4 Flow Chart of Program PFWDSUBGRADE

CHAPTER 6

SUMMARY AND CONCLUSIONS

6.1 SUMMARY

The objective of this study was to investigate whether Prima 100 could be employed for subgrade characterization. A research program, including field and laboratory tests, was undertaken seeking a relation between Prima modulus, E_{PFWD}, and laboratory resilient modulus, M_R. Thirteen as-built subgrade test sections were selected and tested employing FWD, followed by Prima 100 and nuclear device for moisture and unit weight. Disturbed bag samples were collected for particle size analysis, Atterberg limits, standard Proctor test, and resilient modulus test employing AASHTO T-307 protocol. In an attempt to authenticate the Prima modulus, a relationship between FWD elastic modulus, E_{FWD}, and Prima elastic modulus was derived, showing E_{FWD} slightly larger ($\simeq$9%) than E_{PFWD}. Elastic modulus from Prima 100 test was regressed against laboratory resilient modulus in conjunction with three more explanatory variables, namely, density ratio, moisture ratio and PI/P_{200}, resulting in a comprehensive model. Employing the same database, an abbreviated model was also developed deleting the soil index properties, namely, PI/P_{200} ratio. In order to investigate how moisture and density affect Prima modulus measurement, a correction equation was sought by employing density ratio and field moisture as explanatory variables.

6.2 CONCLUSIONS

The multiple linear regression equation established for predicting resilient modulus from Prima modulus, with density ratio, moisture ratio, and PI/P_{200} as secondary explanatory variables is shown to be significant that it is tentatively recommended for estimating resilient modulus. In-situ Prima modulus is shown to be significantly influenced by unit weight with moisture showing

relatively minor influence. What follows are the major conclusions/observations pertaining to the adaptability of Prima 100 for in-situ tests.

1. Prima 100 is a viable device for characterizing subgrade soil provided the stress level is in the linear range (±1730 lbs on a 12-in. plate meets this requirement)
2. Besides soil type, density is the dominant variable, followed by moisture, affecting in-situ modulus. Laboratory studies of other researchers (23, 32), however, reported opposing results, where moisture having the foremost influence.
3. Prima test is significantly affected by inadequate/improper seating of the bearing plate resulting from uneven and/or sloping surface.
4. Verticality of the guide rod is another causal factor affecting the repeatability of Prima 100 test results.
5. Repeatability of Prima 100 is relatively weak in a soft soil as compared to in a stiff soil.
6. When employing Boussinesq's elastic half space equation for calculating elastic modulus, the bearing plate rigidity or stress distribution factor and phase lag should be recognized.
7. Field test results are conclusive to suggest significant spatial variability in stiffness modulus.

6.3 RECOMMENDATIONS FOR FUTURE RESEARCH

This study investigated the feasibility of using Prima 100 to obtain elastic modulus and thereby estimates resilient modulus of subgrade soil. Some suggested recommendations are the following:

1. Despite our initial plans to include a wide variety of soil groups, owing to scarcity of appropriate graded subgrades, the database was deficient in some soils, for

example, A-3 (fine sand) and A-7 (high plasticity clay). Therefore, the model for resilient model prediction shall be enhanced by populating the database with test results from the two groups of soils missing in the present study.

2. The preliminary findings of this study, that suggests the effects of moisture and density on in-situ test results (for elastic modulus) are different from their effects on laboratory test results (for resilient modulus), shall be thoroughly investigated.
3. In view of significant problems with proper seating of the bearing plate, a recommendation would be to equip the plate with a rubber pad mitigating plate slippage and also improving the contact stress distribution close to uniform.
4. Though the peak method of modulus calculation from impulse test is simple and robust, the viability of this approach on different soils need to be investigated by initiating a study of the load and deflection history employing spectral analysis techniques.

6.4 IMPLEMENTATION

With a satisfactory prediction model for estimating resilient modulus from in-situ tests with Prima 100, the use of that device shall be implemented on a trial basis. Validation of the prediction model needs to be considered before state-wide implementation of tests, however. With in-situ elastic modulus obtained from Prima software, resilient modulus may be calculated employing equation 4.2, followed by a plot similar to that in Figure 5.3, partitioning the roadway into subsections. Alternately, the computer program PFWDSUBGRADE performs all of the above steps.

The entire procedure of reading the Prima modulus and soil properties, and making calculations, outputting homogeneous units with mean and standard deviation of resilient

modulus, is programmed and furnished for ready-use by MDOT. The ability to perform the data analysis in the field, if desired, enables the engineer to verify the accuracy of subsectioning, and to some extent validate the resilient modulus values predicted by the analysis procedure.

6.5 BENEFITS

The principle benefit of the prediction model developed in this research lies in being able to use Prima 100 for subgrade characterization. Subgrade resilient modulus for pavement design, as required in the 2002 M-EPDG, can now be determined employing the relation (Eq. 4.2) developed in this investigation, though further validation of the model is recommended. A deflection-based subgrade characterization is preferred over laboratory estimated resilient modulus primarily for two reasons: (i) in-situ tests circumvent disturbance (recompaction/decompaction) affecting the test outcome, and (ii) in-situ tests capture the stress state (resulting from traffic load) in the material better than that can be attained in the harmonized RLT test. With the results accomplished in this research incorporated in a user-friendly program, feasibility of in-situ test using Prima 100 directly on subgrade is indeed enhanced.

Recognition of spatial variability of soil compaction uncovered in this study could lead to better construction control specifications, in terms of employing statistical quality control. As Prima 100 is a cost-effective portable device, and currently receiving recognition, its use in subgrade evaluation is a logical choice and is likely to be adopted by pavement engineers.

REFERENCES

1. Witczak, M., Qi, X. and Mirza, M.W., "Use of Nonlinear Subgrade Modulus in AASHTO Design Procedure", *ASCE Journal of Transportation Engineering,* Vol. 121, No. 3, 1995, pp. 273-282.

2. National Cooperative Highway Research Program, 1-28A Project, *"Harmonized Test Methods for Laboratory Determination of Resilient Modulus for Flexible Pavement Design*, *Annex A-1"*, Transportation Research Board, Washington, DC, 2003.

3. Ali, N.A. and Khosla, N.P., "Determination of Layer Moduli Using a Falling Weight Deflectometer", *Transportation Research Record 1117*, TRB, National Research Council, Washington, DC, 1987, pp. 1-10.

4. Newcomb, D.E., "Comparison of Field and Laboratory Estimated Resilient Modulus of Pavement Materials", Asphalt Paving Technology, *Association of Asphalt Paving Technologists*, Vol. 56, February 1987, pp. 91-106.

5. Von Quintus, H.L. and Killingsworth, B.M., "Comparison of Laboratory and In-Situ Determined Elastic Moduli", Proceedings of the *76th Annual Meeting of the Transportation Research Board*, Washington, DC, January 1998.

6. Chen, B., Dar-Hao, Bilyeu, J. and He, Rong, "Comparison of Resilient Moduli Between Field and Laboratory Testing: A Case Study", Proceedings of the *78th Annual Meeting of the Transportation Research Board*, Washington, DC, January 1999, pp. 25.

7. Houston, W.N., Mamlouk, M.S. and Perera, R.W.S., "Laboratory versus Nondestructive Testing for Pavement Design", *ASCE Journal of Transportation Engineering*, Vol. 118, No. 2, 1992, pp. 207-222.

8. Van Deusan, D.A., Lenngren, C.A. and Newcomb, D.E., "A Comparison of Laboratory and Field Subgrade Moduli at the Minnesota Road Research Project", *Nondestructive Testing of Pavements and Backcalculation of Moduli*, ASTM STP 1198, H.L. Von Quintus et al., eds., ASTM, 1994.

9. Nassar, W., Al-Qadi, I., Flinlsch, G.W. and Appea, A., *"Evaluation of Pavement Layer Response at the Virginia Smart Road"*, Virginia Polytechnic Institute, Blacksburg, VA, 1990.

10. Rahim, A. and George, K.P. "Falling Weight Deflectometer for Estimating Subgrade Elastic Modulus", *ASCE Journal Transportation Engineering*, Vol. 129, No. 1, 2003, pp. 100-107.

11. George, K.P., *"Falling Weight Deflectometer for Estimating Subgrade Resilient Moduli"*, Final Report, FHWA/MS-DOT-RD-03-153, Mississippi Department of Transportation, Jackson, MS, October 2003.

12. Seed, S.B., Ott, W.C., Milchail, M. and Mactutis, J.A. "Evaluation of Laboratory Determined and Nondestructive Test Based Resilient Modulus Values From WesTrack Experiment", *Nondestructive Testing of Pavements and Backcalculation of Moduli*, ASTM STP 1375, S. Tayabji and O. Lukanen eds., ASTM, 2000.

13. Fleming, P.R., Rogers, CDF and Frost, MW, 2000, "A Comparison of Devices for Measuring Stiffness In-Situ", *Proc. of the 5th Int. Symp. on Unbound Aggregates in Roads (UNBAR 5)*, Edited by Dawson, A., Balkema, pp. 193-200.

14. Fleming, P.R., Lambert, J.P., Rogers C.D.F. and Frost M.W., *"In-Situ Assessment of Stiffness Modulus for Highway Foundation During Construction"*, Loughborough University, Loughborough, UK, 2002.

15. Philips, L.D., *"Field Evaluation of Rapid Airfield Assessment Technologies"*, ERDC/GSL TR-05-11, U.S. Army Corps of Engineers, ERDC, Vicksburg, MS, 2005.

16. Gudishala, R., *"Development of Resilient Modulus Prediction Models for Base and Subgrade Pavement Layers from In-Situ Devices Test Results"*, M.S. Thesis, Louisiana State University, Baton Rouge, LA, 2004.

17. Seed, H.B., Chan, C.K. and Lee, C.E., "Resilience Characteristics of Subgrade Soils and Their Relation to Fatigue Failures in Asphalt Pavement", *Proc. First Int. Conf. on Struct. Design of Asphalt Pavements*, University of Michigan, Ann Arbor, 1962.

18. National Cooperative Highway Research Program, *"Guide for Mechanistic-Empirical Design of New and Rehabilitated Pavement Structures Design Inputs"*, Transportation Research Board, Washington, DC, 2004.

19. Van Til, McCullough, B., Vallerga, B. and Hicks, R., "Evaluation of AASHTO Interim Guides for Design of Pavement Structures", NCHRP 128, *Highway Research Board*, 1972.

20. George, K.P., *"Prediction of Resilient Modulus from Soil Index Properties"*, Final Report, FHWA/MS-DOT-RD-04-172, Mississippi Department of Transportation, Jackson, MS, November 2004.

21. George, K.P. and Uddin, W., *"Subgrade Characterization for Highway Pavement Design"*, FHWA/MS-DOT-RD-00-131, Final Report, Mississippi Department of Transportation, Jackson, MS, December 2000.

22. Han, Y., Petry, T.M. and Richardson, D.N., "Resilient Modulus Estimation System for Fine-Grained Soils". *Proceedings of the 85th Annual Meeting of Transportation Research Board*, Washington, DC, January 2006.

23. National Cooperative Highway Research Program, *"Guide for Mechanistic-Empirical Design of New and Rehabilitated Pavement Structures, Appendix DD-1"* Transportation Research Board, Washington, DC, 2000.

24. Fredlund, D.G., Bergan, A.T. and Wong, P.K., "Relation Between Resilient Modulus and Stress Conditions for Cohesive Subgrade Soils", *Transportation Research Record 642*, TRB, National Research Council, 1977, Washington, DC, pp. 73-81.

25. Gehling, W.Y.Y., Ceratti, J.A., Nunez, W.P. and Rodrigues, M.R., "A Study on the Influence of Suction on the Resilient Behavior of Soils from Southern Brazil", *Proceedings of the Second Int. Conf. On Unsaturated Soils*, Vol. 2, Beijing, China, 1998.

26. Lekarp, F., Isacsson, U. and Dawson, A., "State of the Art I: Resilient Response of Unbound Aggregates", *ASCE Journal of Transportation Engineering*, Vol. 126, No. 1, Jan./Feb., 2000, pp. 76-83.

27. Drumm, E.C., Rainwater, R.N., Andrew, J., Jackson, N.M., Yoder, R.E. and Wilson, G.V., "Pavement Response due to Seasonal Changes in Subgrade Moisture Conditions", *Proceedings of the Second Int. Conf. On Unsaturated Soils*, Vol. 2, Beijing, China, 1998.

28. Edil, T.B. and Motan, S.E., "Soil-Water Potential and Resilient Behavior of Subgrade Soils", *Transportation Research Record 705*, TRB, National Research Council, 1979, Washington, DC, pp. 54-63.

29. Yang, S., Huang, W. and Tai, Y., "Variation of Resilient Modulus with Soil Suction for Compacted Subgrade Soils", *Proccedings of the 84th Annual Meeting of Transportation Research Board*, Washington, DC, January 2005.

30. Yau, A. and Von Quintus, H.L., *"Study of LTPP Laboratory Resilient Modulus Test Data and Response Characteristics"*, Final Report, October 2002 (FHWA-RD-02-051), USDOT, FHWA, October 2002.

31. Dai, S. and Zollars, J., "Resilient Modulus of Minnesota Road Research Project Subgrade Soil", *Transportation Research Record 1786*, TRB, National Research Council, Washington, DC, 2002, pp. 20-28.

32. Santha, B.L., "Resilient Modulus of Subgrade Soils: Comparison of Two Constitutive Equations", *Transportation Research Record 1462*, TRB, National Research Council, Washington, DC, pp. 79-90.

33. Newcomb, D.E. and Birgisson, B., "Measuring In-Situ Mechanical Properties of Pavement Subgrade Soils", *NCHRP Synthesis 278*, *Transportation Research Board*, Washington, DC, 1999.

34. Gros, C., "Use of a Portable Falling Weight Deflectometer: Loadman", University of Oulu, *Publications of Road and Transportation Laboratory*, No. 20, 1993.

35. Kudla, W., Floss, R., and Trautmann, C., "Dynamic Plate Compression Test – Rapid Testing Method for Quality Assurance of Unbound Course", *Autobahn 42*, No. 2, (Published in German), 1991.

36. Rogers, C.D.F., Brown, A.J. and Fleming, P.R., "Elastic Stiffness Measurement of Pavement Foundation Layers", *Unbound Aggregates in Roads 4*, Edited by Dawson, A. and Jones, R.H., Nottingham University, 1995.

37. Carl Bro Pavement Consultants website: http://www.carlbro.dk/prima100; Accessed in December 2005.

38. Nazzal, M.D., *"Field Evaluation of In-Situ Test Technology for QC/QA During Construction of Pavement Layers and Embankments"*, M.S. Thesis, Louisiana State University, Baton Rouge, LA, 2003.

39. *"AASHTO Guide for Design of Pavement Structures, 1986/1993"*, AASHTO, Washington, DC, 1986.

40. Daleiden, J.F., Killingsworth, B.M., Simpson, A.L. and Zamora, R.A., "Analysis of Procedures for Establishing In Situ Subgrade Moduli", *Transportation Research Record 1462*, TRB, National Research Council, Washington, DC, 1994.

41. Akram, T., Scullion, T. and Smith, R.E., "Comparing Laboratory and Backcalculated Layer Moduli on Instrumented Pavement Sections", *Special Technical Publication (STP) 1198*, ASTM, Philadelphia, PA, 1994.

42. Nazarian, S., Yuan, D. and Baker, M.R., "Rapid Determination of Pavement Moduli with Spectral-Analysis-of-Surface-Waves Method", *Research Record 1243-1F, Center for Geotechnical and Highway Materials Research,* University of Texas at El Paso, 1995.

43. Von Quintus, H. and Killingsworth, B., *"Design Pamphlet for the Backcalculation of Pavement Layer Moduli in Support of the 1993 AASHTO Guide for the Design of Pavement Structures"*, *Report No. FHWA-RD-97-076, FHWA, USDOT*, Washington, DC, 1997.

44. Newcomb, D.E., Chabourn, B.A., Van-Deusen, D.A. and Burnham, T.R., *"Initial Characterization of Subgrade Soils and Granular Base Materials at the Minnesota Road Research Project"*, Report No. MN/RC-96/19, Minnesota Department of Transportation, St. Paul, MN, December 1995.

45. Nassar, W., Al-Qadi, I., Flinlsch, G.W. and Appea, A., *"Evaluation of Pavement Layer Response at the Virginia Smart Road"*, Virginia Polytechnic Institute, Blacksburg, VA, 1990.

46. Van Gurp, C., Groenendijk, J. and Beuving, E., "Experience with Various Types of Foundation Tests", *Proc. of the 5th Int. Symposium on Unbound Aggregates in Roads (UNBAR 5)*, 2000, Edited by Dawson, A., and Balkema, pp. 239-246.

47. Kestler, M., Eaton, R., Berg, R., Steinert, B., Smith, C., Aldrich, C. and Humphrey, D., *"Handheld In-Situ Testing Devices for Estimating the Stiffness of Trails and Low Volume Roads"*, Transportation System Workshop, Ft. Lauderdale, FL, 2004.

48. Groenendijk, J., Van Haasteren, C.R. and Van Niekerk, A.A., "Comparison of Stiffness Moduli of Secondary Road Base Materials under Laboratory and In-Situ Conditions", *Proc. of the 5th Int. Symposium on Unbound Aggregates in Roads (UNBAR 5)*, Edited by Dawson A., Balkema, pp. 201-208.

49. Carl Bro a/s, *"Prima 100, Portable Falling Weight Deflectometer"*, User Manual, Pavement Consultants, Denmark, 2004.

50. Huang, Y., "Pavement Analysis and Design", Prentice Hall, Inc., 1993.

51. Hoffman, O., Guzina, B. and Drescher, A., *"Enhancement and Verification Tests for Portable Deflectometers"*, Report MN/RC-2003-10, Minnesota Department of Transportation, St. Paul, MN, 2003.

52. Coleman, H.W. and Steels, W.G., *"Experimentation and Uncertainty Analysis for Engineers"*, John Wiley & Sons, New York, 1989.

53. Teng, P. and Crawley, A., *"Pavement Design System for Mississippi Highways"*, Mississippi Department of Transportation, Jackson, MS, 1983.

54. Jin, M.S., Lee, K.W. and Kovacs, W.D., "Seasonal Variation of Resilient Modulus of Subgrade Soils". *ASCE Journal of Transportation Engineering*, Vol. 120, No. 4, July/August, 1994, pp. 603-616.

55. National Cooperative Research Program, *"Guide for Mechanistic-Empirical Design of New and Rehabilitated Pavement Structure, Appendix DD-2"*, Transportation Research Board, Washington, DC, 2000.

APPENDIX A

RESILIENT MODULUS OF SAMPLES AS A FUNCTION OF STRESS STATE

(TYPICAL RESULTS)

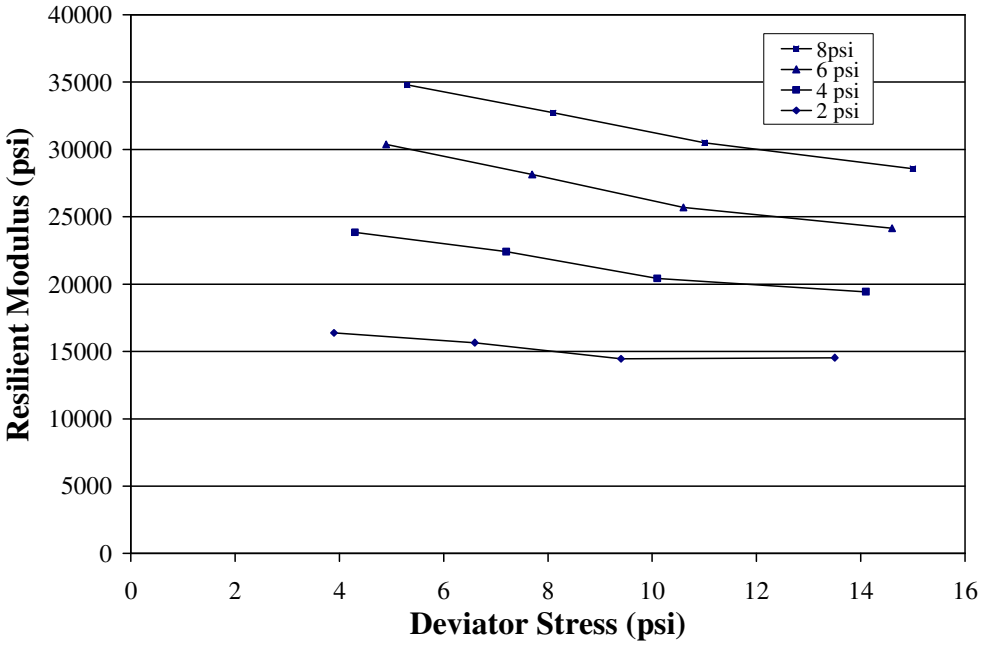

Figure A1 Resilient Modulus versus Deviator Stress of Soil 5(4), 1 psi = 6.89 kPa

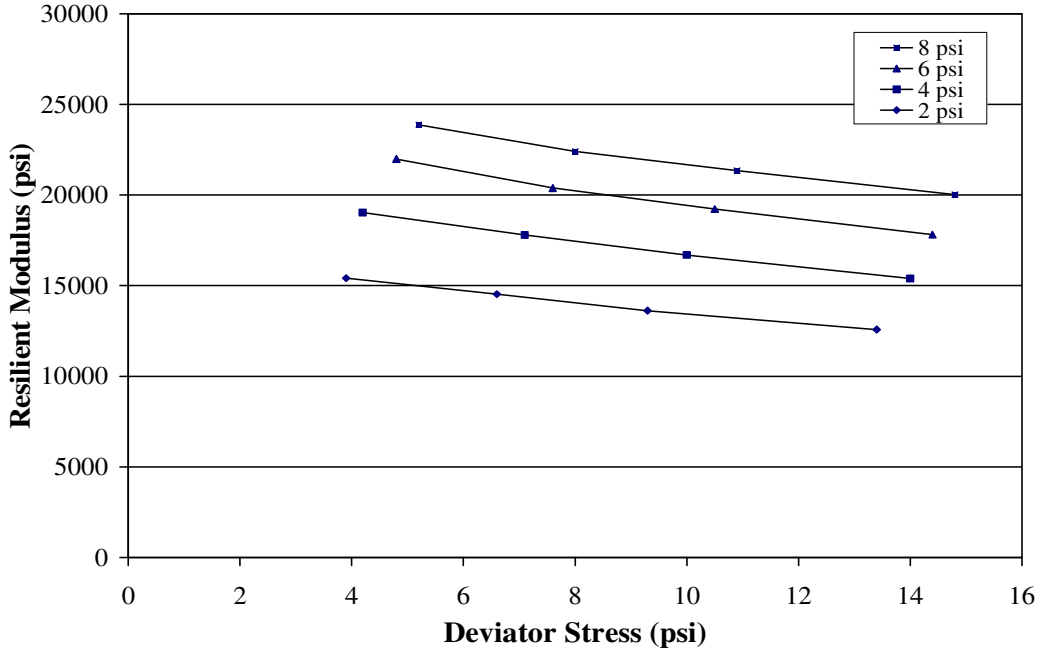

Figure A2 Resilient Modulus versus Deviator Stress of Soil 9(2), 1 psi = 6.89 kPa

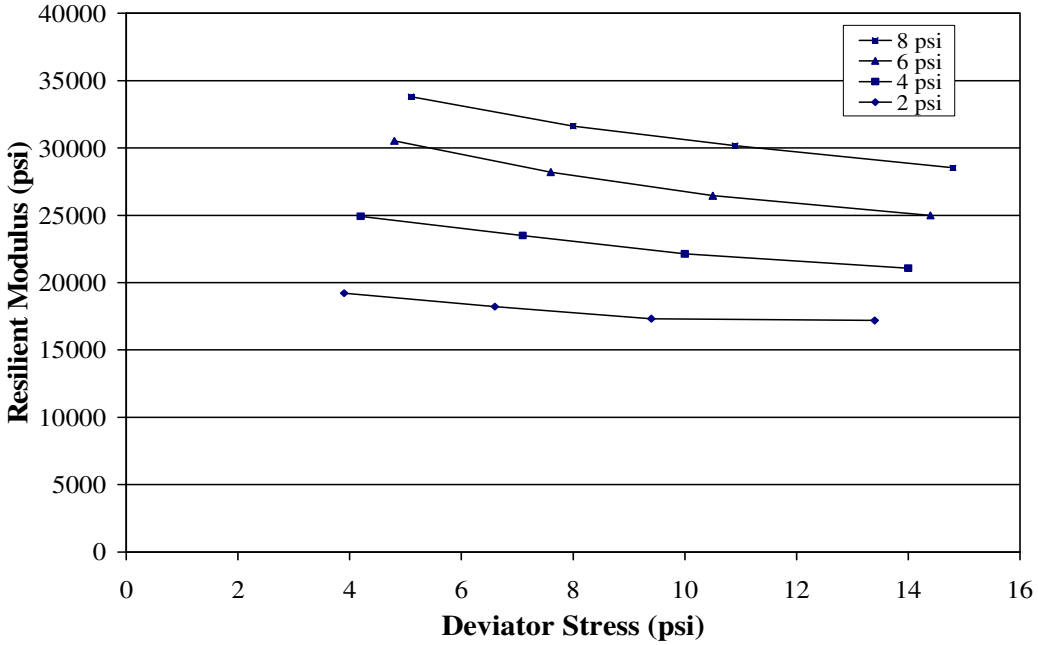

Figure A3 Resilient Modulus versus Deviator Stress of Soil 14(5), 1 psi = 6.89 kPa

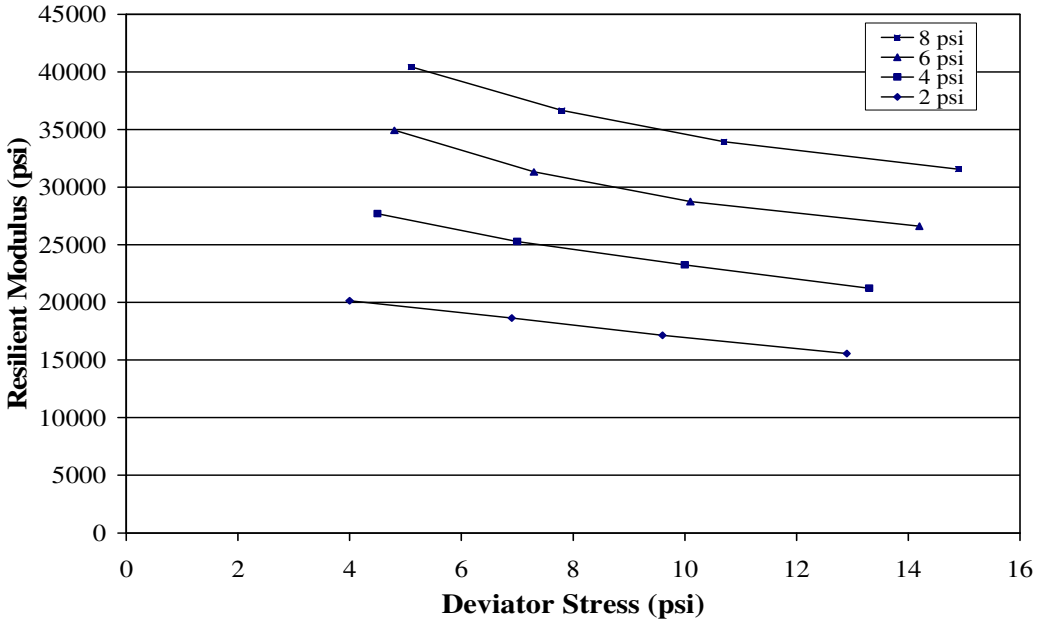

Figure A4 Resilient Modulus versus Deviator Stress of Soil 13(1), 1 psi = 6.89 kPa

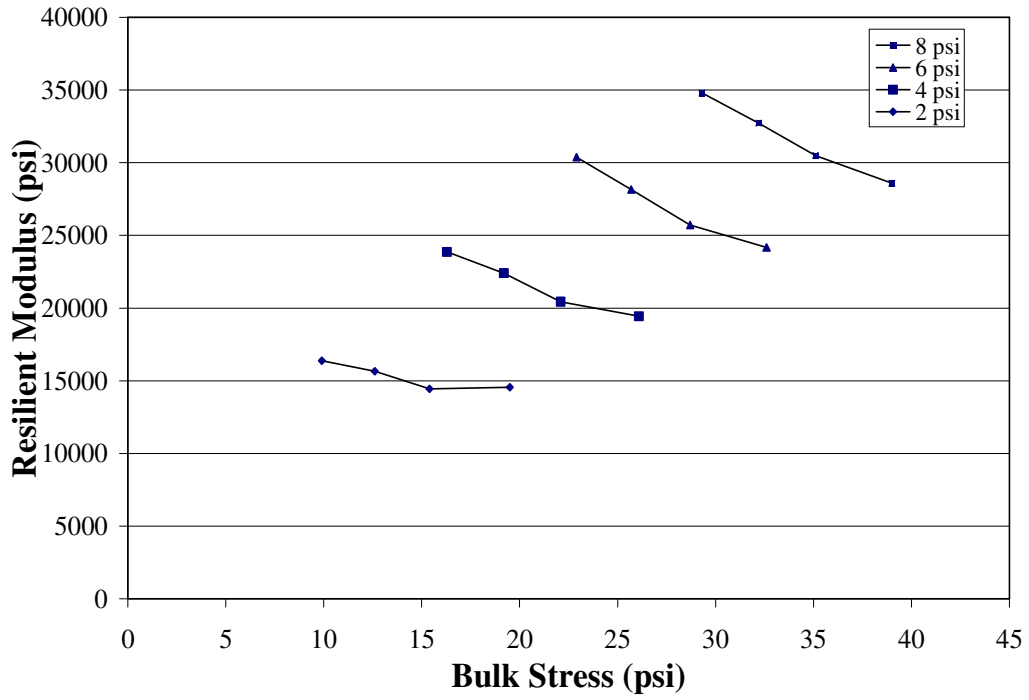

Figure A5 Resilient Modulus versus Bulk Stress of Soil 5(4), 1 psi = 6.89 kPa

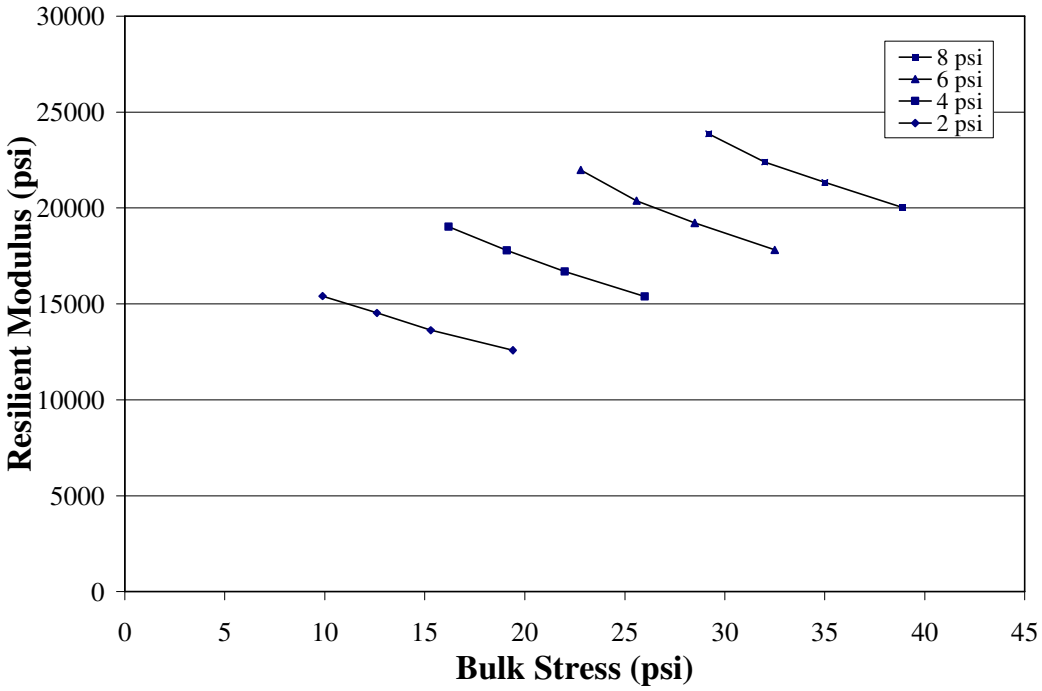

Figure A6 Resilient Modulus versus Bulk Stress of Soil 9(2), 1 psi = 6.89 kPa

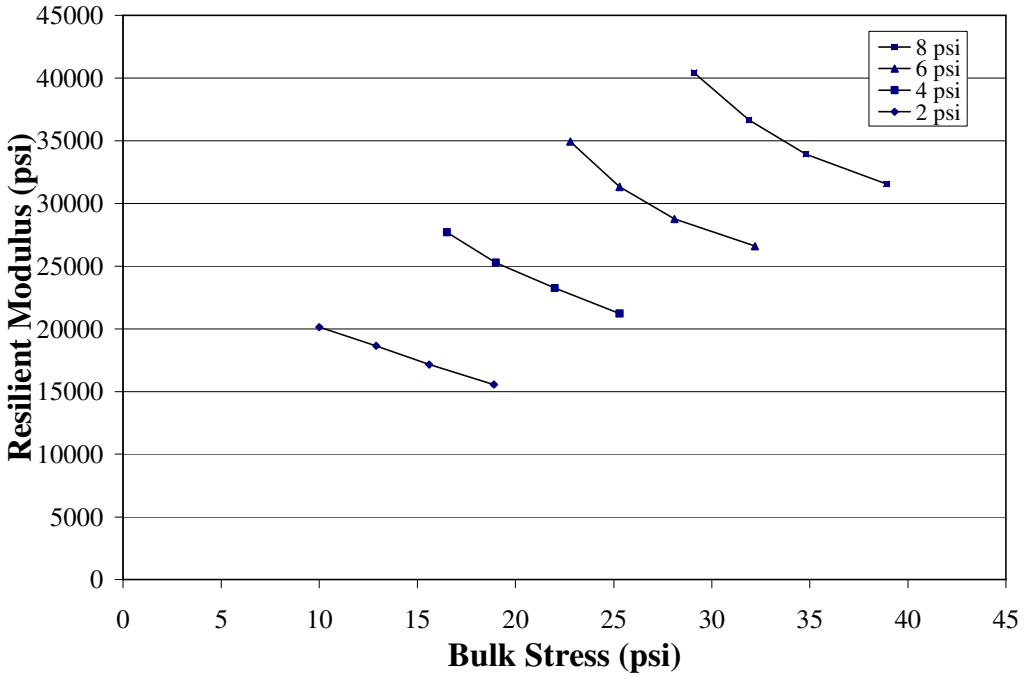

Figure A7 Resilient Modulus versus Bulk Stress of Soil 13(1), 1 psi = 6.89 kPa

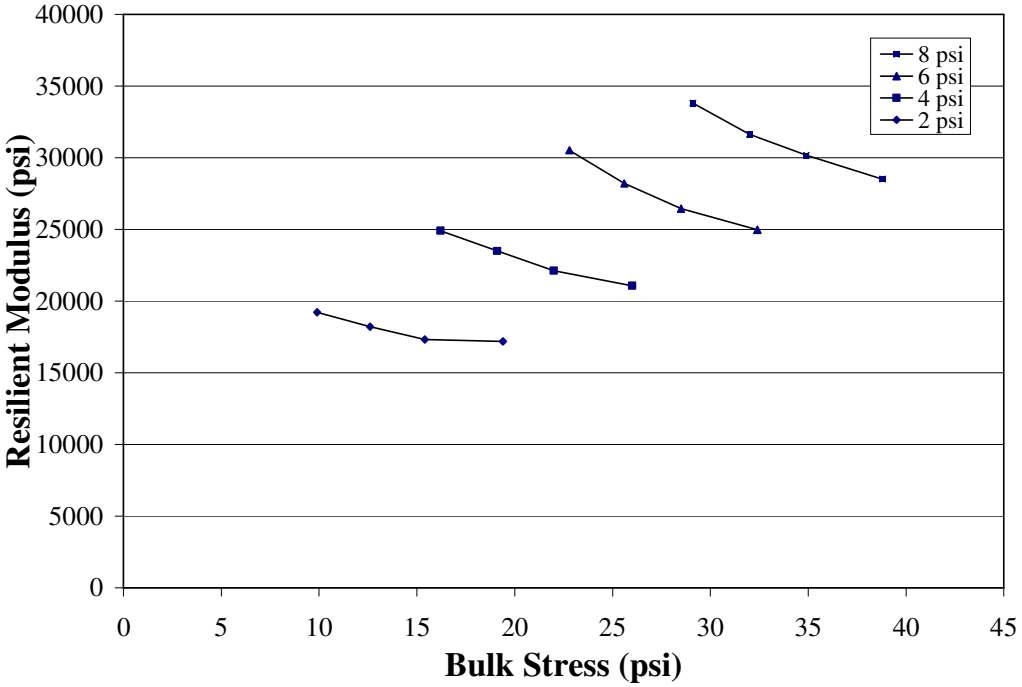

Figure A8 Resilient Modulus versus Bulk Stress of Soil 14(5), 1 psi = 6.89 kPa

APPENDIX B

OPTIONAL PREDICTION MODELS

In addition to Eq. 4.2, which is programmed in the PFWDSUBGRADE software, two other model equations have been derived, with analogous or the same three explanatory variables. The first model with moisture as one of the variables follows:

$$\frac{E_{PFWD}}{M_{R95}} = 3.130 + 4.569 D_{\left(f/95\right)} - 0.011 w - 0.668 \, PI/P_{200} \qquad \text{(B1)}$$

$R^2 = 0.82$; Standard Error = 0.080

Considering the good fit of the model ($R^2 = 0.82$), equation B1 could be an option in predicting M_R, if optimum moisture data is either suspect or not available.

Model B2 is derived with M_{R95} calculated at stress states $\sigma_1 = 10.2$ psi and $\sigma_2 = \sigma_3 = 1.6$ psi, the stress states existed while testing with PFWD (see Table 3.5).

$$\frac{E_{PFWD}}{M_{R95}} = -2.689 + 4.395 D_{\left(f/95\right)} - 0.364 M_{\left(f/o\right)} - 0.572 \, PI/P_{200} \qquad \text{(B2)}$$

$R^2 = 0.67$; Standard Error = 0.128

where: E_{PFWD}/M_{R95} = ratio of measured PFWD elastic modulus to laboratory determined resilient modulus at 95% compaction (Note M_{R95} is calculated at stress states $\sigma_1 = 8$ psi and $\sigma_2 = \sigma_3 = 2$ psi in Eq. B1);

$D_{(f/95)}$ = ratio of field unit weight to unit weight at 95% compaction;

w = field moisture, %,

$M_{(f/o)}$ = ratio of field moisture to optimum moisture; and

PI/P_{200} = ratio of plasticity index (%) to passing sieve size #200 (%).

A summary statistics of these two models are listed in Table B1.

Equation B1 is highly significant since it meets or exceeds the statistical requirements. The impetus for deriving this model was to predict M_{R95} from E_{PFWD} without the use optimum moisture of the soil being tested. Note that the moisture ratio in the original equation (Eq. 4.2) is

Table B1: Summary Statistics of Prediction Models

	Regression Coefficients	Values	t-Statistics	t-Critical	F-Statistics	F-Critical	RMSE	R^2
Model Equation B1	a_1	-3.130	-2.379	1.753	17.884	2.61	0.08042	0.82
	a_2	4.569	3.522					
	a_3	-0.011	-1.430					
	a_4	-0.668	-3.083					
Model Equation B2	a_1	-2.689	-1.127	1.753	7.991	2.61	0.12843	0.67
	a_2	4.395	1.926					
	a_3	-0.364	-1.266					
	a_4	-0.572	-1.644					

subtitled by field moisture, avoiding one piece of data, namely the optimum moisture. As alluded to before in Chapter 4, the fewer the explanatory variables, the better the model will be. One drawback of this model, however, is that the significance or sensitivity of the moisture variable in predicting M_{R95} is diminished, while the role of density is enhanced.

Equation B2 is analogous in all respects to Eq. 4.2, except the E_{PFWD} values employed in the model development. They were calculated with a stress state (σ_1 = 10.2 psi and $\sigma_2 = \sigma_3$ = 1.6 psi) with them tabulated in column 8 of Table 3.4. As can be seen in Table 3.5, those latter stresses resulted from the Prima 100 inducing a 1730-lb load, as opposed to σ_1 = 8 psi and $\sigma_2 = \sigma_3$ = 2 psi, which were the recommendation of M-EPDG. Employing those stresses, the values of column 9 of Table 3.4 were calculated and used to formulate Eq. 4.2. This model, Eq. B2, deserves some attention as the E_{PFWD} values are determined considering the exact stress state at which they are determined in the field, whereas the other set of E_{PFWD} values are based on M-EPDG recommended stress states. Nonetheless, Eq. B2 is not the choice for two reasons: first, the model is not as robust as Eq. 4.2, and second the significance of the moisture ratio is disparaged, which cannot be justified based on the results of previous studies (23).

APPENDIX C

DETAILED FLOWCHARTS OF SOFTWARE PFWDSUBGRADE

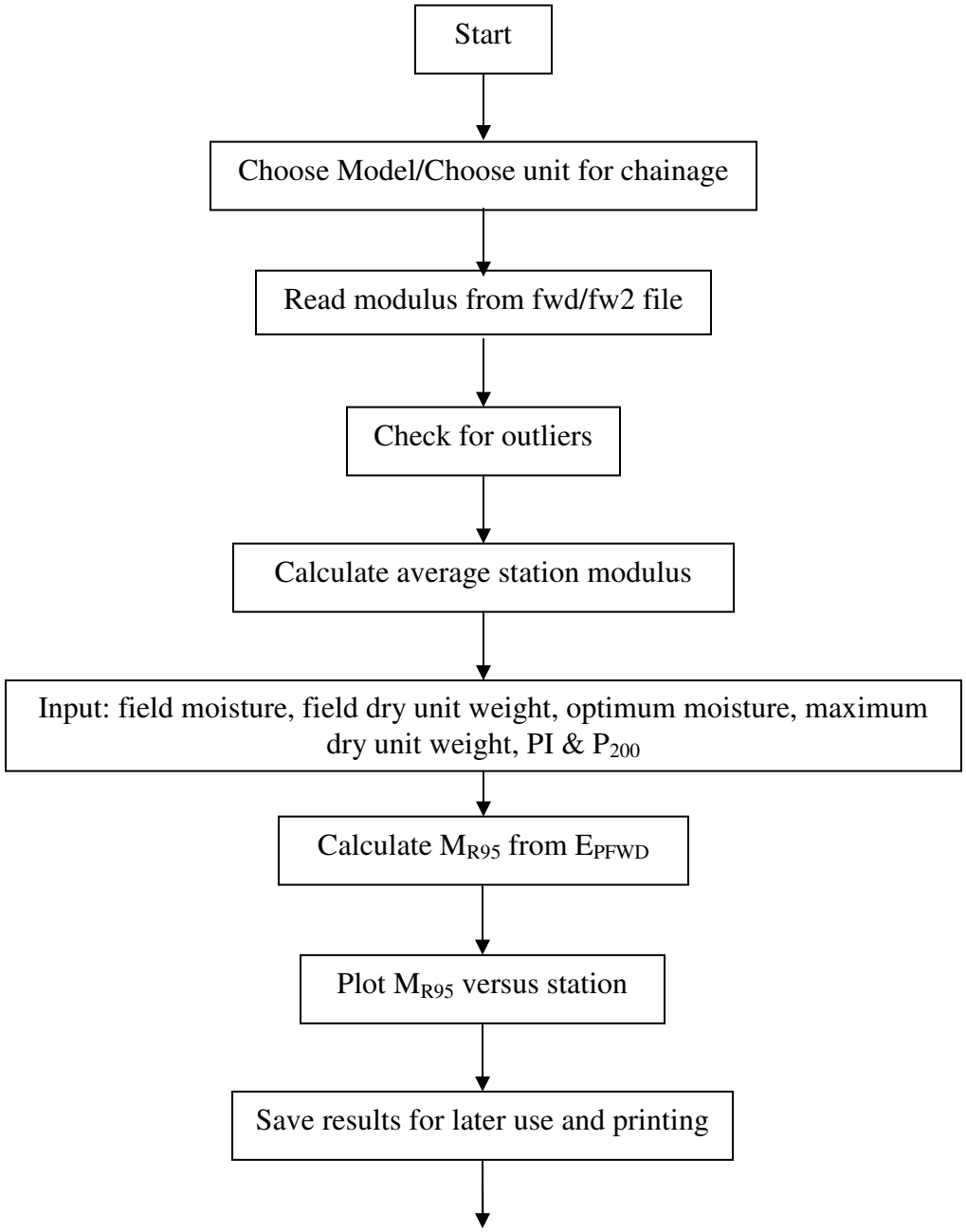

Figure C1 Flow Chart of First Phase of Program Calculating Resilient Modulus from Elastic Modulus

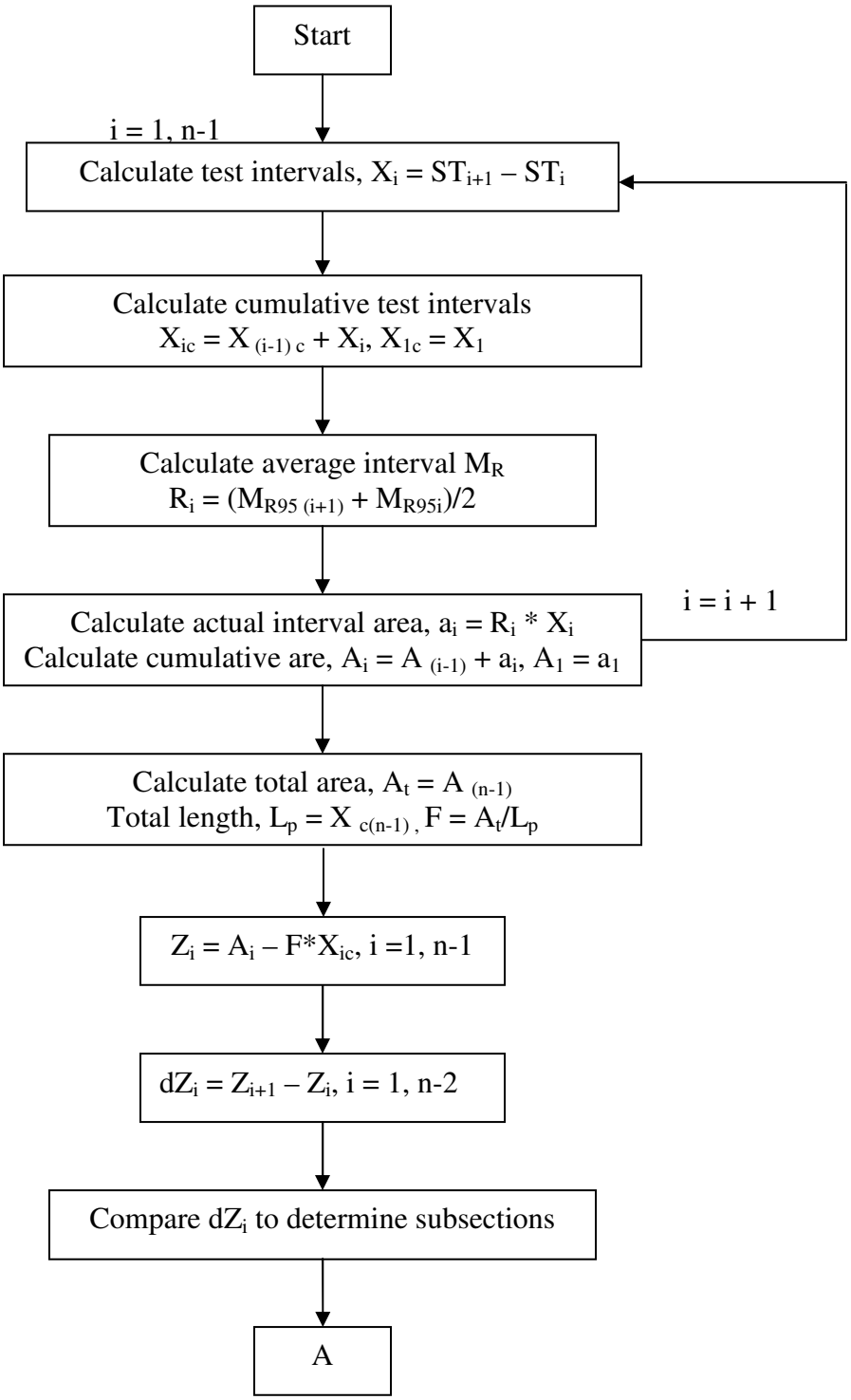

Figure C2 Flow Chart of Second Phase of Program Delineating Homogeneous Sections

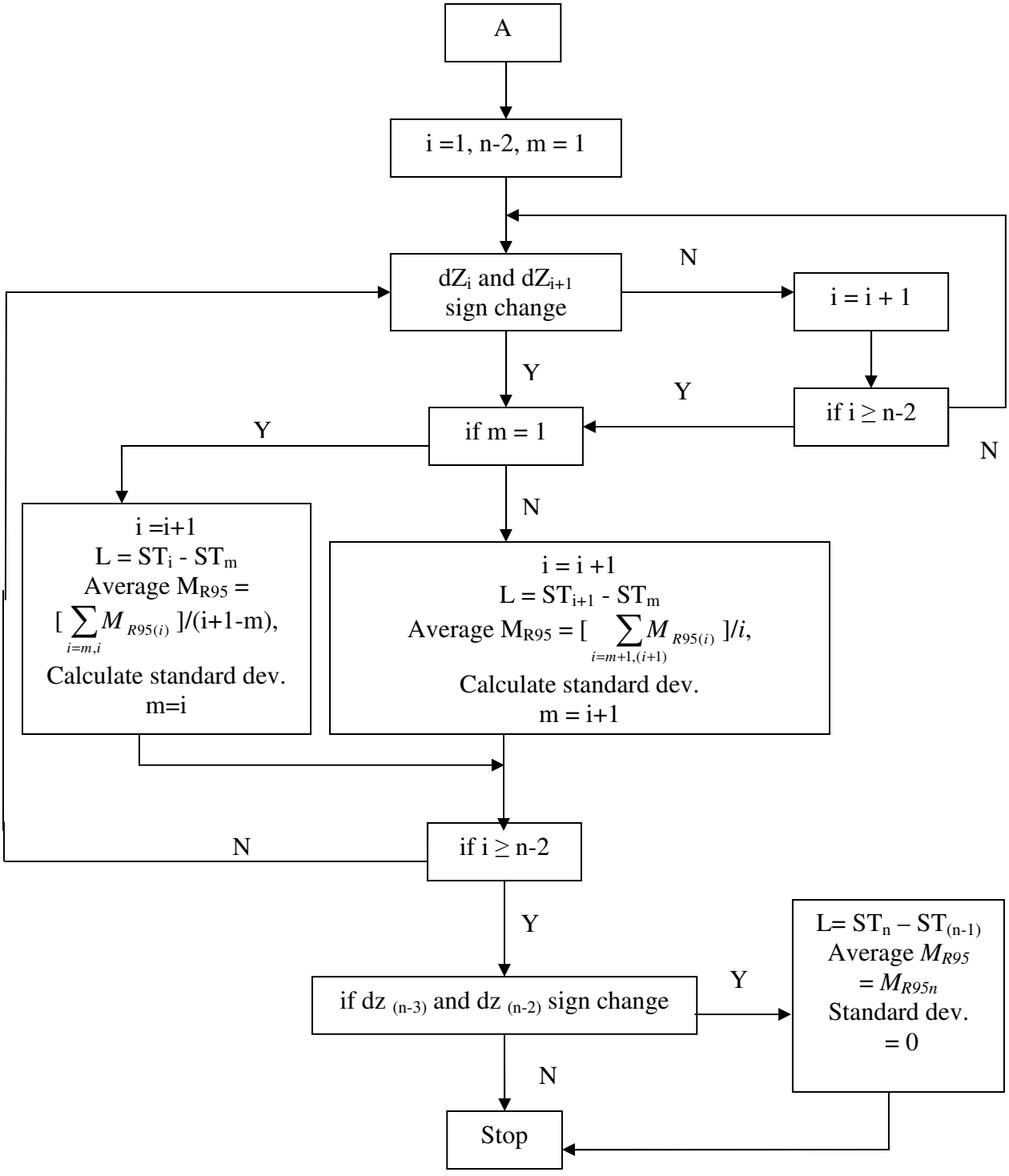

Figure C2 (Ctd) Flow Chart of Second Phase of Program Delineating Homogeneous Sections